COMPUTATION OF SLOWNESS AND EFFECTIVE PERMITTIVITY CURVES FOR STANDARD SAW CRYSTALS

BY

SHAFIQ S. MANJI,
B.Eng.


McMASTER UNIVERSITY LIBRARY
HAMILTON, CANADA

SLOWNESS AND EFFECTIVE PERMITTIVITY FOR STANDARD SAW CRYSTALS

COMPUTATION OF SLOWNESS AND EFFECTIVE PERMITTIVITY CURVES FOR STANDARD SAW CRYSTALS

By

SHAFIQ S. MANJI, B.Eng.

A Thesis

Submitted to the School of Graduate Studies

in Partial Fulfillment of the Requirements

for the Degree

Master of Engineering

McMaster University
Hamilton, Ontario

MASTER OF ENGINEERING (1997)
(Electrical Engineering)

McMASTER UNIVERSITY
Hamilton, Ontario

TITLE: Computation of Slowness and Effective Permittivity Curves for Standard SAW Crystals

AUTHOR: Shafiq S. Manji, B.Eng. (McMaster University)

SUPERVISOR: Professor Peter Morley Smith

NUMBER OF PAGES: viii , 143

ABSTRACT

The subject of this study is the development of software to provide for the computation of the slowness and effective permittivity functions for standard Surface Acoustic Wave (SAW) crystals. These two functions are very important in characterizing the physical properties of a substrate and their determination provides a foundation from which all further SAW device modelling can be undertaken. To achieve the goal, general wave propagation characteristics in the presence of boundaries are examined with particular emphasis on the case for piezoelectric crystals. The slowness and effective permittivity functions are presented only for the common SAW substrates supporting pure Rayleigh wave propagation. To affirm the validity of the software, the computed functions are compared with already published experimental data. Other parameters derived from the permittivity function are also compared to published results providing further justification for the validity of the software.

TABLE OF CONTENTS

TABLE OF CONTENTS (contd.)

LIST OF FIGURES

LIST OF FIGURES (contd.)

ACKNOWLEDGMENTS

I would like to express my sincere appreciation for the consideration and supervision received from my supervisor, Dr. Peter M. Smith. His leadership and guidance provided a stimulating work environment without which the work could not have been completed.

Special thanks also go to Dr. Wen Liu for his invaluable time and support in the laboratory as well as for his input into insightful discussions.

Finally, my parents deserve much of the credit for their constant support and encouragement throughout the duration of the work.

CHAPTER 1

INTRODUCTION TO SAW DEVICES

1.1 INTRODUCTION

In recent years, the market for Surface Acoustic Wave (SAW) devices has increased significantly. With respect to signal processing applications, surface waves are attractive since they offer low velocity non-dispersive propagation, with low attenuation up to microwave frequencies. The resulting shorter wavelength and the accessibility of the propagation path at the surface of the material allow for the manipulation of the waves in ways that would otherwise require huge lengths of cable or complicated delay mechanisms. Furthermore, all this is achieved at a cost orders of magnitude smaller than for other methods, and the resulting devices are comparable, both in size and in fabrication technology, to integrated circuits.

This chapter will serve as a general introduction to SAW devices touching on history and development and various types of devices. Only a brief account will be presented to give the reader adequate knowledge to allow appreciation of the impact these devices are making in the communications industry. Finally, the chapter will conclude with a description of the scope of this Thesis .

1.2 HISTORY

Since the early 1960's when the use of surface waves in electronic devices was first considered, there has been a substantial growth of research into methods of generating and manipulating the waves, and in developing practical devices for use in a wide range of electronic applications. For these devices, the distinguishing trait is that the wave propagation velocity is about 3000 m/s or about 100 000 times slower than the propagation of electromagnetic waves through free space, and the relative ease by which these waves are generated and detected at frequencies between 40 and 2000 MHz. However, the significant advantage of these waves stems from the fact that the propagation path at the surface of the material is accessible. Because two dimensions are available rather than one, there is much more scope to exploit methods of generating and detecting waves, or of modifying them as they propagate, and considerable structural complexity is feasible.

The physics of propagation of surface waves on a crystalline solid have been known since the last century when they were first studied by Lord Rayleigh [1]. On a solid, a surface acoustic wave may be viewed as a disturbance involving deformations of the substrate. These deformations, as shown in Figure 1.1, are caused by the motions and subsequent displacements of atoms. In an ideal elastic solid, internal restoring forces proportional to the amount of deformation will tend to return the solid to its equilibrium position. A surface acoustic wave can be resolved into two components : longitudinal waves, in which atoms vibrate in the propagation direction, and shear waves, where atoms

vibrate in the plane normal to the propagation direction. The displacement components of a Rayleigh wave propagating in the x_1 direction are [2]

$$u_1 = C\left(e^{k\,b_1 x_3} - Ae^{k\,b_2 x_3}\right) e^{ik(x_1 - v_R t)} \tag{1.1a}$$

$$u_3 = -ikb_1 C\left(e^{k\,b_1 x_3} - A^{-1} e^{k\,b_2 x_3}\right) e^{ik(x_1 - v_R t)} \tag{1.1b}$$

where

$$b_1 = \sqrt{1 - (v_R / v_l)^2}$$

$$b_2 = \sqrt{1 - (v_R / v_t)^2}$$

$$A = \sqrt{b_1 b_2}$$

C is a constant

v_R is the phase velocity of the surface wave on the substrate

v_l is the velocity of the longitudinal bulk wave in the substrate

v_t is the velocity of the transverse bulk wave in the substrate

The longitudinal and vertical displacement components, u_1 and u_3 respectively, are in phase quadrature and the elastic displacement is elliptic, with the polarization procession at the free surface being retrograde.

Figure 1.2 shows the variation of the displacement components with substrate depth in a plane perpendicular to the propagation direction. It is apparent that the propagation is along the surface and the displacement amplitudes exist only in a region

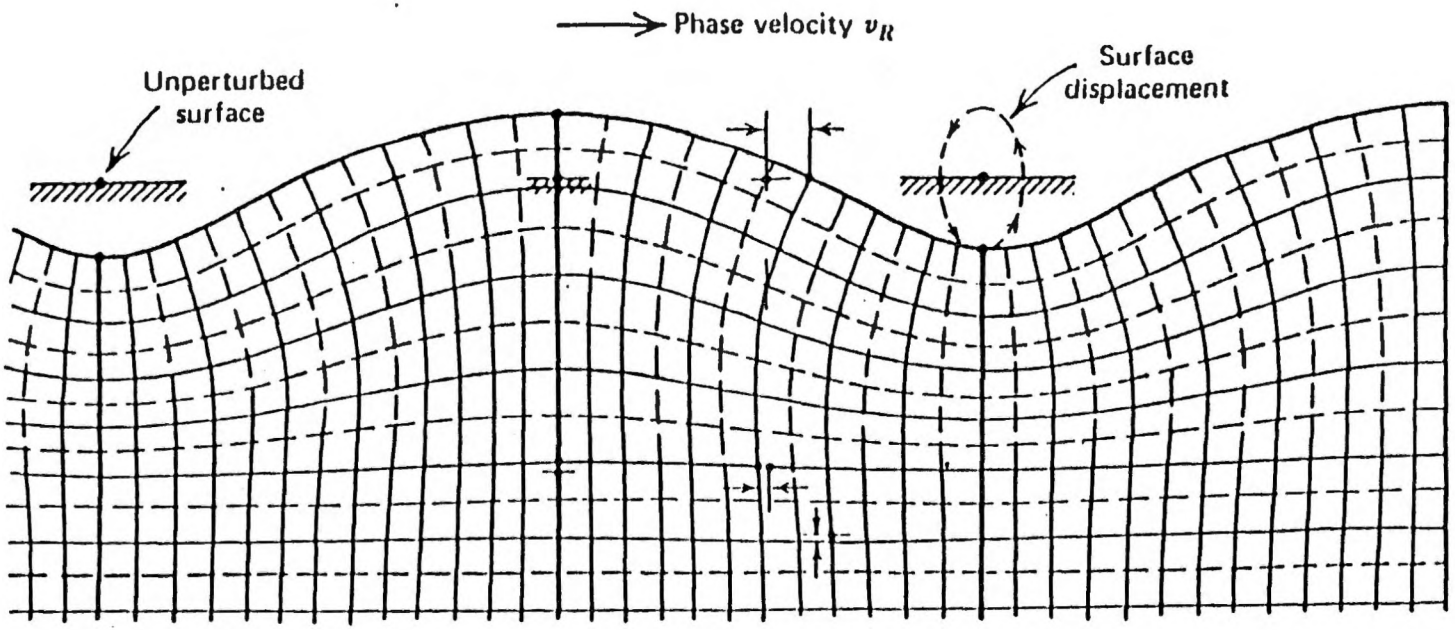

Figure 1.1: Wave propagation on the surface of a crystal [2]

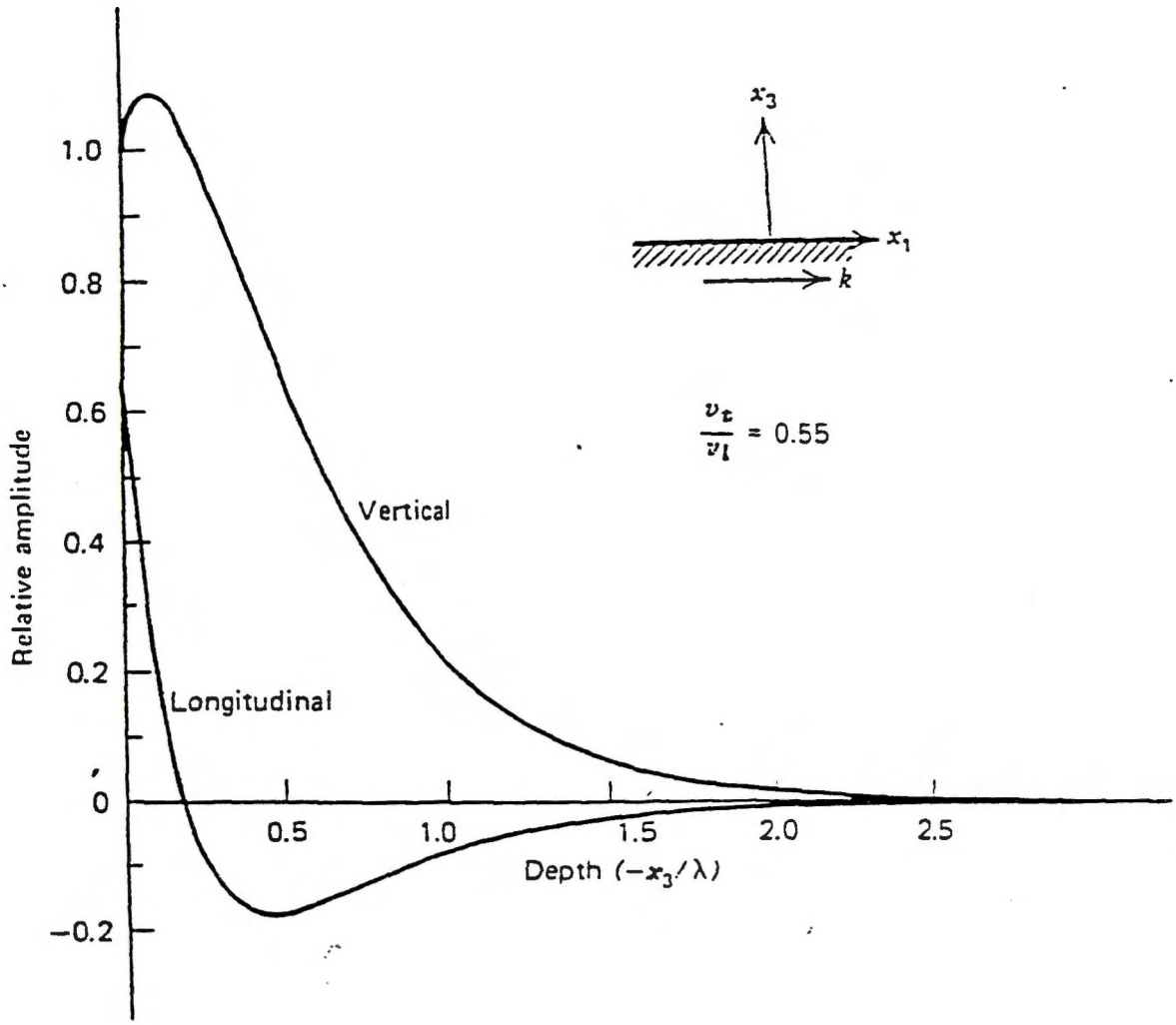

Figure 1.2: Variation of Rayleigh wave components with substrate depth [2]

that extends a few wavelengths from the surface of the crystal. The Poynting vector for this Rayleigh wave is parallel to the x_1 direction everywhere an decreases rapidly with depth indicating that the wave energy is concentrated near the surface.

If this wave is made to propagate along the surface of a *piezoelectric* crystal, an electric field will be induced in the vicinity of the surface due to the perturbations in the crystalline structure. This electric field can be tapped to convert the mechanical wave into an electric signal by means of an *interdigital transducer* (IDT). The interdigital transducer generates surface waves by exploiting the piezoelectric effect. The transducer has a set of identical electrodes connected alternately to two metal bus-bars . When an oscillatory voltage is applied, the transducer generates an electric field which is spatially periodic, with its period, L, equal to the spacing of the electrodes connected to one of the bus-bars. Owing to the piezoelectric effect, a corresponding pattern of mechanical displacements is also produced. Efficient coupling to surface waves occurs if the transducer period L is equal or close to the surface-wave wavelength, and this requires an appropriate frequency for the applied voltage.

Typically, the transducer will be designed for operation at, say, 100MHz, where the wavelength is about 32 microns. The width of each electrode, equal to one quarter of the wavelength, is then 8 microns. Owing to the symmetry, the transducer generates surface waves equally in two opposite directions, so that it is bi-directional. Usually, the waves in one direction are not required, and are eliminated by an absorber comprising a lossy material applied to the surface. This basic component constitutes the basis of operation of all SAW devices and is displayed in Figure 1.3 below.

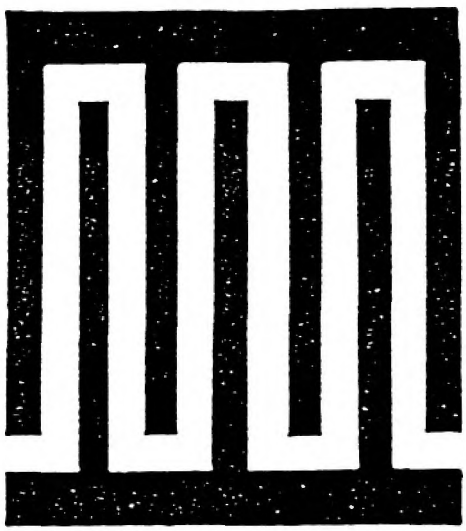

Figure 1.3 : Typical IDT

Over the last several decades, a wide variety of techniques have been developed for use in surface-wave devices. Methods have been developed for electrically generating and detecting the waves (i.e. for transduction), for reflecting, guiding, focusing and amplifying the waves, and for introducing controlled dispersion [3]. These methods employ a variety of physical principles. As in bulk wave devices, an important factor is the use of piezoelectric materials, though for surface waves the usage is somewhat different in that the propagation medium itself is piezoelectric.

Through the efforts of many researchers in surface wave device technology, the field has now reached considerable technical maturity. In modern electronics, surface acoustic wave devices are now used in a considerable range of applications to carry out particular signal processing functions with great technical facility and cost-effectiveness. The important applications such as pass-band filters, pulse compressors and delay line oscillators now constitute a well-proven and reliable component technology for television, radar and communication systems of many kinds.

1.3 TYPES OF DEVICES

The simplest type of surface-wave device is a *delay line*. This structure employs two transducers, one to generate the waves and one to receive them, as shown in Figure 1.4. The propagation medium, often called the substrate, is a piezoelectric crystal typically 1mm thick. If an electrical signal is applied to the input transducer, it will be converted to a corresponding surface wave by exploiting the piezoelectric effect [4]. A voltage will then appear on the output transducer after a delay determined by the transducer separation and the surface wave velocity. Provided the input signal is confined to a frequency band in which the transducers are effective, there is little distortion because the wave is non-dispersive. Typical delays range from 1 to 50 μs [5] .

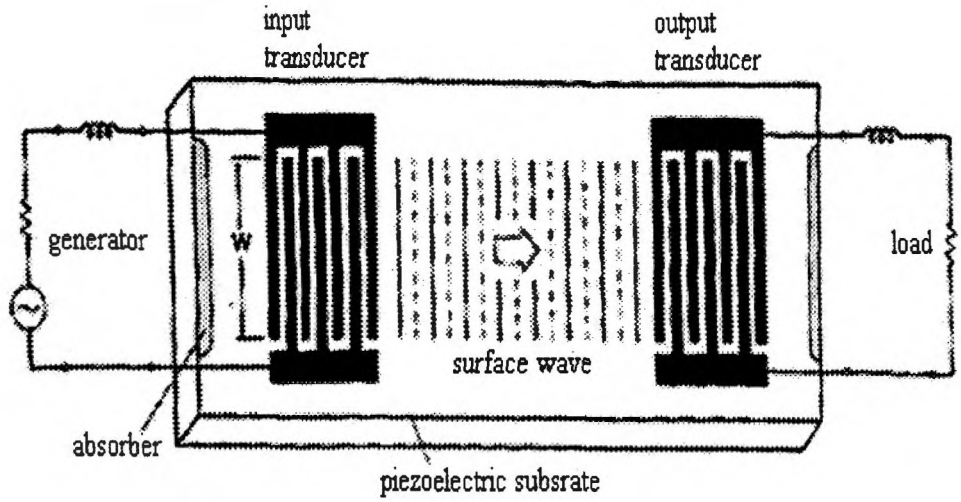

Figure 1.4 : Interdigital delay line [6, p.7]

Most surface wave devices play significant roles in signal processing applications. In this respect, the versatility of the interdigital transducer is a crucial factor. The above description considers only the simplest form of the interdigital transducer. Processing applied electrical signals in a prescribed manner, for example, to reject unwanted frequency components can be achieved by modifying the transducer design in a variety of ways. The two commonest modifications to this component are to vary the electrode lengths and to vary the pitch [7].

The SAW convolver [8] is another type of common device that finds frequent application in signal processing. This device employs two input IDTs with a metal plate covering the space between them. This type of device is depicted in Figure 1.5. The signal to be analyzed is fed into one of the IDTs while a time inverted version of the

reference signal is fed into the other IDT. The metal plate detects a signal which corresponds to the convolution [9] of the two signals.

Alternatively, a surface-wave resonator [10] may be used. In this structure, periodic arrays of either metal strips or grooves form reflectors, two of which form a surface wave cavity. The strips of the reflectors are set at half the desired wavelength in the crystal so that the wave reflections from each strip add constructively with the reflections from other strips. The resulting resonant cavity introduces poles into the response which are not otherwise achievable by other means. The SAW resonator is depicted in Figure 1.6.

In another application of piezoelectricity, a set of metal strips in the path of a surface wave can be used to generate a secondary surface wave, which may be displaced laterally with respect to the input wave, or may propagate in a different direction. This principle is used in the multi-strip coupler, which has a variety of forms with many different applications [11] . Another consequence of piezoelectricity is that a metal strip on the surface may be used as a waveguide for surface waves, enabling a narrow beam to propagate long distances without diffraction spreading.

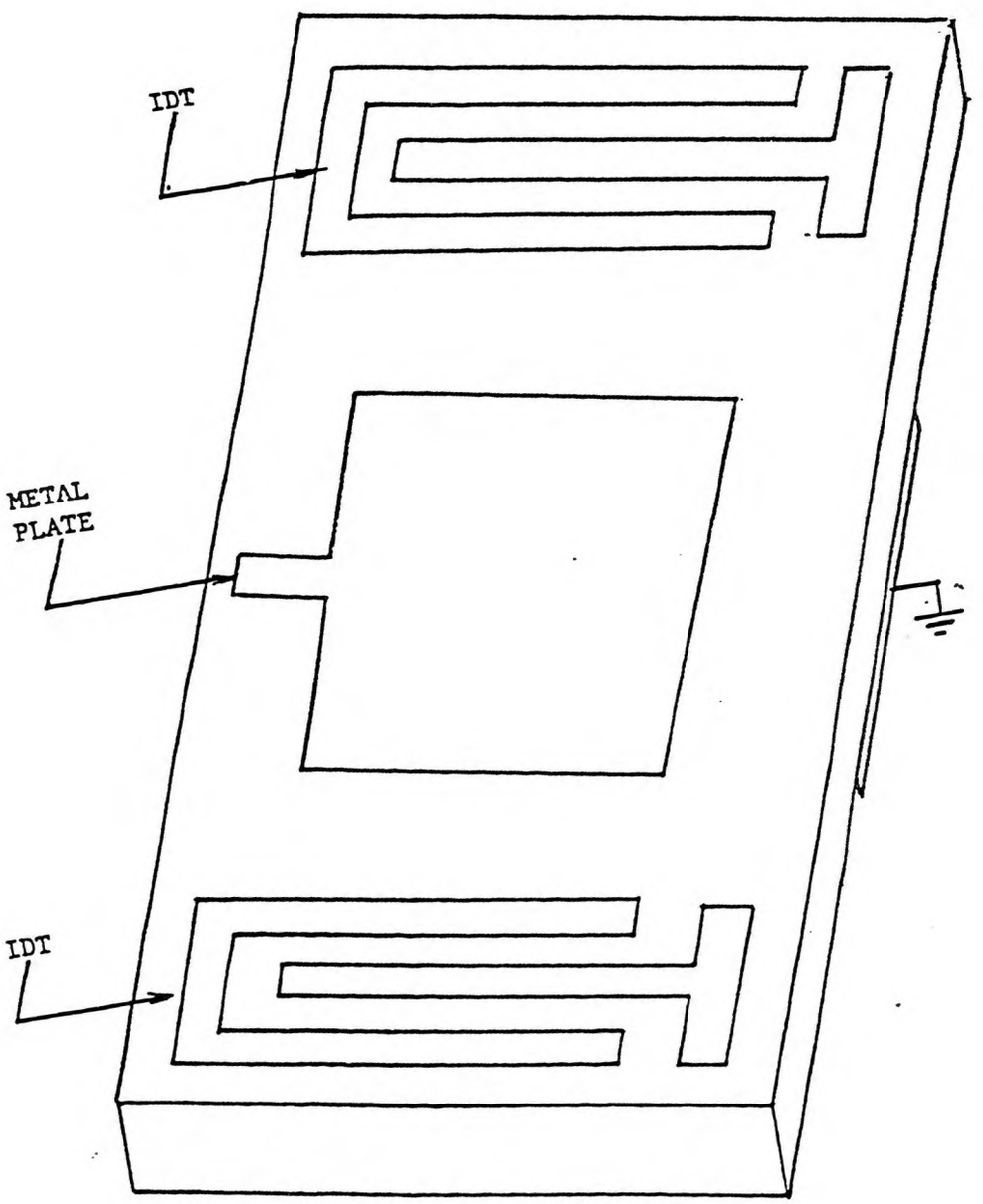

Figure 1.5: The SAW Convolver [12]

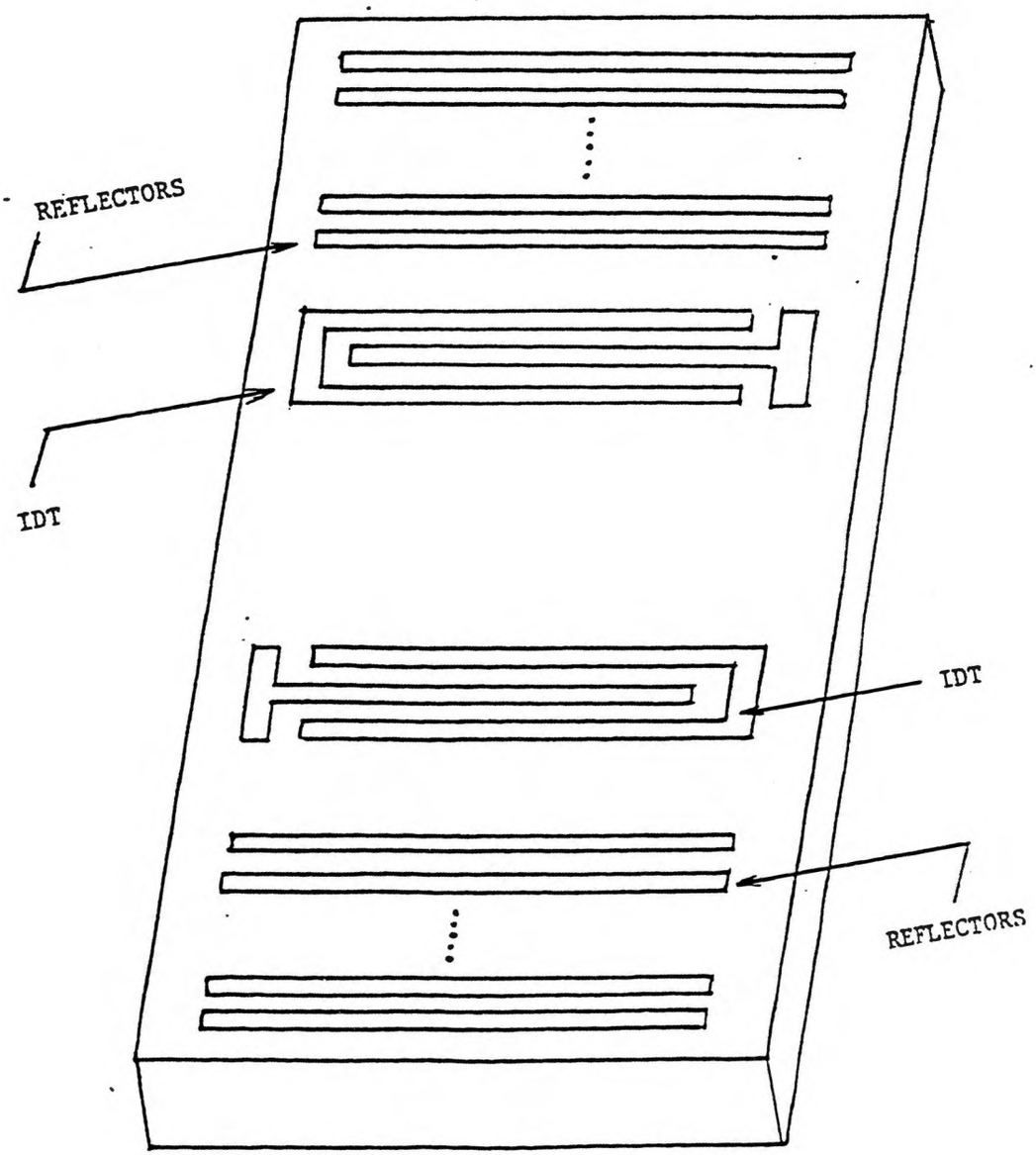

Figure 1.6 : The SAW Resonator [12]

Surface wave technology can also be exploited to produce several types of stable oscillators [13]. In this case, quartz is usually used as the propagation medium because of its good temperature stability. One technique involves connecting an amplifier between the input and output of the interdigital delay line, creating a loop. Then, the small-signal gain of the amplifier will exceed the loss of the delay line, so that the loop oscillates at a frequency related to the surface wave velocity. The details of all the various types of SAW structures are not of particular interest in this thesis and will, therefore, not be discussed further.

The results achieved with the use of surface acoustic wave devices are well suited to a wide range of system requirements, particularly in radar and communication systems. Since they can often be implemented in small, rugged, light and power efficient modules, these devices are also finding ever-increasing application in mobile and space-borne communication systems. In terms of quantity, the most widely used SAW device is the bandpass filter used in the I.F. section of colour television receivers. Bandpass filters are also used extensively in radar and communication systems, and in television broadcasting equipment. Chirp filters (interdigital and reflective array compressors [14]) are widely used in radar systems. Some radar systems make use of delay lines or PSK filters. In spread spectrum communication systems, PSK filters are used as matched filters, and surface wave non-linear convolvers are also having an impact on this area.

In all of the devices described, the structure is simply a piezoelectric medium with a metal film on the surface, etched to give an appropriate geometry. Owing to the simplicity of the structure, and the availability of convenient fabrication methods, nearly all

surface-wave devices use piezoelectric materials. Furthermore, crystalline materials are usually chosen in order to obtain low attenuation of the waves, and the commonest choices are quartz and lithium niobate.

It is obvious then that great consideration must be given as to the choice of substrate material. As noted, the field of SAW devices is mainly concerned with piezoelectric insulators (certain semiconductors, e.g. GaAs can however be used). The qualities required for good surface-wave material can be categorized as follows:

(a) availability at moderate cost;

(b) good temperature stability

(c) fair electromechanical coupling;

(d) good mechanical properties and resistance to environmental effects (e.g. humidity);

At present, availability at moderate cost is really achieved only for the most commonly used materials, e.g. quartz, lithium niobate ($LiNbO_3$) and lithium tantalate ($LiTaO_3$). With regards to piezoelectric properties and temperature stability, an apparent tradeoff exists. For instance, there are good piezoelectric materials, i.e. those with strong electromechanical coupling, like lithium tantalate and, especially, lithium niobate, but their known cuts are very temperature sensitive which excludes them from certain functions. Quartz, on the other hand, exhibits only moderate coupling, but has the advantage of the ST cut whose temperature coefficient is zero to the first order [15, p.20]. Likewise,

Berlinite ($AlPO_4$) is a less commonly used material which also has an ST cut that is more sensitive to the second order than that of quartz, but offers slightly higher coupling. The double oxide of bismuth and germanium ($Bi_{12}GeO_{20}$) is interesting for the realization of long delays because the corresponding velocity is lower by a factor of 2 as compared with other materials.

The primary criteria for substrate choice are the surface wave velocity v, the dimensionless number K^2, which is defined as the coefficient of electromechanical coupling, the relative permittivity ε_r and the temperature behaviour. The velocity v defines the geometry of a device whereas the coefficient K^2 limits its maximum bandwidth : strong coupling allows large relative bandwidths, high velocity allows higher central frequencies but shorter delays. Moreover, the characteristics of propagation (attenuation and anisotropy), diffraction and nonlinear effects can also influence the performance of signal-processing devices [6, pp.145-147].

1.4 Scope of Thesis

The purpose of this Thesis is to develop stand alone software that allows for the computation of two very important functions that characterize a standard SAW crystal substrate. The functions, namely the slowness and effective permittivity, provide a basis on which all further SAW device modelling can be based. The result is the ability for a non-specialist to choose from a select group of commonly used SAW crystals, to enter the

desired cut of the selected crystal and to subsequently obtain precise slowness and effective permittivity curves for evaluation purposes. Only substrates supporting piezoelectric Rayleigh waves are examined.

To provide the groundwork, physical properties of crystals are first discussed including an overview of their representations as tensors. Following this, a rigorous treatment of tensor transformations is given with reference to abbreviated subscript notation. This is followed by a brief description of wave propagation in bulk material placing particular emphasis on piezoelectric solids. Wave propagation in the presence of boundaries is described in detail as this forms the bulk of the underlying theory on which the software was developed. Following this, the slowness and effective permittivity curves for standard SAW crystals obtained using the developed software are presented for comparison with published data. Finally, conclusions and recommendations complete the Thesis.

CHAPTER 2

PROPERTIES OF CRYSTALS

2.1 INTRODUCTION

Surface waves are almost always generated and detected by means of interdigital transducers (IDTs). These consist of metal electrodes deposited on a *piezoelectric crystalline* substrate by means of photolithographic techniques [4, p.216]. The physical properties of the substrate itself are fundamental in determining the performance of a particular device. Since this study involves the calculation of important functions that characterize particular crystal substrates, an examination of the physical properties of crystals is essential.

The physical properties of crystals are defined by relations between measurable quantities. Density, for example, is defined from a relation between mass and volume. Density is a property that does not depend on direction since mass and volume can be measured without reference to direction. On the other hand, a crystal property such as electrical conductivity is defined as a relation between electric field and the current density. These two measurable quantities must be specified in direction as well as magnitude. It is very possible then that a physical property will depend upon the direction

in which it is measured. As an experimental fact, the electrical conductivity of many crystals does indeed vary with direction. In such cases, the crystals are said to be *anisotropic* for the property in question. Further examples of crystal properties that may depend upon the direction of measurement are : the polarization produced in a dielectric by an electric field (dielectric susceptibility) ; the polarization of a crystal that may be produced by mechanical stress (piezoelectricity) ; the deformation caused by a mechanical stress (elasticity); and the birefringence that can be set up by an electric field (electro-optical effect) [4, pp.290-293].

The dilemma then is how to specify the value of a crystal property that can depend on direction as clearly a single number cannot be sufficient. There is also the problem of how the specification, when given, is related to the symmetry of the crystal. For a few properties, such as density, all crystals are isotropic [16]. Cubic crystals happen to be isotropic for certain other properties as well, such as conductivity and refractive index, and this sometimes leads to the misconception that they are isotropic for all properties. However, cubic crystals are in fact markedly anisotropic for elasticity, photoelasticity and certain other properties. All crystals should, therefore, be regarded as potentially anisotropic, and then one can go on to prove that, for certain properties, they are isotropic.

In this chapter, then, a method of specifying the physical properties of a crystal will be introduced. Only the pertinent properties required for the calculation of the slowness and effective permittivity functions will be of concern. These quantities are the elastic constants of the material (stiffness and compliance), the piezoelectric stress and strain

constants and the relative permittivity constants. It will be shown that the relevant crystal properties can be conveniently represented by mathematical quantities called *tensors* and that these standard tensors can be transformed to appropriate values, correctly reflecting different orientations dictated by the cut of the crystal. To begin then, a method of specifying crystal orientations is necessary and this is the subject of the next section.

2.2 CRYSTAL ORIENTATIONS

An ideal crystal is defined to be a body in which the atoms are arranged in a lattice. This implies that (a) when viewed from all the lattice points, the atomic arrangement appears the same, and in the same orientation and (b) the atomic arrangement viewed from a lattice point is different from the arrangement when viewed from any point that is not a lattice point. Crystals are conveniently divided into 32 crystal classes according to the point-group symmetry they possess. The 32 classes are conventionally grouped into seven crystal systems according to the symmetry of the class [16, p.280].

Great care must be taken in specifying the orientation (cut) of a particular crystalline solid. The internal structure for most crystalline materials is referenced to an orthogonal set of axes denoted by the upper case symbols X, Y, Z, with directions defined in relation to the crystal lattice. The standard material tensors are all specified in relation to the internal axes X, Y and Z, so for the analysis, depending on the cut of the crystal, they must be rotated into the frame defined by x_1 , x_2 , x_3 . In surface wave analysis, the cut of a crystal is defined by the surface orientation and the wave propagation direction.

These are most often defined in relation to the crystallographic axes. The convention usually adopted is to define the surface normal x_3, followed by the propagation direction x_1. For example, YZ lithium niobate indicates that x_3 is parallel to the crystal Y-axis, and x_1 is parallel to the crystal Z-axis. The orientation of x_3 is also referred to as the cut, so that for YZ lithium niobate the crystal is said to be Y-cut. Alternatively, crystal cuts are sometimes given with an angle preceding the propagation direction, e.g. Y-cut θ° X-propagating lithium niobate. Here, θ is the angle between the X crystal axis and the propagating direction as depicted in Figure 2.1 below.

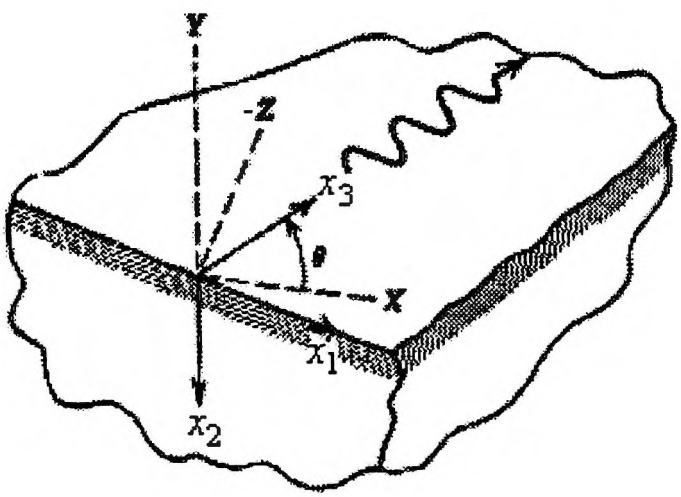

Figure 2.1 : Illustration of the surface wave orientation Y-cut θ° X-propagation. X, Y, Z are the crystal axes while x_1, x_2, x_3 are coordinate axes.

In experimental practice, several different notations are employed to specify rotations of crystallographic axes with respect to the coordinate axes. In essence, three independent parameters are required to specify the orientation of a crystal, and more generally, any rigid body. The IRE Standards on Piezoelectric Crystals, *Proceedings of the IRE*, **37**, pp. 1378-1395 (1949) considers rotations of the coordinates about all three axes. The coordinates axes are labelled *t, l, w* to correspond with thickness, length and width of the usual plate sample geometry. A crystal rotation is described by first aligning the *t, l, w* coordinate axes along the crystal axes and then specifying one, two, or three rotations about particular coordinate axes. This system requires use of a *z*-rotation matrix, *y*-rotation matrix, and, in addition, an *x*-rotation matrix where the rotation angle ξ_x is clockwise about the *x* coordinate axes.

However, the procedure employed in this work, is to consider that the crystal itself is rotated with respect to a *fixed* set of coordinate axes. One can carry out the transformation from a given Cartesian coordinate system to another by means of three successive rotations performed in a specific sequence. The Eulerian angles are then defined as the three successive angles of rotation [17, p.82]. A coordinate rotation described by ξ , η , ξ' thus corresponds to the crystal rotation angles

$\phi = -\xi$ about the *z* axis

$\theta = -\eta$ about the *y'* axis

$\psi = -\xi'$ about the *z'* axis

where the primes indicate an axis obtained as the result of a previous rotation. These three angles are termed the *Euler angles* of rotation.

For example, for Y-cut 128° X-propagating lithium niobate, from the discussion on crystal cut specification, the angle between the X axis and the direction of propagation is 128°. To obtain the Euler angles for this crystal cut, consider the coordinate axes initially coinciding with the crystal axes. With respect to ϕ, no rotation about z is required since the Y axis must remain as the outward normal to the surface. The crystal must be rotated -38° about the y' axis to give an angle of 128° between the X axis and the direction of propagation. Therefore, $\theta = 38°$. And finally, since no rotation about the z' axis is needed, $\psi = 0$. Hence, the Euler angles are determined to be (0, 38, 0). Likewise, the Euler angles can be obtained for any specified cut of a particular crystal.

2.3 DEFINITION OF TENSORS

The physical properties of crystals can be conveniently represented in what is commonly referred to as *tensor* notation. Since this study is concerned only with the physical properties of crystals as they are related to the calculation of the slowness and effective permittivity functions, the explanation of particular properties in terms of crystal structure is not considered. Furthermore, the discussion will be only limited to the physical properties required for the calculations i.e. the stiffness and compliance tensors,

the permittivity tensor and finally the piezoelectric stress and strain tensors. To begin then, the notion of a tensor must be clearly defined.

The equations of physics describe the relations between physical quantities. In the simplest case, if two quantities x and y are linearly related by a scalar quantity, the following relation can be written.

$$y = ax \tag{2.1}$$

where a is called the proportionality factor. The implication here is that the coefficient a is *intrinsic* and depends only on the physical system.

However, if x and y are now considered to be vectors, a vector expression of the form $\boldsymbol{y} = \boldsymbol{ax}$ is needed. In three dimensional space, this takes the form

$$y_i = \sum_{j=1}^{3} a_{ij} x_j \tag{2.2}$$

where the vector equation can be resolved into three scalar equations (i = 1, 2, 3) and the coefficient $\boldsymbol{a}$ is now a matrix of nine coefficients (i, j = 1, 2, 3). It is obvious that the coefficients x_i and y_i are not independent of the coordinate axes even when the vectors $\boldsymbol{x}$ and $\boldsymbol{y}$ are themselves completely intrinsic. It follows that the matrix $\boldsymbol{a}_{ij}$, even though it is supposed to establish an intrinsic relation between intrinsic quantities, will change when the set of coordinates is changed. The intrinsic character of the matrix is indicated by the

fact that its law of variation must be such that the three equations in (2.2) remain valid when the vectors $\boldsymbol{x}$ and $\boldsymbol{y}$ are given in a new coordinate frame i.e. the coefficients in the matrix have to be modified accordingly. When the law of variation of a vector due to a change of the frame of reference is known, the corresponding law of variation of the two index matrix $\boldsymbol{a}_{ij}$ can be deduced from it. Restricting ourselves to orthonormal frames of reference for which

$$x_i \rightarrow X_k = \sum_{i=1}^{3} R_{ki} x_i \tag{2.3}$$

where R_{ki} is an orthogonal matrix, one can verify that [18]

$$\boldsymbol{a}_{ij} \rightarrow \boldsymbol{A}_{kl} = \sum_{i=1}^{3} \sum_{j=1}^{3} \boldsymbol{R}_{ki} \boldsymbol{R}_{lj} \boldsymbol{a}_{ij} \tag{2.4}$$

An intrinsic matrix of this kind (in the sense that its parameters vary in accordance with those of a vector under a change of coordinates), is called a *tensor*.

Therefore, a tensor is an intrinsic entity that possesses a number of indices. A scalar can be considered to be a tensor of zero index or *rank*, and a vector to be a tensor with one index. An intrinsic proportionality between a vector and a two-index tensor can be described by a three-index tensor and so on. For example, the transformation law of a three index tensor under a transformation of the frame of reference is

$$e_{ijk} \rightarrow E_{lmn} = R_{li} R_{mj} R_{nk} e_{ijk} \tag{2.5}$$

where summation convention for the three indices *(i, j, k)* is implied. Note that tensors can represent physical fields (electric field, stress field etc.) as well as properties of the medium (permittivity tensor, elasticity tensor). The physical differences have no effect on the mathematical nature of a tensor whatsoever. Furthermore, any quantity that transforms in the manner described above is defined as a tensor.

2.4 TENSOR REPRESENTATIONS OF PHYSICAL PROPERTIES

The propagation of acoustic waves in a solid involve time-varying deformations, or vibrations, in material media. All material substances are composed of atoms, which may be forced into vibrational motion about their equilibrium positions. When the particles of a medium are displaced from their equilibrium positions, internal restoring forces arise. It is these elastic restoring forces between particles, combined with inertia of the particles, which lead to oscillatory motions of the medium. Assuming the solid to be homogenous, the forces will be expressed in terms of the stress, *T*, while the displacements are expressed in terms of the strain, *S*. In an equilibrium state, consider a particle in the material located at $\mathbf{x} = (x_1 , x_2 , x_3)$. When the material is not in its equilibrium state, this particle is displaced by an amount $\mathbf{u} = (u_1 , u_2 , u_3)$, where the components u_1 ,u_2 and u_3 are in general functions of the coordinates x_1, x_2, x_3. Hence, in non-equilibrium state, the

particle is displaced to a new position **x** + **u**. In the present analysis, the displacement **u** is taken to be independent of time, *t*. If **u** is independent of **x**, there will be no internal forces since this simply denotes displacement of the material as a whole. Internal forces are also absent if the material is rotated. The strain at each point is defined by [6]

$$S_{ij}(x_1, x_2, x_3) = \frac{1}{2}\left(\frac{\partial u_i}{\partial x_j} + \frac{\partial u_j}{\partial x_i}\right), \qquad i, j = 1,\ 2,\ 3. \tag{2.6}$$

With this definition, displacements and rotations of the material as a whole cause no strain, and the strain is related to internal forces. The strain is a second rank tensor and is clearly symmetrical. ($S_{ij} = S_{ji}$), so that six of the nine components are independent [16].

Elasticity is concerned with the internal forces within a solid and the related displacement of the solid from its equilibrium configuration. Elastic deformation in a solid is governed by Hooke's Law [19]. Essentially, this law states that the strain is linearly proportional to the stress, or conversely, that the stress is linearly proportional to the strain. The latter description is stated mathematically by writing each component of stress (elastic restoring force) as a linear function of all the strain components. For example, along the *x* axis

$$\begin{aligned} T_{xx} = {} & c_{xxxx}S_{xx} + c_{xxxy}S_{xy} + c_{xxxz}S_{xz} \\ & + c_{xxyx}S_{yx} + c_{xxyy}S_{yy} + c_{xxyz}S_{yz} \\ & + c_{xxzx}S_{zx} + c_{xxzy}S_{zy} + c_{xxzz}S_{zz} \end{aligned} \tag{2.7}$$

In general then,

$$T_{ij} = c_{ijkl} S_{kl} \tag{2.8}$$

$$i, j, k, l = x, y, z$$

where summation over the repeated subscripts k and l is implied. The constants c_{ijkl} in equation (2.8) are called the elastic *stiffness* constants. Since expansion of equation (2.8) yields nine equations (corresponding to all possible combinations of the subscripts *ij*) and each equation contains nine strain variables, there are 81 elastic stiffness constants in total. However, many of these elements are related. The symmetry of S_{ij} and T_{ij} implies that the stiffness is unchanged if i and j are interchanged or if k and l are interchanged, so

$$c_{ijkl} = c_{jikl} \ , \quad c_{ijkl} = c_{ijlk} \tag{2.9}$$

This constraint reduces the number of independent elements to 36. Thermodynamic considerations also show that the pair of indices can be interchanged without loss of generality [17, p.144]. That is,

$$c_{klij} = c_{ijkl} \tag{2.10}$$

This allows for further reduction of the number of independent elements to 21. In fact, this is the maximum number of constants for any medium. These elements represent physical

properties of the material under consideration, so that the number of independent components may well be further reduced by the microscopic nature of the medium. For example, a crystalline material with cubic symmetry has only 3 independent elements.

Alternatively, the strains may be expressed as general linear functions of all the stresses,

$$S_{ij} = s_{ijkl} T_{kl} \tag{2.11}$$

$$i, j, k, l = x, y, z$$

where the constants s_{ijkl} are called the *compliance* constants, and are measures of the deformability of the medium. Equations (2.8) and (2.11) are appropriately termed the *elastic constitutive relations*. Both the stiffness and compliance constants define fourth rank tensors since their components have four indices. Likewise, the stress and strain fields define second rank tensors.

With respect to electromagnetic properties, the electric displacement vector **D** and the electric field vector **E** in a crystalline medium are not always parallel. In such cases, the components of **D** are related to the components of **E** by three linear equations

$$\begin{aligned} D_x &= \varepsilon_{xx} E_x + \varepsilon_{xy} E_y + \varepsilon_{xz} E_z \\ D_y &= \varepsilon_{yx} E_x + \varepsilon_{yy} E_y + \varepsilon_{yz} E_z \\ D_z &= \varepsilon_{zx} E_x + \varepsilon_{zy} E_y + \varepsilon_{zz} E_z \end{aligned} \tag{2.12}$$

which can be written in summation convention as

$$D_i = \sum_{j=1}^{3} \varepsilon_{ij} E_j \qquad (2.13)$$

where ε_{ij} is defined as the *permittivity* matrix. The permittivity matrix is a second rank tensor as it defines the relation between one vector and another, as in equation (2.2). The stiffness, compliance and permittivity tensors are the material properties of practical interest for the analysis of substrates in this study.

From the above discussion, it is abundantly clear that carrying out tensor transformations in the full subscript notation for stiffness and compliance is inconvenient and can be quite laborious. This difficulty can be avoided by using *abbreviated subscript* notation which is always possible when the stress components are symmetric ($T_{ij} = T_{ji}$). If this condition is satisfied, then terms like $c_{xyxy}S_{xy}$ and $c_{yxxy}S_{xy}$ are equal. Furthermore, since $S_{ij} = S_{ji}$ there is no way to distinguish experimentally between terms like $c_{xyxy}S_{xy}$ and $c_{xyyx}S_{yx}$. Therefore, no purpose is served in distinguishing c_{ijkl} from c_{ijlk}. Similar arguments reveal that $s_{ijkl} = s_{jikl}$ and $s_{ijkl} = s_{ijlk}$. With these constraints on the stiffness and compliance constants, the four subscripts may be reduced to two by using an abbreviated subscript notation where [17, p.65]

I	ij
1	xx
2	yy
3	zz
4	yz, zy
5	xz, zx
6	xy, yx

Then, capitallized indices will refer to the abbreviated notation while lower case letters will refer to the full subscript form. Relationships between the stiffness with full subscripts and those with abbreviated subscripts can be established by considering individual terms in equation (2.8). For example,

$$T_{xx} = c_{xxyy} S_{yy} \tag{2.14}$$

is replaced in abbreviated subscript notation by

$$T_1 = c_{12} S_2 \tag{2.15}$$

The general relationship is therefore,

$$c_{IJ} = c_{ijkl} \tag{2.16}$$

Similarly, it can be found that [17, p.66]

$$s_{IJ} = s_{ijkl} \times \begin{cases} 1 \text{ for } I \text{ and } J = 1,\ 2,\ 3 \\ 2 \text{ for } I \text{ and } J = 4,\ 5,\ 6 \\ 4 \text{ for } I \text{ and } J = 4,\ 5,\ 6 \end{cases} \tag{2.17}$$

where the multiplying factors (1, 2, 4) arise from the definition of strain in abbreviated notation [17, p.27]. Clearly then, abbreviated subscripts provide for economy of space and simple algebraic manipulation.

As discussed, the physical properties of crystals are conveniently expressed as tensors. Actual values for the elements comprising these material tensors are normally given with respect to the crystallographic axes. In this case, the tensors are commonly referred to as the standard material constants. However, the crystallographic axes may not always be the convenient choice of axes for analyzing specific problems, and it is therefore necessary to consider how these standard crystal constants may be transformed into other coordinate systems. Transformation of the standard material tensors is examined in the next section.

2.5 TENSOR TRANSFORMATIONS

The physical properties of crystalline materials are normally given in tensor notation with respect to the crystallographic axes. In this study particularly, various different crystal orientations are examined, so it is necessary to transform the standard crystal tensors to appropriate values reflecting the particular cut of crystal under investigation.

The preceding description clearly demonstrates the economy of space and the ease of algebraic manipulation provided by *abbreviated* subscript notation. As such, it is of considerable importance to have a method of performing coordinate transformations directly in this notation without the additional effort of converting to full subscripts, applying the transformation, and then reconverting to the abbreviated notation. A very efficient matrix technique has been developed specifically for this purpose by W. L. Bond [20]. In essence, the technique involves the construction of 6 x 6 transformation matrices that may be used to transform the standard material tensors by means of a single matrix multiplication.

To obtain the transformation matrices, consider the stress field **T**. In full subscript notation this transforms according to

$$T'_{ij} = a_{ik} a_{jl} T_{kl}$$

$$i, j, k, l = x, y, z \qquad (2.18)$$

where the a_{ij} are elements of the standard coordinate rotation matrices [19, p.109]. To convert to abbreviated subscripts, each stress component must be examined individually. For example, from equation (2.18), the transformed stress T'_{xx} is

$$T'_{xx} = a_{xx}^2 T_{xx} + a_{xy}^2 T_{yy} + a_{xz}^2 T_{zz} + 2a_{xy}a_{xz}T_{yz} + 2a_{xx}a_{xz}T_{xz} + 2a_{xx}a_{xy}T_{xy} \tag{2.19}$$

Converting to abbreviated subscript notation and repeating the same procedure for each component of $\boldsymbol{T'}$ yields the matrix transformation law

$$T'_H = M_{HI}T_I \tag{2.20}$$

$$H, I = 1, 2, 3, 4, 5, 6$$

where the coefficients M_{HI} define the following 6 x 6 transformation matrix [17, p.74]

$$[M] = \begin{bmatrix} a_{xx}^2 & a_{xy}^2 & a_{xz}^2 & 2a_{xy}a_{xz} & 2a_{xz}a_{xx} & 2a_{xx}a_{xy} \\ a_{yx}^2 & a_{yy}^2 & a_{yz}^2 & 2a_{yy}a_{yz} & 2a_{yz}a_{yx} & 2a_{yx}a_{yy} \\ a_{zx}^2 & a_{zy}^2 & a_{zz}^2 & 2a_{zy}a_{zz} & 2a_{zz}a_{zx} & 2a_{zx}a_{zy} \\ a_{yx}a_{zx} & a_{yy}a_{zy} & a_{yz}a_{zz} & a_{yy}a_{zz} + a_{yz}a_{zy} & a_{yx}a_{zz} + a_{yz}a_{zx} & a_{yy}a_{zx} + a_{yx}a_{zy} \\ a_{zx}a_{xx} & a_{zy}a_{xy} & a_{zz}a_{xz} & a_{xy}a_{zz} + a_{xz}a_{zy} & a_{xz}a_{zx} + a_{xx}a_{zz} & a_{xx}a_{zy} + a_{xy}a_{zx} \\ a_{xx}a_{yx} & a_{xy}a_{yy} & a_{xz}a_{yz} & a_{xy}a_{yz} + a_{xz}a_{yy} & a_{xz}a_{yx} + a_{xx}a_{yz} & a_{xx}a_{yy} + a_{xy}a_{yx} \end{bmatrix} \tag{2.21}$$

The above matrix is referred to as the *Bond stress transformation* matrix. Similarly, following the same line of argument, the matrix transformation law for strain is

$$S'_K = N_{KJ} S_J \tag{2.22}$$

$$K, J = 1, 2, 3, 4, 5, 6$$

where [17, p.75]

$$[N] = \begin{bmatrix} a_{xx}^2 & a_{xy}^2 & a_{xz}^2 & a_{xy}a_{xz} & a_{xz}a_{xx} & a_{xx}a_{xy} \\ a_{yx}^2 & a_{yy}^2 & a_{yz}^2 & a_{yy}a_{yz} & a_{yz}a_{yx} & a_{yx}a_{yy} \\ a_{zx}^2 & a_{zy}^2 & a_{zz}^2 & a_{zy}a_{zz} & a_{zz}a_{zx} & a_{zx}a_{zy} \\ 2a_{yx}a_{zx} & 2a_{yy}a_{zy} & 2a_{yz}a_{zz} & a_{yy}a_{zz}+a_{yz}a_{zy} & a_{yx}a_{zz}+a_{yz}a_{zx} & a_{yy}a_{zx}+a_{yx}a_{zy} \\ 2a_{zx}a_{xx} & 2a_{zy}a_{xy} & 2a_{zz}a_{xz} & a_{xy}a_{zz}+a_{xz}a_{zy} & a_{xz}a_{zx}+a_{xx}a_{zz} & a_{xx}a_{zy}+a_{xy}a_{zx} \\ 2a_{xx}a_{yx} & 2a_{xy}a_{yy} & 2a_{xz}a_{yz} & a_{xy}a_{yz}+a_{xz}a_{yy} & a_{xz}a_{yx}+a_{xx}a_{yz} & a_{xx}a_{yy}+a_{xy}a_{yx} \end{bmatrix} \tag{2.23}$$

It is apparent that the *Bond strain transformation* matrix , [N], will be the same as [M], except for a shift of the factor 2 from the upper right-hand corner of the matrix, to the lower left-hand corner.

Application of the Bond stress transformation matrix to equation (2.8) yields

$$[T'] = [M]\,[c]\,[S] \tag{2.24}$$

where, for convenience, the matrix form is now invoked to replacing the cumbersome summation notation. The inverse of equation (2.22) is

$$[S] = [N]^{-1}[S'] \tag{2.25}$$

and substituting this for [S] in equation (2.24) yields

$$[T'] = [M]\,[c]\,[N]^{-1}[S'] \tag{2.26}$$

Comparison with equation (2.8) reveals that the transformed stiffness matrix is simply

$$[c'] = [M]\cdot[c]\cdot[N]^{-1} \tag{2.27}$$

In a similar manner, the transformation law for the compliance matrix can be derived and is [17, p.76]

$$[s'] = [N]\cdot[s]\cdot[M]^{-1} \tag{2.28}$$

From equations (2.27) and (2.28), it is apparent that the stiffness and compliance transformation laws require the inversion of 6 x 6 matrices, [N] and [M], the prospect of which seems to be no easy task. This may lead one to question the usefulness of Bond's

transformation method. However, a bit of thought reveals that these matrix inversions are unnecessary. Since the inverse of the coordinate rotation matrix [a] is simply its transpose, [a]′, the matrix $[N]^{-1}$ corresponding to $[a]^{-1} = [a]'$ is obtained simply by transposing all the subscripts in equation (2.23). Comparison with equation (2.21) shows that the result is simply [M]′. That is,

$$[N]^{-1} = [M]' \tag{2.29}$$

Making this substitution into equation (2.26) yields the easily applied stiffness transformation law

$$[c'] = [M] \cdot [c] \cdot [M]' \tag{2.30}$$

In a completely parallel way, the compliance transformation law is simplified to

$$[s'] = [N] \cdot [s] \cdot [N]' \tag{2.31}$$

Finally, since the permittivity matrix is a second rank tensor that relates the electric displacement vector to **D** to the electric field vector **E**, it must transform in the same way as strain and stress. In matrix notation, this is

$$[\varepsilon'] = [a] \cdot [\varepsilon] \cdot [a]' \tag{2.32}$$

The calculation of the slowness and effective permittivity functions for various crystal substrates requires the use of the material tensors which must be transformed to the appropriate reference frame dictated by the cut of the crystal. The great advantage of the *Bond method* for transforming material constants is that it can be applied directly to the standard material tensors as they appear in published tables of crystal properties. It also involves shorter and less complicated algebra, and provides a more effective book-keeping system and guard against error. All coordinate transformations in this study are carried out using the Bond transformation method outlined above.

All surface wave devices employ a piezoelectric substrate on which a metal film is deposited. For piezoelectric crystals, two additional material constants are needed in addition to the ones already presented to appropriately characterize the substrate. These constants, along with their respective transformation laws are the subject of the following section.

2.6 PIEZOELECTRIC CRYSTALS

In some cases, Hooke's Law does not fully describe the response of a solid to acoustic strain. Certain materials become electrically polarized when they are strained. This phenomenon, known as piezoelectricity, occurs in many materials and couples elastic

stresses and strains to electric fields and displacements. Because of the coupling between electric and acoustic fields in piezoelectric solids, measurements of the electrical properties depend upon the mechanical constraints imposed on the medium, and vice versa. As a result, the elastic constitutive equations must be modified to take adequately reflect this coupling phenomenon.

In a homogenous *piezoelectric* insulator, the stress components T_{ij} at each point are dependent on the electric field **E** (or, equivalently, the electric displacement **D**) in addition to the strain components S_{ij}. Assuming all these quantities are appropriately small, the relationship can be taken to be linear and T_{ij} is, therefore, given by the relation [6, p.17]

$$T_{ij} = \sum_k \sum_l c^E_{ijkl} S_{kl} - \sum_k e_{kij} E_k \tag{2.33}$$

The superscript on c^E_{ijkl} identifies this as a tensor that relates changes of T_{ij} to changes of S_{kl} if the electric field, **E** , is held constant. That is, it denotes the stiffness tensor for constant electric field. Similarly, the electric displacement is usually determined by the field **E** and the permittivity tensor so that [6, p.17]

$$D_i = \sum_j \varepsilon^S_{ij} E_j + \sum_j \sum_k e_{ijk} S_{jk} \tag{2.34}$$

where ε^{S}_{ij} denotes the permittivity tensor for constant strain. The forms of these equations can be justified from thermodynamic considerations, the details of which are not important here. Equations (2.33) and (2.34) are referred to as the *piezoelectric constitutive relations*. The tensor, e_{ijk} , relating elastic to electric fields, is called the piezoelectric stress tensor.

Alternatively, **D** can be related to the stress instead of strain, and this can be achieved by eliminating S_{ij} from equations (2.33) and (2.34). The result is

$$D_i = \sum_j \varepsilon^{T}_{ij} E_j + \sum_j \sum_k d_{ijk} T_{jk} \tag{2.35}$$

where the new tensors, ε^{T}_{ij} and d_{ijk} , are related in a rather complicated manner to the tensors in equations (2.33) and (2.34). The tensor ε^{T}_{ij} is the permittivity tensor for constant stress and d_{ijk} is defined as the piezoelectric strain tensor. **E** can also be eliminated to obtain an equation giving T_{ij} in terms of S_{kl} and **D**; the coefficients of S_{kl} then give a stiffness tensor for constant electric displacement. Therefore, the following relation is also valid :

$$S_{ij} = \sum_k \sum_l s^{E}_{ijkl} T_{kl} + \sum_k d_{kij} E_k \tag{2.36}$$

The piezoelectric stress and strain constants define third rank tensors. From the symmetry of T_{ij}, the tensors themselves have the symmetry

$$e_{ijk} = e_{ikj} \quad \text{and} \quad d_{ijk} = d_{ikj} \tag{2.37}$$

The symmetry arguments for the stress and strain imply that abbreviated subscript notation can be introduced once again [17, p.271]. The piezoelectric constitutive relations then take the form

$$D_i = \varepsilon_{ij}^T E_j + d_{iJ} T_j \tag{2.38}$$

$$T_I = c_{IJ}^E S_J - e_{Ik} E_k \tag{2.39}$$

where the matrices d_{iJ} and e_{iJ} now define 3x6 matrices [16, p.116].

Transformation laws for the piezoelectric strain and stress constants can be derived by the Bond method considered in the previous section for the compliance and stiffness constants. In any case, the simplified transformation properties can be written in matrix form as [17, p.273]

$$[d'] = [a] \cdot [d] \cdot [M]^{-1} = [a] \cdot [d] \cdot [N]' \tag{2.40}$$

$$[e'] = [a] \cdot [e] \cdot [N]^{-1} = [a] \cdot [e] \cdot [M]' \tag{2.41}$$

The discussion on the physical properties of crystals and their tensor representations given in this chapter provides a strong foundation from which all further surface wave analysis can be undertaken. An overview of wave propagation in bulk material is presented in the following chapter and this will provide an introduction to the mathematics involved in all substrate modelling.

CHAPTER 3

WAVE PROPAGATION IN BULK MATERIAL

3.1 INTRODUCTION

In a solid, an acoustic wave is a form of disturbance involving deformations of the material. Deformation occurs when the motions of individual atoms are such that the distances between them change, and this is accompanied by internal restoring forces which tend to return the material to its equilibrium state. If the deformation is time-variant, the motion of each atom is determined by these restoring forces and by inertial effects. This can give rise to propagating wave motion with each atom oscillating about its equilibrium position. In most materials, the restoring forces are proportional to the amount of deformation, provided the latter is small, and this can be assumed for most practical purposes. The material is then described as elastic, and the propagating waves are often referred to as elastic or acoustic waves. In an ideal elastic solid, acoustic waves propagate with no attenuation [21, p.23].

The simplest types of waves are the plane waves that can propagate in an infinite homogenous medium. The deformation is harmonic in space and time, and all the atoms on a particular plane, normal to the propagation direction, have the same motion. There

are two types of plane waves: longitudinal waves, in which atoms vibrate in the propagation direction, and shear waves, in which the atoms vibrate in the plane normal to the propagation direction. These are directly analogous to the longitudinal and transverse waves that can propagate on an elastic string. The waves are non-dispersive at the frequencies of interest here, with velocities usually between 1000 and 10 000 m/s.

This chapter provides an overview of wave propagation in isotropic solids, anisotropic solids and finally, in piezoelectric solids. Emphasis is placed on the latter since SAW devices primarily consist of metal electrodes deposited on piezoelectric substrates, which are necessarily anisotropic. For these cases, wave properties can usually only be found by employing numerical techniques due to the complexity of the elasticity equations. In contrast, wave solutions for isotropic materials are more readily obtainable, and since they have many features in common with the solutions for anisotropic materials, it will be instructional to begin by considering wave propagation for this case.

3.2 EQUATION OF MOTION

In addition to the elasticity equations described in the previous chapter, wave motion will be subject to Newton's laws if the stress and strain are functions of time as well as position. These constraints can be combined in the form of an *equation of motion.* Consider, for example, an elementary cube within the material with edges parallel to the x_1 , x_2 and x_3 axes and of length δ as shown in Figure 3.1.

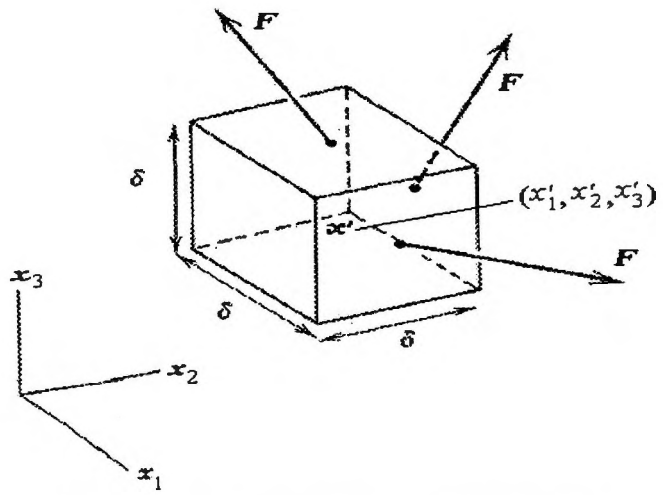

Figure 3.1 : **Forces on an elementary cube within a solid**

The cube is centered at $\mathbf{x}' = (x_1', x_2', x_3')$. Forces are exerted on all six faces by the material surrounding the cube. For the faces at $x_1 = x_1' \pm \delta/2$, the components of force in the x_i direction are $\pm \delta^2 T_{i1}(x_1' \pm \delta/2, x_2', x_3')$. The forces on the faces normal to x_2 and x_3 can be obtained in the same manner. Summing all these forces yields the total force on the cube. Assuming that δ is small, the total force will have an x_i component

$$\delta^3 \left[\sum_j \frac{\partial T_{ij}}{\partial x_j} \right]_{\mathbf{x}'} \tag{3.1}$$

This must be equal to the mass $\rho\delta^3$ multiplied by the acceleration $\partial^2 u_i(\mathbf{x}')/\partial t^2$, where ρ is the density. This equality must hold for all points $\mathbf{x}'$, so that

$$\rho \frac{\partial^2 u_i}{\partial t^2} = \sum \frac{\partial T_{ij}}{\partial x_j}, \qquad i.j = 1, 2, 3 \tag{3.2}$$

which is defined as the equation of motion.

3.3 WAVE PROPAGATION IN ISOTROPIC SOLIDS

In an isotropic material, the stiffness tensor c_{ijkl} has only two independent components which are known as the Lame constants and can be denoted by λ and μ. From symmetry considerations, it can be shown [22] that the stiffness can be written as

$$c_{ijkl} = \lambda \delta_{ij} \delta_{kl} + \mu \left(\delta_{ik} \delta_{jl} + \delta_{il} \delta_{jk} \right) \tag{3.3}$$

where $\delta_{ij} = 1$ for $i=j$ and $\delta_{ij} = 0$ for $i \neq j$. Substituting into equation (2.8), the stress can be written as

$$T_{ij} = \lambda \delta_{ij} \Delta + 2\mu S_{ij} \tag{3.4}$$

where $$\Delta = \sum_i S_{ii} = \sum_i \frac{\partial u_i}{\partial x_i} \tag{3.5}$$

Upon substituting equation (3.3) , the equation of motion is modified to become

$$\rho \frac{\partial^2 u_j}{\partial t^2} = (\lambda + \mu) \frac{\partial \Delta}{\partial x_j} + \mu \nabla^2 u_j \tag{3.6}$$

where $$\nabla^2 = \sum \frac{\partial^2}{\partial x_i^{\,2}} \tag{3.7}$$

For an infinite medium supporting plane waves, with frequency ω, the displacement **u** takes the general form

$$\mathbf{u} = \mathbf{u}_o \exp[j(\omega t - \mathbf{k} \cdot \mathbf{x})] \tag{3.8}$$

where $\mathbf{u}_o$ is a constant vector, independent of **x** and t. Note that the actual displacement is the real part of equation (3.8). The direction of propagation is given by the wave vector $\mathbf{k} = (k_1, k_2, k_3)$, The wavefronts are perpendicular to **k** and are solutions of $\mathbf{k} \cdot \mathbf{x}$ = constant. The phase velocity of the wave is defined as $V = \omega / |\mathbf{k}|$. If **u** takes the form of equation (3.8), this implies that

$$\frac{\partial \mathbf{u}}{\partial x_j} = -jk_j \mathbf{u} \tag{3.9}$$

Substituting into equation (3.6) yields

$$\omega^2 \rho u_j = (\lambda + \mu)(\mathbf{k} \cdot \mathbf{u}) k_j + \mu |\mathbf{k}|^2 u_j, \quad j = 1, 2, 3 \tag{3.10}$$

where

$$|\mathbf{k}|^2 = k_1^2 + k_2^2 + k_3^2 \tag{3.11}$$

Then, using equation (3.8) for u_j yields the following expression in vector form

$$\omega^2 \rho \mathbf{u}_0 = (\lambda + \mu)(\mathbf{k} \cdot \mathbf{u}_0)\mathbf{k} + \mu |\mathbf{k}|^2 \mathbf{u}_0 \tag{3.12}$$

Inspection of equation (3.10) reveals that there is one term parallel to **k** (which includes the scalar product $\mathbf{k} \cdot \mathbf{u}_0$.) and two terms parallel to $\mathbf{u}_0$. It is obvious, then, that two cases must be considered. In the first, if $\mathbf{u}_0$ is not perpendicular to **k** the product $\mathbf{k} \cdot \mathbf{u}_0$ is non-zero. This implies that for non-trivial solutions $\mathbf{u}_0$ must be parallel to **k**. Secondly, if $\mathbf{u}_0$ is perpendicular to **k** the scalar product is zero, and the remaining terms in the equation are parallel. These two cases give longitudinal wave solutions and shear wave solutions, respectively.

For shear or transverse waves, $\mathbf{u}_0$ is perpendicular to **k** and the wave vector, $\mathbf{k}_t$, can be found from equation (3.10) yielding

$$|\mathbf{k}_t|^2 = \frac{\omega^2 \rho}{\mu} \tag{3.13}$$

The phase velocity for shear waves, V_t , is then equal to $\omega / |\mathbf{k}_t|$ so that

$$V_t = \sqrt{\mu / \rho} \tag{3.14}$$

taking V_t to be positive. The fact that this is independent of frequency means the wave is non-dispersive.

For longitudinal waves, solutions to equation (3.10) with $\mathbf{u}_0$ parallel to $\mathbf{k}$ must be considered. In this case, $\mathbf{k}$ is given by

$$\mathbf{k} = \pm \mathbf{u}_0 \frac{|\mathbf{k}|}{|\mathbf{u}_0|} \tag{3.15}$$

from which we find

$$(\mathbf{k} \cdot \mathbf{u}_0)\mathbf{k} = \mathbf{u}_0 |\mathbf{k}|^2 \tag{3.16}$$

For longitudinal waves, the wave vector is denoted by $\mathbf{k}_l$ and is obtained by substituting equation (3.16) into equation (3.10). Therefore,

$$|\mathbf{k}_t|^2 = \frac{\omega^2 \rho}{(\lambda + 2\mu)} \tag{3.17}$$

The phase velocity for longitudinal waves, V_l , is then given by $\omega / |\mathbf{k}_l|$ or

$$V_l = \sqrt{\frac{\lambda + 2\mu}{\rho}} \tag{3.18}$$

As shown, this wave is also nondispersive. Comparing equations (3.14) and (3.18) reveals that the velocity of longitudinal waves will always be greater than the velocity of shear waves since λ and μ are always positive. The velocities are typically in the region of 6000 m/s for longitudinal waves and 3000 m/s for shear waves.

3.4 WAVE PROPAGATION IN ANISOTROPIC SOLIDS

For isotropic materials, there were two solutions, the shear wave and the longitudinal wave, with $\mathbf{u}_0$ respectively perpendicular and parallel to $\mathbf{k}$. Solutions for anisotropic materials are obtained in the same manner by again forming an equation of motion with solutions of the form

$$\mathbf{u} = \mathbf{u}_o \exp[j(\omega t - \mathbf{k} \cdot \mathbf{x})] \tag{3.19}$$

In this case, three solutions representing non-dispersive acoustic waves are obtained. Usually, one solution has the displacement $\mathbf{u}_0$ almost parallel to $\mathbf{k}$, and is called the *quasi-*

longitudinal wave. The other two solutions with different velocities usually have $\mathbf{u}_0$ almost perpendicular to **k**, and are called *quasi-shear* waves. For certain propagation directions, the longitudinal wave can have $\mathbf{u}_0$ parallel to **k**, in which case it is then called a pure longitudinal wave. Shear waves that are perpendicular to **k** are called pure shear waves. Owing to anisotropy, each of the three waves will have a phase velocity dependent on the propagation direction.

Piezoelectricity is the phenomenon which, in many materials, couples elastic stresses and strains to electric fields and displacements. It occurs only in anisotropic materials whose internal structure lacks a centre of symmetry. It occurs in many crystal classes but is often weak, thus having little effect on the elastic behaviour. However, SAW device technology is concerned with devices that make crucial use of piezoelectricity, so it is necessary to take account of the effect in the analysis. In the following discussion of wave propagation in piezoelectric solids, only insulating materials will be considered.

3.5 WAVE PROPAGATION IN PIEZOELECTRIC SOLIDS

In one way or another, piezoelectric crystals provide the physical basis for almost all practical applications of acoustic fields. This is because they provide ~~and~~ an effective means for electrically generating and detecting acoustic vibrations. This section is concerned with acoustic wave propagation in piezoelectric materials, which must of course be anisotropic. Because of the complexity of the equations for this case, the

solutions can usually only be found using numerical techniques. Subsequently, the account here is mainly descriptive for the sake of simplicity. A more formal mathematical treatment is given in the next chapter.

The mechanical equation of motion given by equation (3.2) is valid for a piezoelectric material. It is convenient, however, to express this in terms of the displacements u_i and the electric potential, Φ. Since elastic disturbances travel much more slowly than electromagnetic ones, the *quasi-static* approximation [6, pp.67-70] can be invoked. That is, the electric field is given by the gradient of the potential, so that

$$E_i = -\frac{\partial \Phi}{\partial x_i} \tag{3.20}$$

Substituting this relation into equation (2.33), and using equation (2.6) for stress, the equation of motion is modified to yield

$$\rho \frac{\partial^2 u_i}{\partial t^2} = \sum_j \sum_k \left[e_{kij} \frac{\partial^2 \Phi}{\partial x_j \partial x_k} + \sum c^E_{ijkl} \frac{\partial^2 u_k}{\partial x_j x_l} \right] \tag{3.21}$$

In addition, since the material is assumed to be an insulator, there are no free charges. Therefore, div $\mathbf{D} = 0$. Applying this to equation (2.34) gives

$$\sum_i \sum_j \left[\varepsilon_{ij}^s \frac{\partial^2 \Phi}{\partial x_i x_j} - \sum_k e_{ijk} \frac{\partial^2 u_j}{\partial x_i x_k} \right] = 0 \tag{3.22}$$

Four equations relating the four quantities u_i and Φ can be derived from equations (3.21) and (3.22), and if appropriate boundary conditions are specified, the wave motion can be determined.

In all practical cases of interest, the wave propagates on a half-space of some material. The boundary conditions introduced can substantially alter the characteristics of the waves. The solution of primary interest in this study is the surface acoustic wave (SAW), whose existence was first shown by Lord Rayleigh in the 19th century. This type of wave can exist in a homogenous material with a plane surface. It is guided along the surface, with its amplitude decaying exponentially with depth. The wave is strongly confined, with typically 90% of the energy propagating within one wavelength of the surface. It is non-dispersive, with a velocity of typically 3000 m/s. In general, the surface wave velocity is less than the velocities of plane waves propagating in an infinite material. Of the three plane wave solutions, the slow shear wave has the lowest velocity, so the surface wave velocity must be less than this. In practice, the surface wave velocity is usually quite close to the slow shear velocity.

For some particular orientations the piezoelectric Rayleigh wave can have its displacement confined to the sagittal plane. This occurs if the sagittal plane is a plane of mirror symmetry for the crystal [16, p.278]. The wave is then called a pure mode, and

the propagation direction is called a pure mode direction. For a given surface orientation, the wave velocity is symmetrical with respect to a pure mode direction.

A bounded medium also supports many other types of acoustic waves, and the boundary conditions can substantially affect the nature of the waves. For example, in a plate with two plane parallel boundaries, a series of dispersive modes with different velocities can propagate. On the other hand, a medium with dimensions much larger than the wavelength can support waves with characteristics similar to those of waves in an infinite medium. The term bulk waves is often used to describe waves which are not bound to a surface.

CHAPTER 4

WAVE PROPAGATION IN THE PRESENCE OF BOUNDARIES

4.1 INTRODUCTION

This thesis is primarily concerned with the propagation of acoustic Rayleigh waves in *piezoelectric* media which must, of course, be *anisotropic*. In the previous chapter, wave propagation in bulk material was considered with reference to isotropic, anisotropic and piezoelectric solids. For isotropic materials, we saw that there were two wave solutions, namely the *shear* wave and the *longitudinal* wave. For the shear wave, $\mathbf{u}_0$ is perpendicular to the wave vector $\mathbf{k}$ whereas for the longitudinal wave, it is parallel to $\mathbf{k}$. For piezoelectric materials, which are of primary interest in this study and in the fabrication of practical SAW devices, there are two shear wave solutions in addition to the longitudinal wave i.e. there are three plane wave solutions in total. This chapter extends the development in the previous chapter for wave propagation in piezoelectric solids to include the case for piezoelectric Rayleigh wave propagation in the presence of boundaries, a necessary condition for all SAW analysis . The analysis will culminate in the definition of an effective permittivity function for a piezoelectric half-space, a concise formulation of which is given in the next chapter.

4.2 GENERAL WAVE EQUATIONS FOR A PIEZOELECTRIC HALF-SPACE

The potential and charge density at the surface of a non-piezoelectric half-space are related by a parameter known as the *effective permittivity* [6, pp.39-42]. However, the case of most interest for SAW device modelling is that of a piezoelectric half-space and, as such, a rigorous treatment for this case is imperative. The method of analysis invoked in this study was first proposed by Ingebrigtsen [23] and developed later by Greebe *et al.* [24] and by Milsom *et al.* [25,26]. Perturbation theory [27] and normal mode theory [28] are other approaches which give essentially the same results as the effective permittivity approach. However, they are not considered in this study.

For a piezoelectric material, the equation of motion takes on the same form as equations (3.14) given in the previous chapter, in terms of the displacement **u** and the potential Φ. Again, we shall consider plane wave solutions with frequency ω and wave vector **k**. As in Chapter 3, it is assumed that the potential and acoustic displacements are proportional to $\exp(j\omega t)$, with frequency ω positive. The displacement and potential then take on the familiar form

$$\mathbf{u} = \mathbf{u}_0 \exp\left[j(\omega t - \mathbf{k} \cdot \mathbf{x}) \right] \tag{4.1}$$

$$\Phi = \Phi_0 \exp\left[j(\omega t - \mathbf{k} \cdot \mathbf{x}) \right] \tag{4.2}$$

where $\mathbf{u}_0$ and Φ_0 are constants, independent of $\mathbf{x}$ and t, and $\mathbf{k}$ is real. Initially, we consider a harmonic solution with variables proportional to $\exp(j\beta x_1)$, with β real. Fourier synthesis will then be used later to generalize the solution. The procedure here is very similar to that described for calculating the bulk-wave velocities as discussed previously. However, the electric boundary conditions at the surface will not be specified initially. This enables a solution for any value of β to be obtained. Note that wave motion propagating in the $-x_1$ direction is denoted by positive values of β. This is done for convenience when using Fourier synthesis.

To begin the analysis, we assume a *piezoelectric half-space* as depicted in Figure 4.1 below:

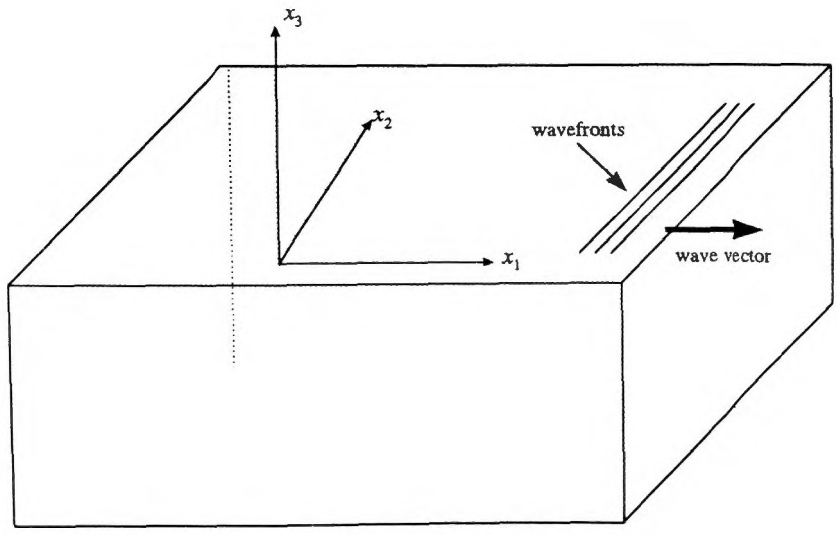

Figure 4.1: Axes for surface wave analysis

From the discussion in the previous chapter, an applied electrical force on a piezoelectric solid will result in an appropriate mechanical response in the form of acoustic vibrations and vice versa. Acoustic waves in a typical material are some five orders of magnitude slower than electromagnetic waves and, as such, the piezoelectrically coupled electric field can be assumed to be quasistatic. In light of this, Maxwell's equations reduce to [25]

$$D_{i,i} = \rho_S \tag{4.3}$$

and

$$E_i = -\phi_{,i} \tag{4.4}$$

where D, E, ϕ and ρ_S are electric flux density, field, electrostatic potential and free charge density. The comma here denotes differentiation in the usual tensor notation [29].

The above equations must be satisfied for the piezoelectric solid which occupies the half-space ($x_3 < 0$) and for the free space region ($x_3 > 0$). In addition, the free charge density, ρ_S, can be taken as zero since the solid is assumed to be a perfect insulator. Equation (4.3) reduces to Laplace's equation in the free space region. That is,

$$\phi_{,ii} = 0 \tag{4.5}$$

Newton's stress equation of motion, equation (3.21), must also be satisfied by the elastic field quantities discussed previously. In the absence of internal body forces, this becomes

$$T_{ij,j} - \rho \ddot{u}_i = 0 \tag{4.6}$$

where T is stress, u is elastic displacement and ρ is the density. In the discussion of tensors in Chapter 2, we saw that strain, S, was defined by

$$S_{ij} = \frac{1}{2}\left(u_{i,j} + u_{j,i}\right) \tag{4.7}$$

The above equations are coupled through the piezoelectric equations of state (constitutive relations) given in chapter 3. For convenience, these are listed again below:

$$T_{ij} = c^E_{ijkl} s_{kl} - e_{kij} E_k \tag{4.8}$$

$$D_i = e_{ikl} s_{kl} + \varepsilon^s_{ik} E_k \tag{4.9}$$

where c^E, e and ε^S are, respectively , the elastic, piezoelectric and permittivity tensors of the solid. As before, the superscripts E and S simply imply that the constants describe elastic and dielectric properties measured under conditions of constant electric field and stress, respectively.

A few assumptions will be made in obtaining a solution. Firstly, the electrodes are assumed to be *massless*, in order that mass loading effects be neglected. The electrodes

are also assumed to be *perfectly conducting* and of sufficient length in the x_2 direction to make all differentials with respect to x_2 negligible. In addition, the time dependence will be suppressed throughout the analysis, since all quantities will be assumed to vary as $\exp(j\omega t)$. Finally, the x_3 dependence of the field variables for the region $x_3 \leq 0$ is assumed to take the form of $\exp(j\alpha x_3)$, where α is a dimensionless decay coefficient.

With these criteria, partial wave solutions with displacements $\mathbf{u}'$ and potential Φ' take on the general form

$$\mathbf{u}' = \mathbf{u}_0' \exp(j\alpha x_3)\exp[j(\omega t + \beta x_1)] \tag{4.10}$$

$$\Phi' = \Phi_0' \exp(j\alpha x_3)\exp[j(\omega t + \beta x_1)] \tag{4.11}$$

where $\mathbf{u}_0'$ and Φ_0' are constants and α is the x_3 component of the wave vector which, by definition, has no x_2 component. These equations are required to satisfy the homogenous second-order differential equations of motion for an infinite medium, which are rewritten here in shorthand tensor notation [29] for ease of reference.

$$-\rho \ddot{u}_j + c^E_{ijkl} u_{k,li} + e_{kij}\phi_{,ki} = 0 \tag{4.12}$$

$$e_{ikl} u_{k,li} - \varepsilon^S_{ik}\phi_{,ki} = 0 \tag{4.13}$$

Note that the standard material tensors for a crystal are usually given with regards to the crystallographic frame of reference and, hence, must be rotated into the appropriate canonical frame of x_1 , x_2 , x_3 , defined by the cut of the crystal.

Substitution of the elastic quantities into the equations of motion, equations (4.12) and (4.13), yields four linear homogenous equations in the four variables $\mathbf{u}_0'$, Φ_0'. In simplified matrix form, the transformed equations become

$$\begin{bmatrix} \alpha^2 c_{55}^E - 2j\alpha c_{15}^E - c_{11}^E + \rho v^2 & \alpha^2 c_{45}^E - j\alpha(c_{14}^E + c_{56}^E) - c_{16}^E & \alpha^2 c_{35}^E - j\alpha(c_{13}^E + c_{55}^E) - c_{15}^E & \alpha^2 e_{35} - j\alpha(e_{15} + e_{31}) - e_{11} \\ \alpha^2 c_{45}^E - j\alpha(c_{14}^E + c_{56}^E) - c_{16}^E & \alpha^2 c_{44}^E - 2j\alpha c_{46}^E - c_{66}^E + \rho v^2 & \alpha^2 c_{34}^E - j\alpha(c_{36}^E + c_{45}^E) - c_{56}^E & \alpha^2 e_{34} - j\alpha(e_{14} + e_{36}) - e_{16} \\ \alpha^2 c_{35}^E - j\alpha(c_{13}^E + c_{55}^E) - c_{15}^E & \alpha^2 c_{34}^E - j\alpha(c_{36}^E + c_{45}^E) - c_{56}^E & \alpha^2 c_{33}^E - 2j\alpha c_{35}^E - c_{55}^E + \rho v^2 & \alpha^2 e_{33} - j\alpha(e_{13} + e_{35}) - e_{15} \\ \alpha^2 e_{35} - j\alpha(e_{15} + e_{31}) - e_{11} & \alpha^2 e_{34} - j\alpha(e_{14} + e_{36}) - e_{16} & \alpha^2 e_{33} - j\alpha(e_{13} + e_{35}) - e_{15} & -\alpha^2 \varepsilon_{33}^S + 2j\alpha \varepsilon_{13}^S \\ & & & \varepsilon_{11}^S \end{bmatrix} \begin{bmatrix} \bar{u}_1 \\ \bar{u}_2 \\ \bar{u}_3 \\ \bar{\phi} \end{bmatrix} = 0$$

(4.14)

where v $(= \omega / k)$ is the component of phase velocity in the x_1 direction corresponding to the wave number k and where the material constants c^E , e and ε^S have been reduced to the standard matrix notation of abbreviated subscripts.

For a non-trivial solution to exist, the determinant of the left-hand matrix must be set to zero [30]. Inspection of equation (4.14) reveals that the determinant of this matrix will be an eighth order polynomial in α. Then, each of the eight roots will represent an

elementary mode of the half-space. Furthermore, for each root, the equations also yield the relative values of $\mathbf{u}_0'$ and Φ_0'. However, since the solution will not in general be a surface wave solution, great care is needed in choosing acceptable roots. Four of the roots will not correspond to excitation at the surface and are, therefore, unacceptable. To ensure decay into the substrate for positive k (or v), those roots which are real or complex must have positive real parts while imaginary roots which represent nondecaying bulk modes must also be positive for propagation away from the surface. This is not always the case, however, because for an anisotropic material the power flow direction and the wave vector are not, in general, collinear with one another [17, p.135]. This second order effect is commonly referred to as beam steering. Note that the power flow direction may be found by examining the variation of phase velocity with propagation direction [6, p.47].

The four acceptable elementary solutions to equation (4.14) corresponding to the selected roots α_n, take on the general form

$$\bar{\mathbf{u}}_m^{(n)} = \bar{\mathbf{u}}_{0m} \exp(j\alpha_n x_3)\exp[j(\omega t + \beta x_1)] \tag{4.15}$$

$$\bar{\Phi}_m^{(n)} = \bar{\Phi}_{0m} \exp(j\,\alpha_n x_3)\exp[j(\omega t + \beta x_1)] \qquad \text{for } m, n = 1, 2, 3, 4 \tag{4.16}$$

where each solution has been normallized with respect to $\bar{\Phi}_m^{(n)}$ which has been rewritten as $\bar{\mathbf{u}}_4^{(n)}$ for convenience. A more general solution is given by a linear combination of the elementary solutions. That is

$$\bar{\mathbf{u}}_i = \sum_{n=1}^{4} A_n \bar{u}_i^{(n)} \exp(\alpha_n k x_3), \qquad i = 1, 2, 3, 4 \tag{4.17}$$

Then, the *total* solution in the half-space has displacements $\tilde{\mathbf{u}}$ and potential $\tilde{\Phi}$, where the tilde indicates that the solution is harmonic, with variables proportional to $\exp(j \beta x_1)$. The total solution is taken to be a linear combination of the partial waves, so that

$$\tilde{\mathbf{u}} = \sum_{m=1}^{4} A_m \bar{\mathbf{u}}_m \tag{4.18}$$

and

$$\tilde{\Phi} = \sum_{m=1}^{4} A_m \bar{\Phi}_m \tag{4.19}$$

4.3 MECHANICAL BOUNDARY CONDITION

The exclusion of mass loading effects implies that there must be no force on the free surface ($x_3 = 0$) of the solid. The homogenous mechanical boundary condition at the interface can be expressed as

$$T_{13} = T_{23} = T_{33} = 0, \qquad \text{at } x_3 = 0 \tag{4.20}$$

or in more compact form

$$N_3 T_{i3} = 0 , \quad \text{at } x_3 = 0 \tag{4.21}$$

where N_i is the unit surface normal and the stresses are defined by equations (2.33). This stress-free boundary condition is used to determine the relative values of the coefficients A_m in equations (4.17) and (4.18) above. The relative values of these constants can be found since there are three equations relating the four constants A_m. Subsequently, the relative values of the displacements $\tilde{\mathbf{u}}$ and potential $\tilde{\Phi}$ for the harmonic solution can then be obtained from equations (4.17) and (4.18) yielding a solution for any value of β.

4.4 ELECTRICAL BOUNDARY CONDITIONS

In addition to the mechanical boundary condition stated in the previous section, the solution for an interdigital array of electrodes on the surface of a piezoelectric solid must adhere to certain electrical boundary conditions. The normal component of electric displacement $\tilde{D}_3$ in the piezoelectric may be denoted by $\tilde{D}_3(0^-)$ at the surface while that above the surface may be denoted by $\tilde{D}_3(0^+)$. The electrical boundary conditions are as follows :

- The discontinuity in the normal component of flux is equal to the free charge density at the surface, $\sigma(x_1)$, which must be zero on free surfaces. Therefore,

$$\tilde{D}_3(0^+) - \tilde{D}_3(0^-) = \sigma \quad \text{(metallized surface at } x_3 = 0) \tag{4.22}$$

$$\tilde{D}_3(0^+) - \tilde{D}_3(0^-) = 0 \quad \text{(free surface at } x_3 = 0) \tag{4.23}$$

- At the free surface $x_3 = 0$, tangential electric field E_1 and hence potential ϕ, must be continuous. (Since all differentials with respect to x_2 are negligible, note that $E_2 = 0$.)
- Apart from time variation, potential ϕ must be constant over all electrodes that are connected.

It is obvious that the normal component of electric displacement $\tilde{\mathbf{D}}$, and the potential ϕ are the variables of primary interest in problems concerning electrical excitation at the surface of a piezoelectric. These variables must satisfy the boundary conditions cited above. The electric displacement can be calculated from the potential, acoustic displacements and material tensors by using equation (4.9). The acoustic displacements, of course, define the stress tensor [see equation (4.7)] and the potential is obtained from the solution described in section 4.2. The potential at the surface can be denoted as $\tilde{\phi}(x_1)$, so that

$$\tilde{\phi}(x_1) = \tilde{\Phi}(x_1,\ 0) \tag{4.24}$$

The electric field can then be obtained using equation (4.4). The determination of these two variables allows for the definition of the ratio $\tilde{D}_3(0^-)/\tilde{\phi}(x_1)$, which will, in general, be a function of β.

The potential $\tilde{\Phi}(x_1,\ x_3)$ must also satisfy Laplace's equation $\nabla^2\tilde{\Phi} = 0$ [25] in the free space region, $x_3 > 0$. Furthermore, the x_3 dependence of potential must be of the form $\exp(-|\beta|\ x_3)$ since $\tilde{\Phi}$ must vanish at $x_3 = \infty$. Together with the fact that the potential is also proportional to $\exp(j\ \beta\ x_1)$, the following general relation is valid for $x_3 > 0$.

$$\tilde{\Phi}(x_1,\ x_3) = \tilde{\phi}(x_1)\exp(-|\beta|\ x_3) \tag{4.25}$$

Ultimately, the goal is to derive an *effective surface permittivity function* for piezoelectric solids similar to that of Greebe *et al* [24]. Basically, the permittivity function relates the *Fourier transforms* [9] of charge density and potential at the surface $x_3 = 0$. However, the formulation given in this study will differ slightly from Greebe's definition in that contributions from both the internal and external field will now be included in the same function. For completeness, Fourier transforms and inverse transforms can be defined, respectively, as

$$\overline{\psi}(k,x_3)=\frac{1}{2\pi}\int_{-\infty}^{\infty}\psi(x_1,x_3)\exp(jkx_1)dx_1$$

$$\psi(x_1,x_3)=\int_{-\infty}^{\infty}\overline{\psi}(k,x_3)\exp(-jkx_1)dk \qquad (4.26)$$

where Ψ can be any of the field variables presented .

The permittivity function is significant in that it embodies an exact solution to equations (4.12) and (4.13) satisfying the stress-free boundary condition. For a particular crystal orientation the effective permittivity, ε_S , is a function only of the horizontal component of phase velocity v. Once it has been determined, the complete system of equations defining a particular transducer configuration reduces to the one-dimensional problem of satisfying the electrical boundary conditions. In addition, the function embraces all values of v including those for which bulk waves form part of the solution. A concise formulation of the effective permittivity function is treated in the following chapter.

CHAPTER 5

SLOWNESS AND EFFECTIVE PERMITTIVITY

5.1 INTRODUCTION

As described in chapter 1, surface acoustic wave devices consist of metal electrodes deposited on piezoelectric substrates. For the effective modelling of such devices, analysis of the substrate is critical in determining its suitability for the intended end use of the device. Two functions of great interest in substrate analysis are the ***slowness*** and the ***effective permittivity*** functions. These functions serve as the basis for the modelling of all SAW devices. Slowness is simply the inverse of phase velocity and is useful for depicting the three plane wave solutions travelling in a plane of propagation for the media in question. The form of the slowness curve will depend on the substrate material and the orientation of the surface normal. Similarly, the effective permittivity is a very robust tool for solving problems concerning a one-dimensional set of electrodes on the surface of a piezoelectric half-space. The evaluation of this function is crucial because, for a given substrate orientation, it effectively stores all the relevant mechanical information in a scalar electrical quantity. To begin then, a concise formulation of the slowness surface must be presented and this is the topic of the following section.

5.2 SLOWNESS OR INVERSE PHASE VELOCITY

Differentiating the wave equation given in chapter 3 with respect to time, and making appropriate substitutions allow it to be rewritten in matrix form with abbreviated subscripts as

$$\nabla_{iK}\, c_{KL}\, \nabla_{Lj}\, v_j = \rho \frac{\partial^2 v_i}{\partial t^2} - \frac{\partial}{\partial t} F_i \tag{5.1}$$

with v_j being the particle velocity variable. The matrix-differential operators ∇_{iK} and ∇_{Lj} have also been introduced and they are defined by

$$\nabla_{Lj} = \begin{bmatrix} \frac{\partial}{\partial x} & 0 & 0 \\ 0 & \frac{\partial}{\partial y} & 0 \\ 0 & 0 & \frac{\partial}{\partial z} \\ 0 & \frac{\partial}{\partial z} & \frac{\partial}{\partial y} \\ \frac{\partial}{\partial z} & 0 & \frac{\partial}{\partial x} \\ \frac{\partial}{\partial y} & \frac{\partial}{\partial x} & 0 \end{bmatrix} \quad \text{and} \quad \nabla_{iK} = \begin{bmatrix} \frac{\partial}{\partial x} & 0 & 0 & 0 & \frac{\partial}{\partial z} & \frac{\partial}{\partial y} \\ 0 & \frac{\partial}{\partial y} & 0 & \frac{\partial}{\partial z} & 0 & \frac{\partial}{\partial x} \\ 0 & 0 & \frac{\partial}{\partial z} & \frac{\partial}{\partial y} & \frac{\partial}{\partial x} & 0 \end{bmatrix}$$

(5.2)

A uniform plane wave propagating in a source-free region (**F** = 0) along the direction

$$\hat{\mathbf{l}} = l_x\,\hat{\mathbf{x}} + l_y\,\hat{\mathbf{y}} + l_z\,\hat{\mathbf{z}} \tag{5.3}$$

has fields proportional to $\exp[j(\omega t - k\,\hat{\mathbf{l}}\cdot\mathbf{r})]$. As such the matrix operators may be replaced by matrices $-j\,k_{iK}$ and $-jk_{Lj}$ where

$$-j\,k_{iK} = -j\,k\,l_{iK} = -jk\begin{bmatrix} l_x & 0 & 0 & 0 & l_z & l_y \\ 0 & l_y & 0 & l_z & 0 & l_x \\ 0 & 0 & l_z & l_y & l_x & 0 \end{bmatrix} \tag{5.4}$$

and

$$-j\,k_{Lj} = -j\,k\,l_{Lj} = -jk\begin{bmatrix} l_x & 0 & 0 \\ 0 & l_y & 0 \\ 0 & 0 & l_z \\ 0 & l_z & l_y \\ l_z & 0 & l_x \\ l_y & l_x & 0 \end{bmatrix} \tag{5.5}$$

For the determination of plane wave solutions, the wave equation given in equation (5.1) with **F** = 0 (absence of internal body forces), reduces to [17, p.165]

$$k^2(l_{iK}c_{KL}l_{Lj})\,v_j = k^2\Gamma_{ij}v_j = \rho\omega^2 v_i \tag{5.6}$$

This is called the *Christoffel equation* and the matrix, Γ_{ij} , is called the *Christoffel matrix.* This matrix is determined solely by the plane wave propagation direction and the stiffness constants of the medium. The formulation of the Christoffel equation applies to uniform plane waves in both isotropic and anisotropic media. However, the analysis for anisotropic media is of more significance since these are the materials used in the fabrication of all practical SAW devices.

In an anisotropic solid, the propagation characteristics of plane waves can be found by rewriting the Christoffel equation (5.6) in the form

$$\left[k^2\Gamma_{ij} - \rho\omega^2\delta_{ij}\right]\left[v_j\right] = 0 \tag{5.7}$$

By setting the characteristic determinant of equation (5.7) equal to zero, the following dispersion relation is obtained.

$$\Omega\left(\omega,\ k_x,\ k_y,\ k_z\right) = \left|k^2\Gamma_{ij}\left(l_x,\ l_y,\ l_z\right) - \rho\omega^2\delta_{ij}\right| = 0 \tag{5.8}$$

At fixed frequency, ω, equation (5.8) defines a surface in k-space that gives k as a function of its direction $\hat{\mathbf{l}}$. This is termed the *wave vector surface.* However, examination of equation (5.8) reveals that the first term is proportional to k^2 while the second term is proportional to ω^2. The dispersion relation can, therefore, always be expressed entirely in terms of the variable k/ω which has units of inverse of velocity and

is termed the *slowness*. In other words, the wave vector **k** will always be proportional to ω. As such, it is more convenient to consider the *slowness (or inverse velocity) surface*. This surface gives the inverse of the phase velocity $k/\omega = 1/V_p$ as a function of propagation direction and is independent of ω. It is preferred over the wave vector surface, because it does not scale with ω. A typical slowness curve and its relation to the wave vector is depicted in Figure 5.1 below. Note that for an isotropic material, k and v are independent of θ, resulting in a slowness curve that is circular in nature [17, p.385].

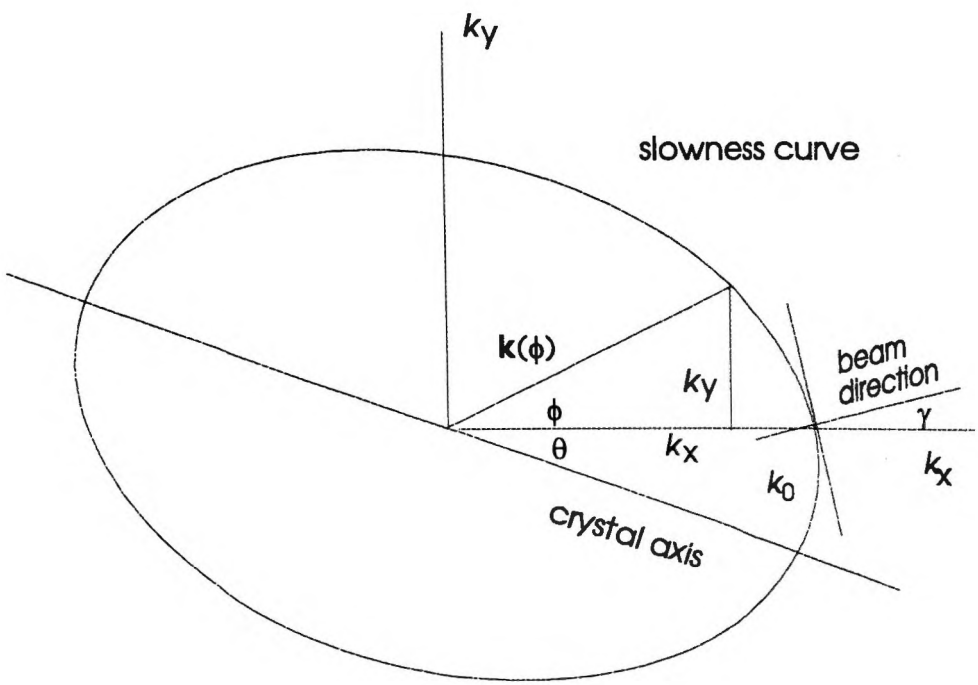

Figure 5.1 : Typical slowness curve and its relation to the wave vector.

However, the scope of this study is concerned with acoustic wave propagation in *piezoelectric* media. As such, a *stiffened Christofell equation* which takes piezoelectricity into account must be employed in the analysis. The stiffened equation takes the exact same form as equation (5.6) above, but with c_{KL} replaced by a *piezoelectrically stiffened* constant defined by the expression below [17, p.300].

$$c_{KL} \quad \rightarrow \quad \left\{ c^{E}_{KL} + \frac{\left[e_{Kj}\ l_j \right]\left[l_i\ e_{iL} \right]}{l_i\ \varepsilon^{S}_{ij}\ l_j} \right\} \tag{5.9}$$

In order to generalize the analysis for all possible cases, we assume anisotropic solids of the type represented by the classes 1 and $\bar{1}$ in the triclinic crystal system [16, p.280]. Since these crystals have no effective symmetries whatsoever, the compliance and stiffness matrices have the full complement of 21 elastic constants. In substituting the piezoelectrically stiffened constant into equation (5.6) and performing the matrix multiplications, the Christoffel equation appears in the form

$$k^2 \begin{bmatrix} -\sin^2\theta c^E_{55} - c^E_{11}\cos^2\theta & -\sin^2\theta c^E_{45} - c^E_{16}\cos^2\theta & -\sin^2\theta c^E_{35} - c^E_{15}\cos^2\theta & -\sin^2\theta e^E_{35} - e^E_{11}\cos^2\theta \\ -2c^E_{15}\sin\theta\cos\theta & -(c^E_{14}+c^E_{56})\sin\theta\cos\theta & -(c^E_{13}+c^E_{55})\sin\theta\cos\theta & -(e^E_{15}+e^E_{31})\sin\theta\cos\theta \\ -\sin^2\theta c^E_{45} - c^E_{16}\cos^2\theta & -\sin^2\theta c^E_{44} - c^E_{66}\cos^2\theta & -\sin^2\theta c^E_{34} - c^E_{56}\cos^2\theta & -\sin^2\theta e^E_{34} - e^E_{16}\cos^2\theta \\ -(c^E_{14}+c^E_{56})\sin\theta\cos\theta & -2c^E_{46}\sin\theta\cos\theta & -(c^E_{36}+c^E_{45})\sin\theta\cos\theta & -(e^E_{14}+e^E_{36})\sin\theta\cos\theta \\ -\sin^2\theta c^E_{35} - c^E_{15}\cos^2\theta & -\sin^2\theta c^E_{34} - c^E_{56}\cos^2\theta & -\sin^2\theta c^E_{33} - c^E_{55}\cos^2\theta & -\sin^2\theta e^E_{33} - e^E_{15}\cos^2\theta \\ -(c^E_{13}+c^E_{55})\sin\theta\cos\theta & -(c^E_{36}+c^E_{45})\sin\theta\cos\theta & -2c^E_{35}\sin\theta\cos\theta & -(e^E_{13}+e^E_{35})\sin\theta\cos\theta \\ -\sin^2\theta e^E_{35} - e^E_{11}\cos^2\theta & -\sin^2\theta e^E_{34} - e^E_{16}\cos^2\theta & -\sin^2\theta e^E_{33} - e^E_{15}\cos^2\theta & \sin^2\theta \varepsilon^E_{33} - \varepsilon^E_{11}\cos^2\theta \\ -(e^E_{15}+e^E_{31})\sin\theta\cos\theta & -(e^E_{14}+e^E_{36})\sin\theta\cos\theta & -(e^E_{13}+e^E_{35})\sin\theta\cos\theta & +2\varepsilon^E_{13}\sin\theta\cos\theta \end{bmatrix} \begin{bmatrix} v_x \\ v_y \\ v_z \\ j\omega\phi \end{bmatrix} = \rho\omega^2 \begin{bmatrix} v_x \\ v_y \\ v_z \\ j\omega\phi \end{bmatrix} \tag{5.10}$$

Setting the characteristic determinant of the Christoffel equation to zero and solving for the roots yields three values for $(k / \omega)^2$ from which the slownesses are readily obtained. It is seen that there will be three uniform plane wave solutions for each propagation direction. Each have particle velocity polarizations oriented at right angles to one other [17, p.219] and are pure transverse (shear) or pure longitudinal for certain propagation directions only. Plane wave solutions for **v** are found by the method outlined above. Once **v** has been found, the electric potential is easily calculated. Furthermore, once the characteristic equation has been solved, the particle velocity polarization can be obtained from equation (5.5). Note that the general Christoffel equations given by equations (5.6) and (5.10) are not restricted to any particular coordinate system. It is only necessary that the propagation direction $\hat{\mathbf{l}}$ and the stiffness constants c_{ij} be referred to the same coordinate system.

5.3 EFFECTIVE PERMITTIVITY

A basic concept used in the analysis and modelling of SAW devices is the effective permittivity, which gives a description of the electrical behaviour of the surface taking account of the acoustic behaviour of the material. This function is a powerful tool for solving problems concerning a one-dimensional set of electrodes on the surface of a piezoelectric half-space. As such, it provides an effective means of SAW transducer analysis. For variables proportional to $\exp(j\omega t)$, the surface potential $\phi(x_1)$ and charge

density $\sigma(x_1)$ are related by the *effective permittivity*, and the solution is then determined if appropriate boundary conditions are applied. Usually, $\phi(x_1)$ is specified at the electrode locations, while $\sigma(x_1)$ must be zero on all unmetallized regions. It should be noted that acoustic wave excitation is allowed for implicitly by the definition of effective permittivity. This includes all forms of acoustic wave that can be excited. Therefore, in addition to the usual excitation of piezoelectric Rayleigh waves, the effective permittivity will, when appropriate, include the effects of *Bleustein-Gulyaev* waves [31, pp.41-42], *pseudo-surface* waves [32, pp.29-31] and *bulk* waves. In fact, many of the properties of these waves may be deduced by examining the effective permittivity function. However, the effective permittivity does not show the effect of any waves which are not piezoelectrically coupled at the surface. Such waves, which may occur in a piezoelectric material, cannot of course be excited by electrodes on the surface; nevertheless, they may be present in a practical device owing to mode conversion at a discontinuity, for example an edge of the substrate.

At the surface $x_3 = 0$ of a piezoelectric half-space, the normal displacement in the vacuum is denoted $\tilde{D}_3(0^+)$, and is given by

$$\tilde{D}_3(+) = \varepsilon_0 |\beta| \, \tilde{\phi}(x_1) \tag{5.11}$$

The electrical boundary conditions stipulate that the surface potential $\tilde{\phi}(x_1)$ must be the same on both sides of the boundary. However, the normal component of electric

displacement can be different. This discontinuity be related to the potential by the *effective permittivity* function, $\varepsilon_S(\beta)$, defined as [6, p.44]

$$\varepsilon_S(\beta) = \frac{\tilde{D}_3(0^+) - \tilde{D}_3(0^-)}{|\beta|\,\tilde{\phi}(x_1)} \tag{5.12}$$

where β is the wavenumber of the surface wave, $\tilde{D}_3(0^+)$ is the electric flux density on the free-space side of the surface and $\tilde{D}_3(0^-)$ denotes the electric flux density on the piezoelectric side. In addition, the x_1 dependence cancels on the right side, so that $\varepsilon_S(\beta)$ is not dependent on x_1. In essence, the effective permittivity gives the electrical behaviour of the interface between the vacuum and the piezoelectric half-space.

If $\tilde{D}_3(0^+)$ and $\tilde{D}_3(0^-)$ differ, there must obviously be free charges present at the surface, implying the presence of electrodes. Thus, if the total charge density at x_1, including both sides, is denoted $\tilde{\sigma}(x_1)$, equation (5.12) becomes

$$\varepsilon_S(\beta) = \frac{\tilde{\sigma}(x_1)}{|\beta|\,\tilde{\phi}(x_1)} \tag{5.13}$$

where $\tilde{\sigma}(x_1)$ and $\tilde{\phi}(x_1)$ are both proportional to $\exp[j(\omega t + \beta x_1)]$. If $\tilde{D}_3(0^+) = \tilde{D}_3(0^-)$ no electrodes are present, and hence no free charges, giving $\tilde{\sigma}(x_1) = 0$.

In the above equations, the potential $\tilde{\phi}(x_1)$ and charge density $\tilde{\sigma}(x_1)$ are proportional to $\exp(j\omega t)$, and the frequency ω was taken to be constant throughout. If ω s changed, the value of $\varepsilon_S(\beta)$ changes, so $\varepsilon_S(\beta)$ is a function of ω as well as β. However, since $\varepsilon_S(\beta)$ is essentially the ratio of $\tilde{D}_3$ to $\tilde{E}_1$ as shown by equation (5.10), it it will remain unchanged if ω and β are changed in proportion. Thus, $\varepsilon_S(\beta)$ is a function of the normalized variable $s = \beta / \omega$ This has dimensions the same as the reciprocal of velocity, as discussed in the last section is termed the *slowness*. In this study, the analysis applies for constant frequency, and for brevity the effective permittivity is written as $\varepsilon_S(\beta)$, without showing the frequency dependence explicitly.

A more general solution, with surface potential $\phi(x_1)$ and charge density $\sigma(x_1)$ can be obtained by Fourier synthesis [6, pp. 39-42]. In any case , the general solution obtained from equation (5.13) is [6, p.44]

$$\varepsilon_S(\beta) = \frac{\bar{\sigma}(\beta)}{|\beta|\,\bar{\phi}(\beta)} \tag{5.14}$$

where $\bar{\sigma}(\beta)$ and $\bar{\phi}(\beta)$ are the Fourier transforms of $\sigma(x_1)$ and $\phi(x_1)$. Thus, given some general potential function $\phi(x_1)$ in the x_1 domain, the corresponding charge density may be determined by transforming to obtain $\bar{\phi}(\beta)$, and then using $\varepsilon_S(\beta)$ to obtain $\bar{\sigma}(\beta)$. A transformation back to the x_1 domain then yields $\sigma(x_1)$. In solving a particular problem it is usually found that the potential and the charge density are functions of frequency, so

their transforms $\overline{\phi}(\beta)$ and $\overline{\sigma}(\beta)$ will also be functions of frequency. In the Fourier transform, the frequency ω is held constant during the integration. The relationship given by the effective permittivity, equation (5.14) applies for all values of ω

The form of $\varepsilon_S(\beta)$ depends markedly on the type of acoustic wave involved. This study is concerned primarily with the excitation of piezoelectric Rayleigh waves. However, bulk wave excitation has been investigated quite extensively by others because it occurs in most surface-wave devices to some extent. Some devices, in fact, use bulk waves as the main form of acoustic propagation. For the excitation of Bleustein-Gulyaev waves, the effective permittivity can be expressed as an analytical formula [24, 33].

Since the effective permittivity is, generally, a complicated function of β, it must be found numerically. A number of important properties of this function, however, can be readily deduced. Firstly, the function is symmetrical, so that

$$\varepsilon_S\,(-\beta) = \varepsilon_S\,(\beta) \tag{5.15}$$

This follows directly from the general reciprocity relation [6, p.348]. The effective permittivity is usually complex for some values of β and real for other values. Complex values of $\varepsilon_S(\beta)$ indicate that energy is being radiated away from the surface into the bulk of the material, in the form of acoustic waves. This can be seen from the definition involving the harmonic solution, equation (5.11). Figures 5.2 and 5.3 below depict the permittivity functions for YZ lithium niobate and 128° lithium niobate as found in [34].

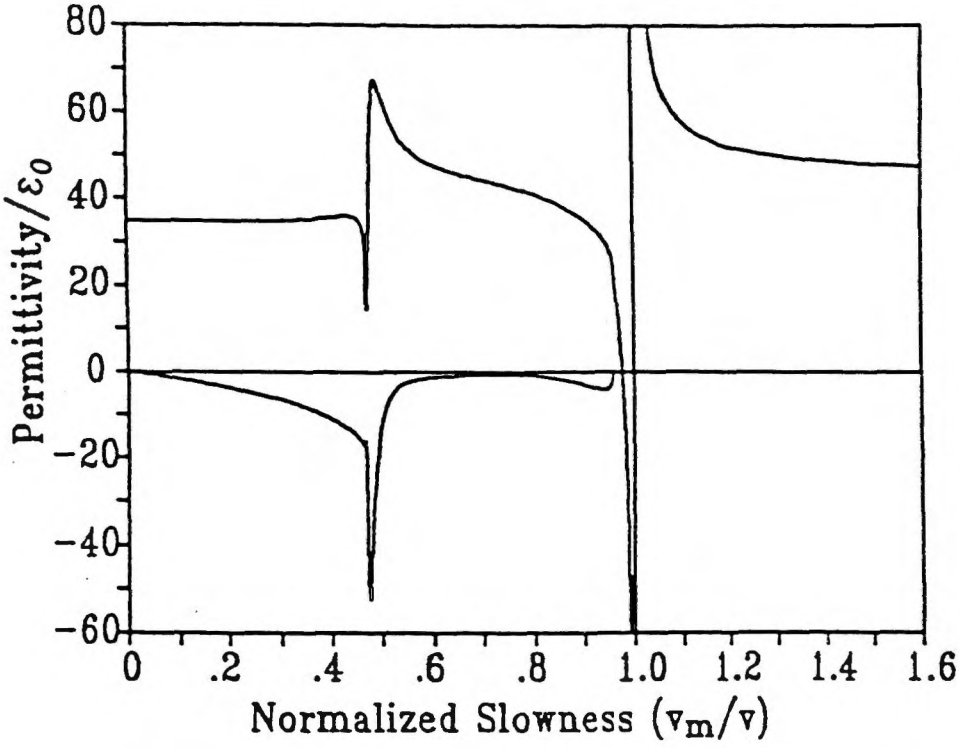

Figure 5.2 : Effective permittivity function for YZ $LiNbO_3$ [34] .

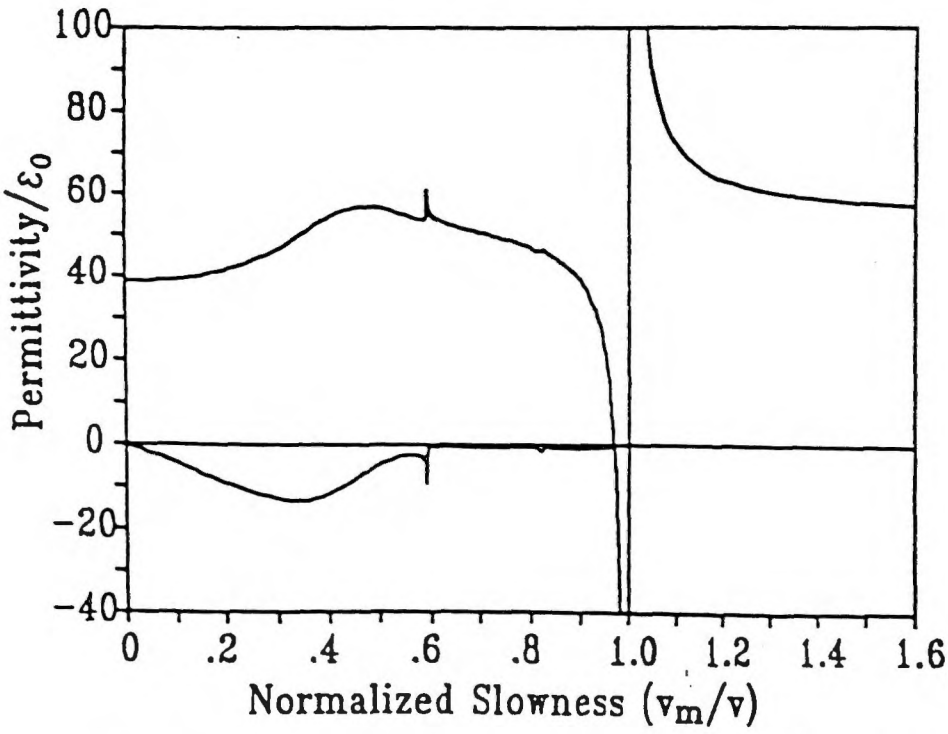

Figure 5.3 : Effective permittivity function for 128° $LiNbO_3$ [34].

CHAPTER 6

COMPUTED RESULTS

6.1 INTRODUCTION

The slowness and effective permittivity functions are two very important parameters that form the basis of all further SAW device modelling. The accurate characterization of substrate performance that these two parameters provide allow for the determination of other properties that are significant in device modelling. The ability to accurately compute these two functions for a given substrate is, therefore, of great merit. Using the underlying analysis present in the previous chapter, subroutines were developed to predict the slowness and effective permittivity functions for various crystal substrates. Since this thesis concerns piezoelectric Rayleigh waves in crystal media, only the most common substrates supporting the propagation of such waves are considered. These standard crystals are listed below.

(i) 128^0 $LiNbO_3$

(ii) YZ $LiNbO_3$

(iii) YZ $LiTaO_3$

(iv) 112^0 $LiTaO_3$

(v) ST Quartz

Additional parameters defining suitable choices of substrate for practical SAW devices were outlined in Chapter 1. It should be noted that the substrates chosen for analysis in this study find considerable application in the fabrication of most SAW devices.

6.2 SLOWNESS CURVES FOR STANDARD BULK CRYSTALS

A typical slowness surface for propagation in the YZ plane of lithium niobate is depicted in Figure 6.1. As seen from the figure, *three* uniform plane wave solutions exist for each propagation direction. The three solutions will have mutually orthogonal particle velocity polarizations. This orthogonality condition must always be satisfied and details of the proof are available in [17, p.22]. Two of the waves have the particle displacement velocity polarized transverse to the propagation direction and are termed quasishear waves. The third wave has particle displacement velocity along the direction of propagation and is termed the quasilongitudinal wave. The prefix "quasi" refers to the notion that, in general, the wave is not polarized strictly along a coordinate axes but is composed of two vector components. If, however, the wave propagates strictly along a coordinate axes it is termed "pure". Special directions for which the wave solutions become pure transverse and pure longitudinal are called pure mode directions and can often be deduced from symmetry conditions.

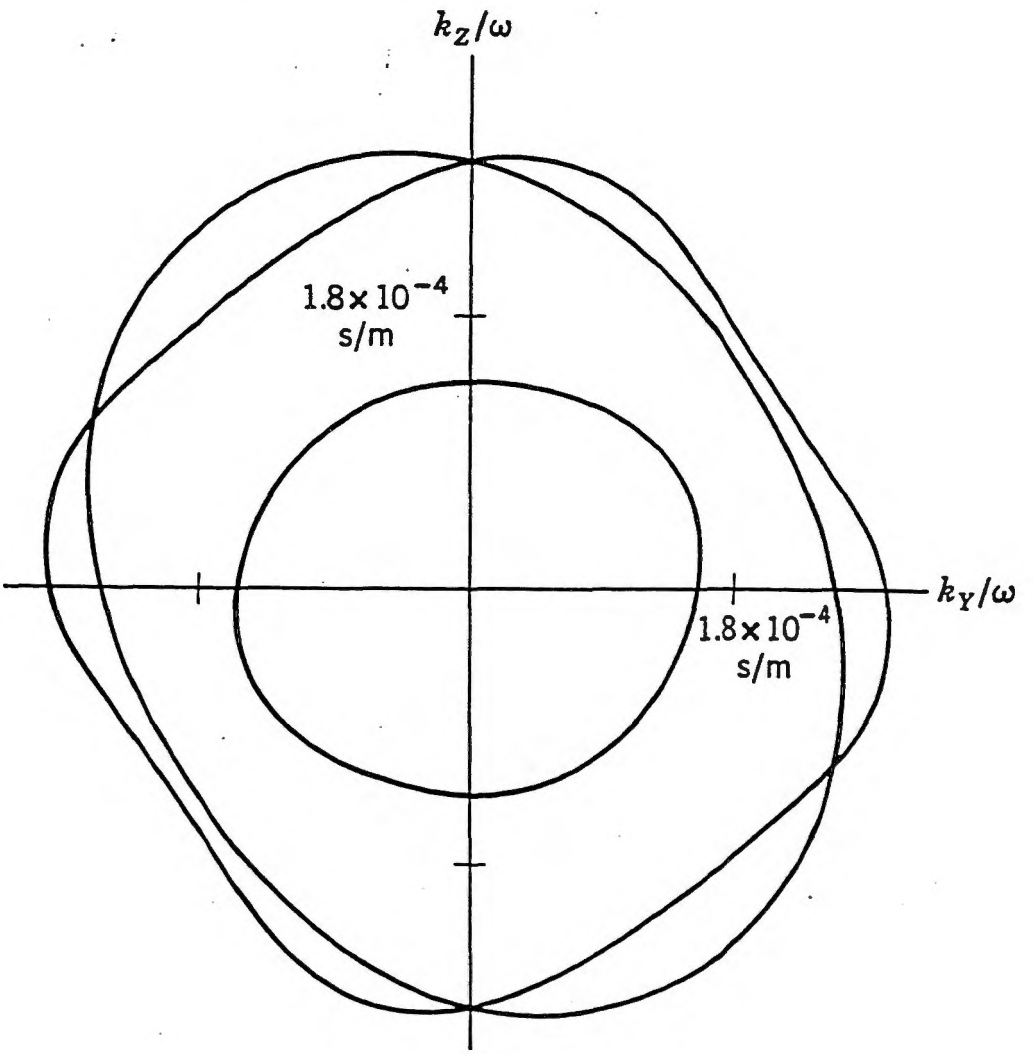

Figure 6.1 : Slowness surface for propagation in the YZ plane of lithium niobate [17, p.308].

In this study, the wave components are restricted to the sagittal plane since we are concerned with pure SAW or Rayleigh wave type propagation only. The wave with greatest velocity (or with smallest "slowness") is defined as the longitudinal wave while the one with lowest velocity (greatest "slowness") is termed the slow shear wave. The wave with intermediate velocity is defined as the fast shear wave.

A number of subroutines were written in MATLAB to calculate the slowness surfaces for the selected crystal substrates mentioned at the beginning of the chapter. A preliminary program allows the user to choose the desired crystal and to also specify the cut (orientation) by entering the appropriate Euler angles. Another subroutine then transforms the standard material tensors [see Appendix C] to the appropriate coordinate system using the Bond transformation method outlined in Chapter 2. Finally, a separate subroutine calculates and plots the slowness surfaces for the selected crystal substrates using the Christoffel equation method described in the previous chapter. All these subroutines can be found in Appendix C at the conclusion of the Thesis.

Using the developed software presented in Appendix C, results for the selected substrates are presented in Figures 6.2 through 6.6 on the following pages. The longitudinal wave for each case is represented by the inner "dashed" line while the two shear waves are denoted by the "solid" lines.

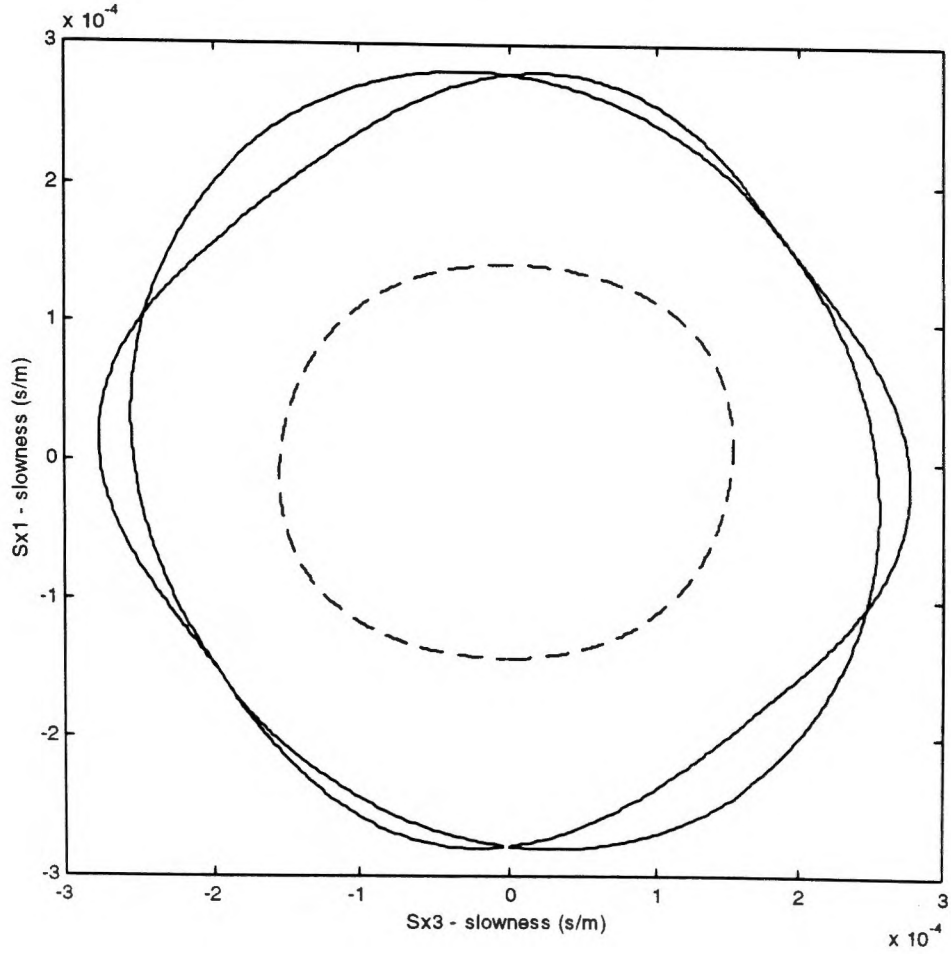

Figure 6.2 : Inverse velocity (or slowness) curves for propagation in the sagittal plane of YZ lithium niobate.

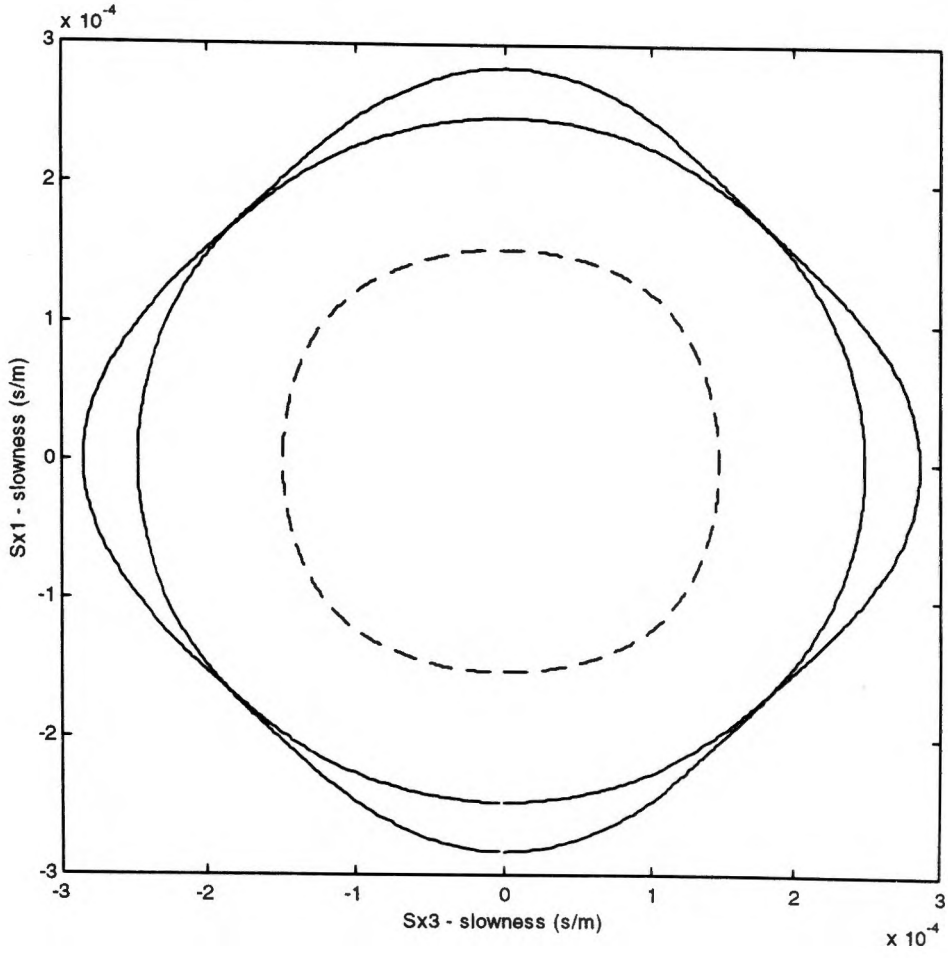

Figure 6.3 : Inverse velocity (or slowness) curves for propagation in the sagittal plane of 128° lithium niobate.

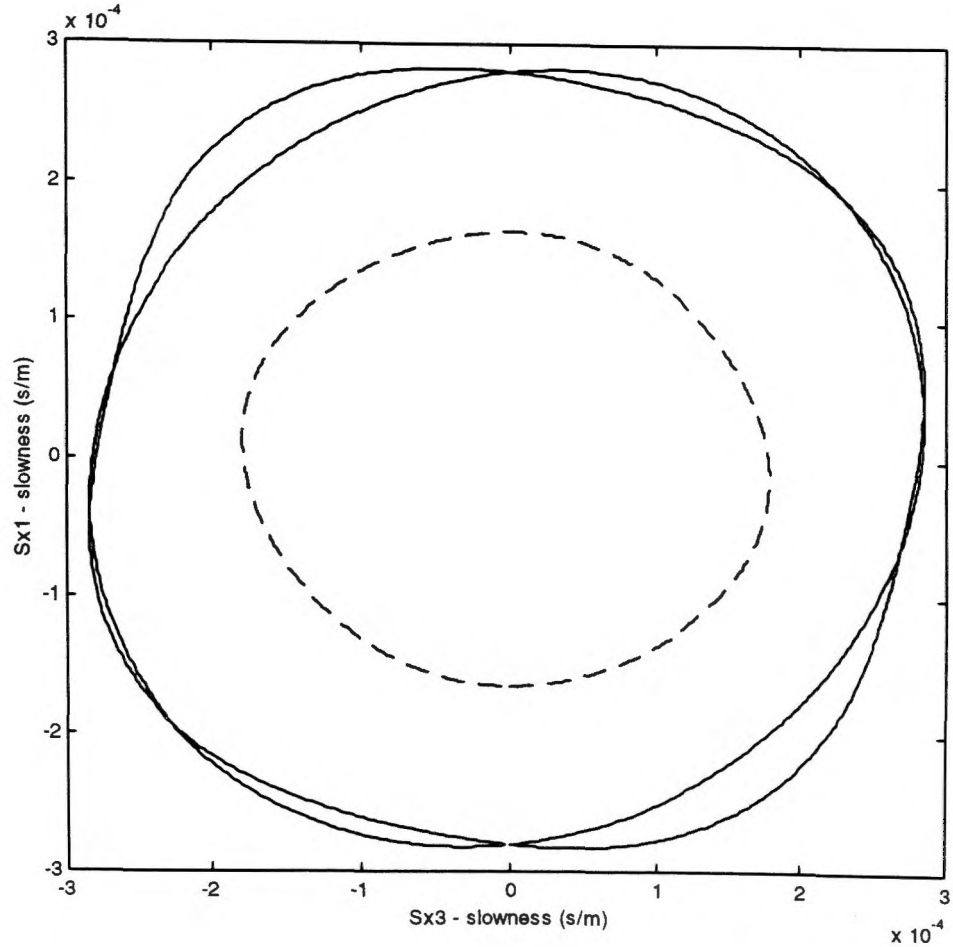

Figure 6.4 : Inverse velocity (or slowness) curves for propagation in the sagittal plane of YZ lithium tantalate.

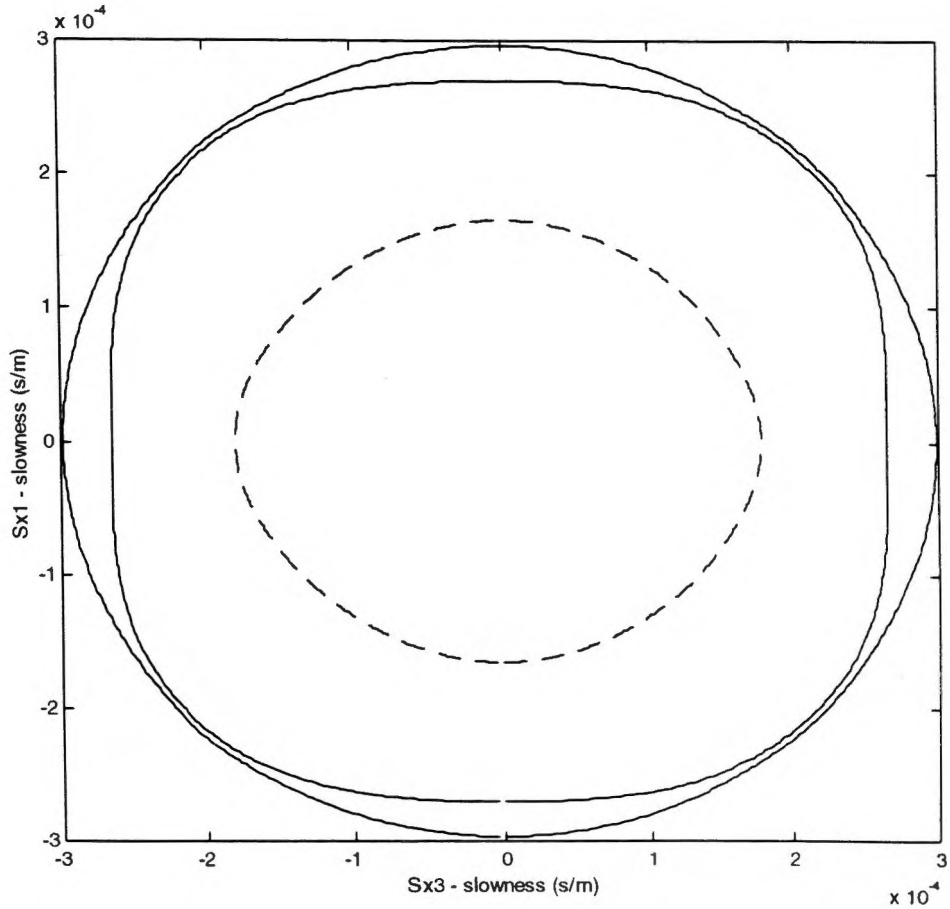

Figure 6.5 : Inverse velocity (or slowness) curves for propagation in the sagittal plane of 112° lithium tantalate.

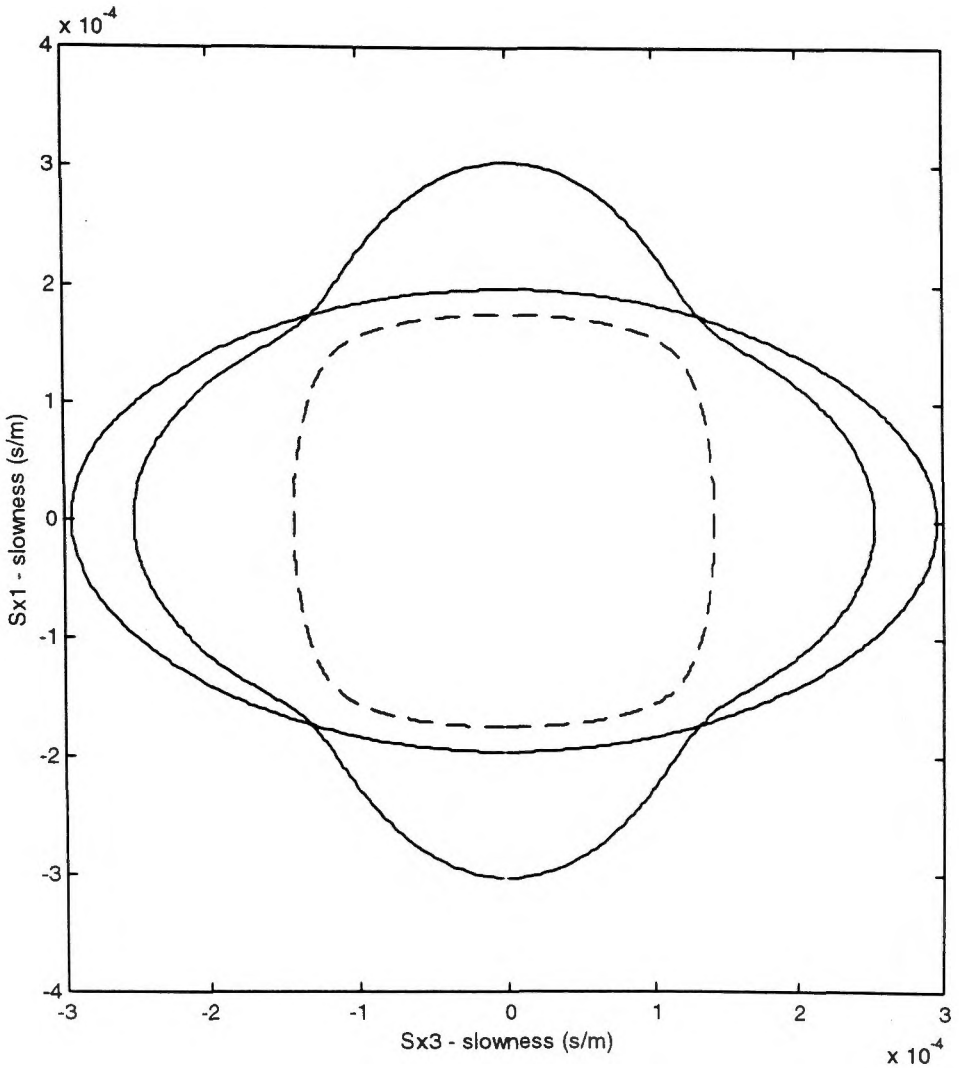

Figure 6.6 : Inverse velocity (or slowness) curves for propagation in the sagittal plane of ST quartz.

As seen from the plots, the wave solutions will, in general, be nondegenerate i.e. for each propagation direction they will each have three different values of phase velocity and hence slowness. Cases can exist, however, when shear wave solutions become degenerate i.e. propagate along the same direction with the same velocity. This can be seen from the plots where we see that, for some substrates, the two shear wave solutions become degenerate for certain propagation directions.

The slowness surface predicted by the software for YZ lithium niobate (Figure 6.2) compares favourably with the one cited in [17] which was depicted in Figure 6.1. Since not all the slowness surfaces for the common SAW crystal substrates have been published, the fact that the two results compare above gives justification that the remaining computed slowness functions provide an accurate model for the other selected substrates.

6.3 EFFECTIVE PERMITTIVITY FOR STANDARD SAW CRYSTALS

A program was written to compute the effective permittivity functions for the crystal substrates of concern and is given in Appendix C. Again, the preliminary program for rotating the standard material tensors into the appropriate coordinate system must be run prior to the effective permittivity subroutine. After the transformation is carried out, the program takes the characteristic determinant of equation (4.14) yielding an eighth order polynomial from which the eight decay coefficients are obtained. The program then selects the appropriate roots according to the criteria given in chapter 5, and then solves for the relative values of acoustic displacement and potential. The effective permittivity is then obtained by forming the ratio defined at the conclusion of chapter 5. The effective permittivity functions obtained via the programs are depicted in Figures 6.7 through 6.11 on the following pages.

An important limitation of the method used throughout the analysis for this thesis follows from the assumption, used in the derivation, that there are no mechanical forces on the surface of the substrate. This implies that any electrodes on the surface must be sufficiently thin that mechanical perturbations can be assumed to be negligible i.e. mechanical loading effects are neglected. In practice, this is usually a valid approximation.

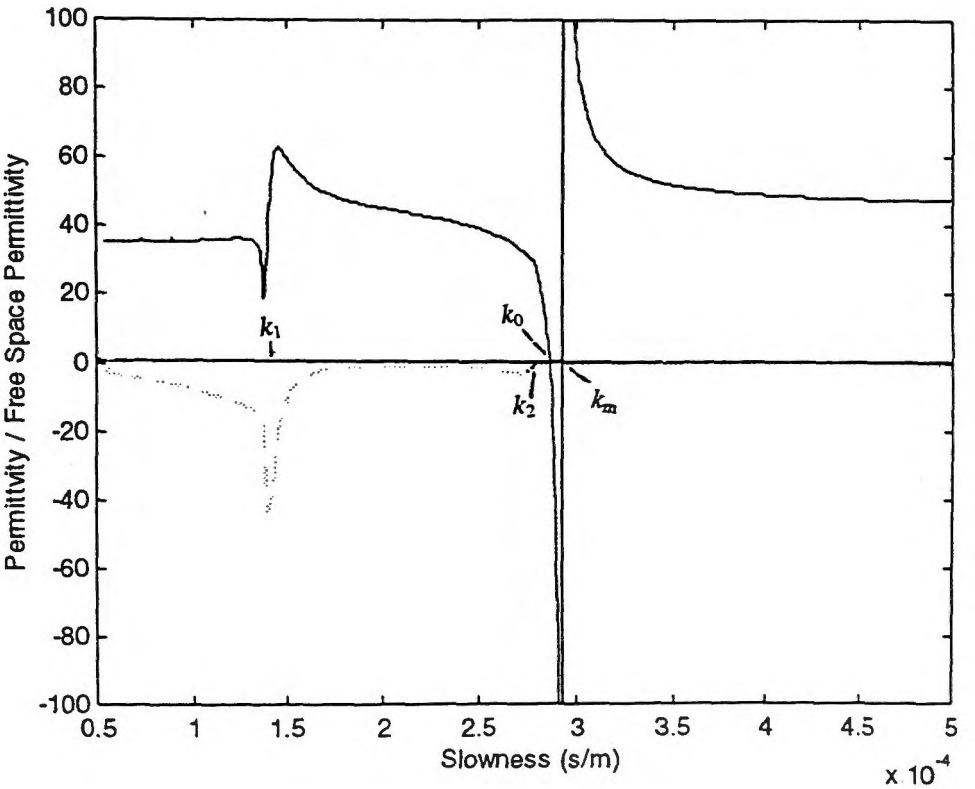

Figure 6.7 : Effective Permittivity for YZ $LiNbO_3$.

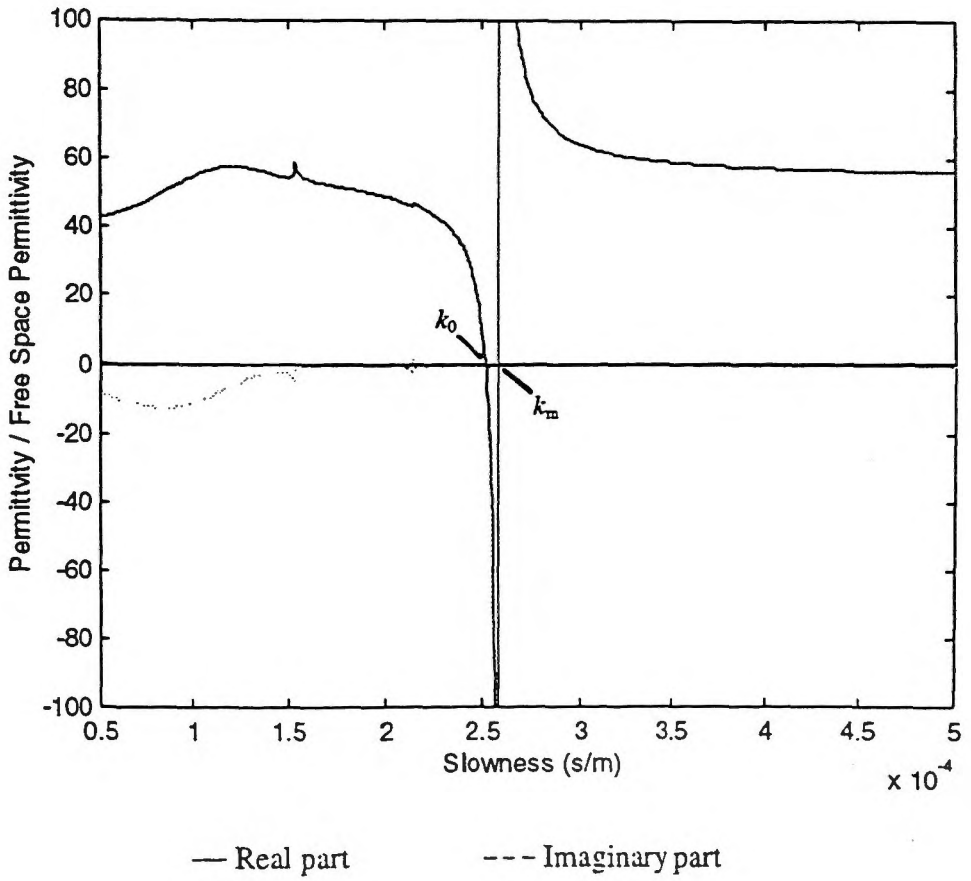

Figure 6.8 : Effective Permittivity for 128° $LiNbO_3$.

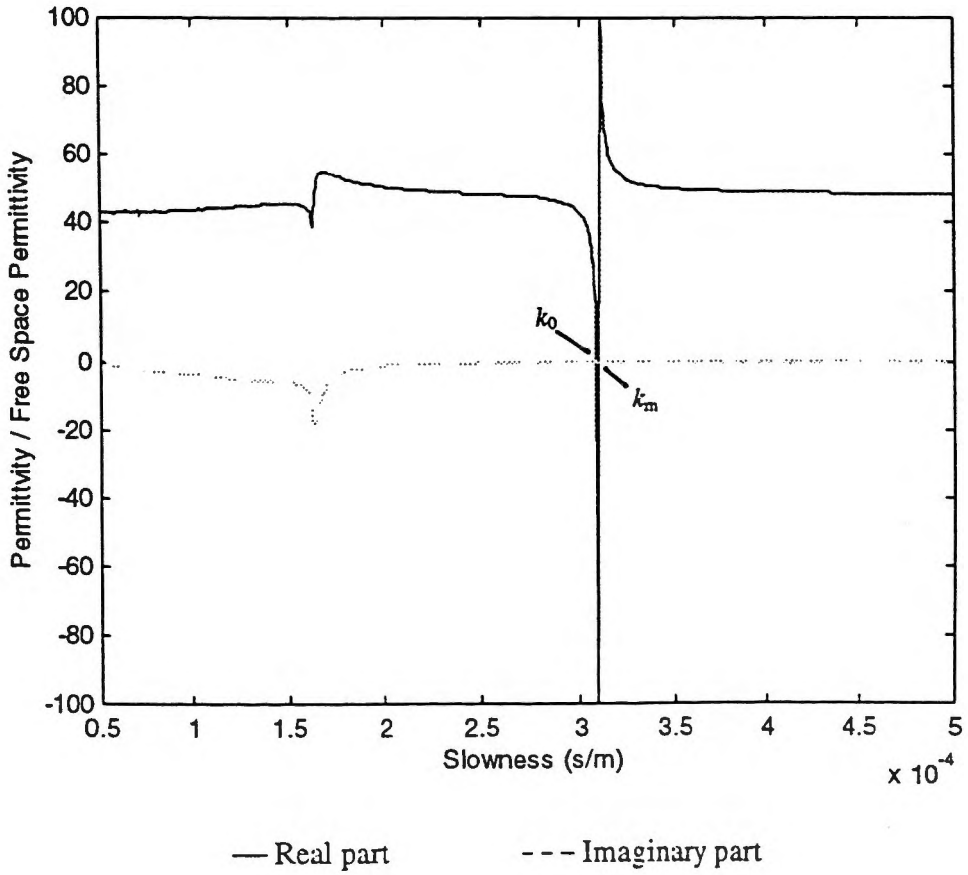

Figure 6.9 : Effective Permittivity for YZ $LiTaO_3$.

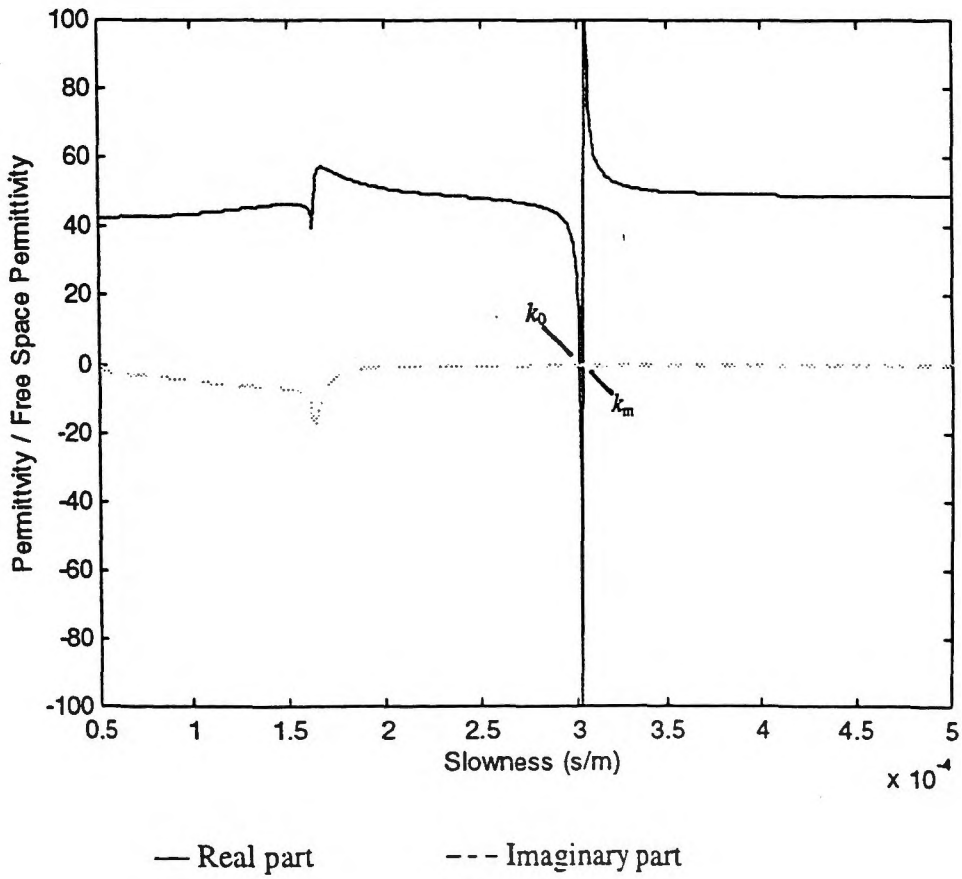

Figure 6.10 : Effective Permittivity for 112° $LiTaO_3$.

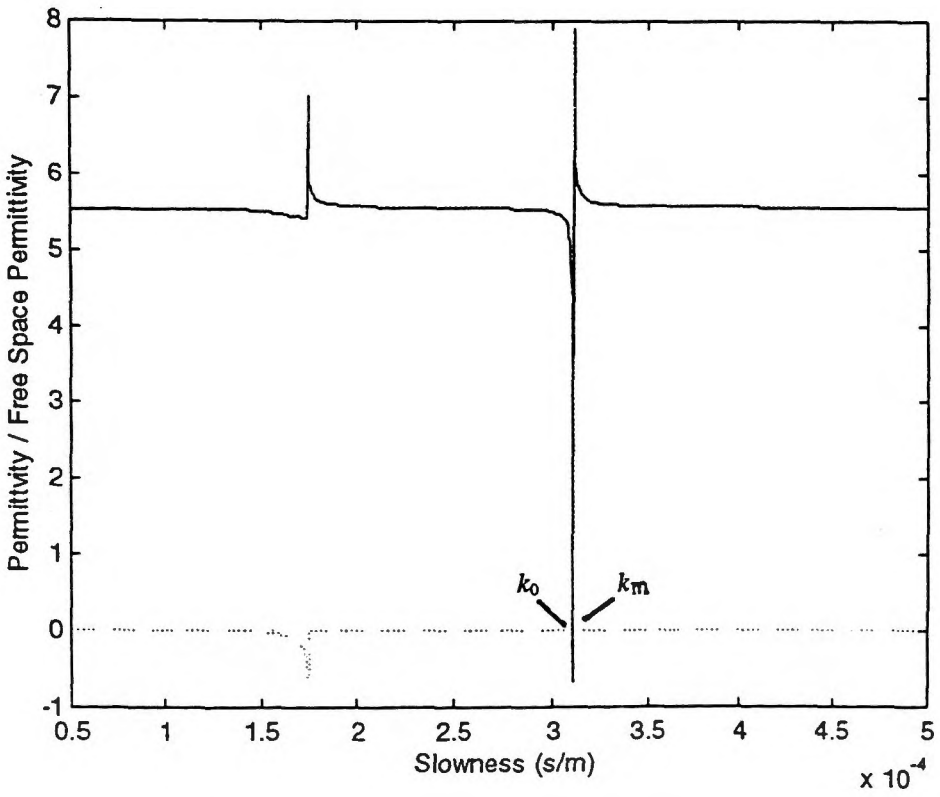

Figure 6.11 : Effective Permittivity for ST quartz.

Figure 5.2 in the previous chapter depicted typical forms of the effective permittivity function for YZ lithium niobate and 128° lithium niobate. These functions were reproduced in Figures 6.7 and 6.8 using the designed simulation programs and compare favourably with those of Figure 5.2. Since not all the effective permittivity curves for the most commonly used SAW substrates have been published in literature, it can be assumed that because the correct function was obtained for a select few of them, the remaining computed functions provide for an accurate characterization of the other crystal substrates. Further justification for this is cited later.

As in Figure 5.2, only positive values of slowness are shown in the plots since the function is even. Examination of all the plots reveals the existence of both *zeros* and *poles* in the respective functions. The zero of a particular permittivity function corresponds to a surface wave solution for the free surface since, by definition, the charge density must be zero. The wavenumber here can be denoted by k_0 , which is taken to be positive, so that the zeros of $\varepsilon_S(\beta)$ occur at $\beta = \pm k_0$. On the other hand, a pole of $\varepsilon_S(\beta)$ indicates a surface wave solution for a metallized surface, since it defines a finite charge density potential approaching zero. In this case, the wavenumber is $k_m > 0$, so that the poles occur at $\beta = \pm k_m$. The *surface wave velocities* for these two cases are v_0 and v_m , respectively, so that $k_0 = \omega/v_0$ and $k_m = \omega/v_m$. In general, these velocities are functions of the propagation direction. Figure 6.12 below depicts the variation of the free-surface and metallized velocities with propagation direction for Y-cut lithium niobate. Note that v_m is less than v_0, which is always the case for a piezoelectrically coupled wave.

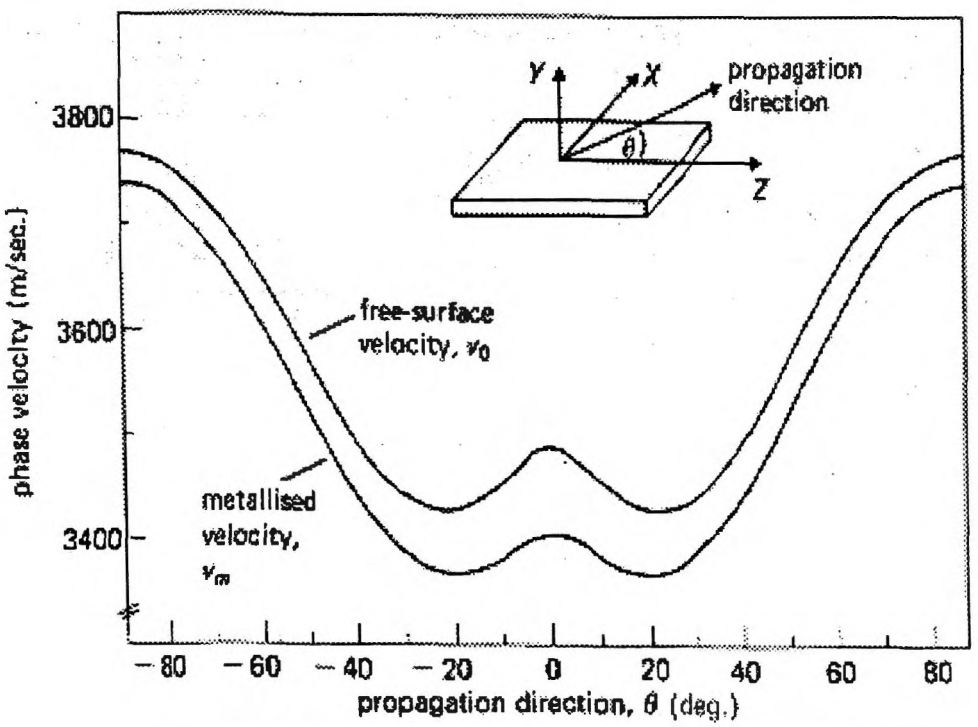

Figure 6.12: Rayleigh-wave velocities for Y-cut lithium niobate [6, p.33].

The marked difference between the two velocities for Y-cut lithium niobate implies that piezoelectric coupling is strong for this case. From Figure 6.12, the coupling is strongest for propagation in the Z direction ($\theta = 0°$), and this orientation, denoted YZ, is often used for SAW device fabrication.

For YZ lithium niobate, the poles at $\pm k_m$ and zeros at $\pm k_0$ corresponding to zero $\overline{\phi}$ and $\overline{\sigma}$ are, respectively, the metallized and free surface Rayleigh wave slownesses as found by Campbell *et al.* [35] using the same analysis. Certain discontinuities are also present in the plot. A discontinuity will arise when one decay coefficient α_n changes from purely imaginary below cutoff to either real or complex above. The discontinuities in

$d\varepsilon_s / ds$ at $\pm k_1$ and $\pm k_2$ are the cutoff slownesses of bulk-longitudinal and vertically polarized bulk-shear waves (slow shear waves). The type of bulk wave associated with each imaginary α_n is determined by the direction of the corresponding particle displacement vector $u_j^{(n)}$. For YZ lithium niobate, the third type of bulk wave (namely, horizontally polarized or fast shear) decouples from the electric field and therefore does not enter into $\varepsilon_s(\beta)$. Figure 6.7 shows that $\varepsilon_s(\beta)$ is purely real above the shear wave cutoff slowness k_2. In addition, at lower values of β, denoted by k_b in Figure 6.7, the permittivity becomes complex, and it remains complex for all smaller values of β. In this region, bulk wave excitation is occurring. For most practical purposes including this study, it is not necessary to consider bulk wave excitation in any detail.

The effective permittivity function for a given substrate also allows for the determination of a very important parameter used in modelling of SAW devices. The *electromechanical coupling coefficient*, K^2, is a measure of the efficiency of a given piezoelectric in converting an applied electrical signal into mechanical energy associated with a surface acoustic wave. This parameter along with the SAW velocity, v, represent the two most important practical material parameters used in SAW filter design. The values of the coupling coefficient usually tend to be very small and, as such, they are usually expressed as percentages.

As cited, the parameter K^2 may be obtained theoretically i.e. from the effective permittivity curves. In this case, the parameter is defined as [31, p.31]

$$K^2 = -\frac{2\,\Delta v}{v_0} \tag{6.1}$$

Here, v_0 is the unperturbed free-surface SAW velocity as defined before. However, $|\,\Delta v\,|$ is the magnitude of the SAW velocity change that occurs when the free surface of the piezoelectric is shorted by a thin highly conducting metal film. That is,

$$\Delta v = v_0 - v_m \tag{6.2}$$

Therefore, in order to determine the respective values of v_0 and v_m , and hence K^2 , for the substrates in question, it is necessary to accurately determine the free-surface and metallized Rayleigh wave slownesses. Accurate determination of these is not possible by inspection of the plots alone. A separate subroutine was written to precisely evaluate the zeros and poles of each of the permittivity functions plotted. The subroutine isolates the region of interest containing the poles and zeros and then recalculates the effective permittivity in that region for a greater number of points. Thus, the location of zeros and poles can be accurately determined. The reciprocal of the respective slowness values then yield the free surface and metallized velocities. For example, for YZ lithium niobate, the program determined the free surface velocity to be 3487.4 m/s and the metallized velocity to be 3411.1 m/s. These values indeed corroborate the marked difference shown in Figure 6.12 for a propagation angle of zero (i.e. YZ lithium niobate) . The electromechanical coupling coefficient was then calculated using equation (6.1) , and for YZ lithium niobate,

this value was determined to be approximately 4.4 % . The same procedure was carried out for the remaining crystal substrates, the results of which are tabulated in Table 6.1. Results reported in other literature are tabulated in Table 6.2 for ease of comparison. In all cases, the values obtained via the developed software agree favourably with values cited in other works.

For SAW propagation in piezoelectrics, crystal properties can also be used to determine the *electromechanical coupling coefficient,* K^2 . In this case , the relation is can be expressed as follows [15, p.17]

$$K^2 = \frac{e'^2}{c'\varepsilon'} \tag{6.3}$$

where e is the piezoelectric coefficient , c is the elastic coefficient and ε is the dielectric permittivity as defined in Chapter 2. Note that in equation (6.3), the tensor subscripts have been dropped. The appropriate constants depend on both the crystal cut and the propagation direction of the surface acoustic wave.

Table 6.1 : **Principle characteristics of selected crystals as determined from the poles and zeros of the computed effective permittivity functions.**

Substrate	Euler Angles (ϕ, θ, φ)	v_0 (m/s)	v_m (m/s)	K^2 (%)
YZ $LiNbO_3$	(0, 90, 90)	3487.4	3411.1	4.4
128° $LiNbO_3$	(0, 38, 0)	3979.3	3870.9	5.5
YZ $LiTaO_3$	(0, 90, 90)	3237.3	3224.6	0.8
112° $LiTaO_3$	(90, 90, 112.2)	3301.0	3285.9	0.9
ST Quartz	(0, 132.75, 0)	3158.0	3156.2	0.1

Table 6.2 : **Principle characteristics of selected crystals as reported in other literature.**

Substrate	Euler Angles (ϕ, θ, φ)	v_0 (m/s)	v_m (m/s)	K^2 (%)
YZ $LiNbO_3$ [34]	(0, 90, 90)	3494.0	3415.0	4.5
128° $LiNbO_3$ [36]	(0, 38, 0)	3979.5	3871.3	5.4
YZ $LiTaO_3$ [34]	(0, 90, 90)	3272.0	3254.0	1.1
112° $LiTaO_3$ [34]	(90, 90, 112.2)	3328.0	3310.0	1.1
ST Quartz [36]	(0, 132.75, 0)	3159.7	3157.9	0.1

published data used to define the standard crystal tensors and to roundoff error. Nonetheless, the results obtained via the software are very comparable with those cited in other literature. Examining the electromechanical coupling coefficients, the values determined using the computed permittivity functions compare very well with the values cited in other literature as can be seen by examining Tables 6.1 and 6.2 . Since the calculation of K^2 involved determining the poles and zeros of the computed permittivity functions, and since these compared with values cited in other work, this reinforces the validity of the designed simulation programs in correctly modelling the selected substrates.

From Tables 6.1, it is observed that the YZ lithium niobate substrate possesses a relatively high electromechanical coupling coefficient of approximately 4.4 %. This is one of the highest values attainable in a substrate suitable for high frequency surface wave devices. The 128° lithium niobate substrate, however, was found to have the highest value for this parameter, at about 5.4%. These relatively high values for the electromechanical coupling coefficients indicate that these substrates are used frequently in the production of SAW devices . YZ lithium niobate generally finds application in wideband SAW filters as well as in radar pulse compression filters with very large time-bandwidth products. ST-X quartz has a value of K^2 that is about 40 times less than for lithium niobate. It finds application in narrow-band filters and delay lines. Moreover, it is widely employed in SAW oscillator designs because of its zero temperature coefficient of delay about room temperature. Lithium tantalate with a higher K^2 than ST-X quartz (but poorer temperature stability), has also found application in oscillator design.

The usefulness of the effective permittivity function stems from the fact that the input admittance of a transducer can be calculated from this function including the effects of radiation of all possible surface and bulk modes. It , therefore, provides and effective basis for further modelling of SAW devices. In most cases, we are concerned with problems in which the boundary conditions are expressed in the x_1 domain. The relationship in this domain can be expressed using a Green's function [36, 37]. The Green's function can be derived from the effective permittivity and can be used to find a numerical solution for the surface charge and field distribution on an interdigital array of electrodes.

CHAPTER 7

CONCLUSIONS

This study was concerned with the acoustic propagation of piezoelectric Rayleigh waves in crystalline media, commonly referred to as surface acoustic waves. Devices based on the propagation of such waves (SAW devices) have for a long time been a key technology in the communications industry. Two functions of great interest when concerned with which substrate is practical for the intended use of a device are the *slowness* and the *effective permittivity*. Slowness is simply the inverse of phase velocity and is useful for depicting the three plane wave solutions travelling in any plane of the media in question. Generally, the form of the slowness curve will depend on the substrate material and the orientation of the surface normal. The permittivity function is significant because, for a given substrate orientation, it effectively stores all the relevant mechanical information in a scalar electrical quantity. In addition, the function embraces all values of v including those for which bulk waves form part of the solution.

To compute these two important functions, various programs were designed. Initially, a subroutine was designed to transform the standard tensor properties of a crystal into the appropriate coordinate system based on the prescribed cut of the crystal. Another program was designed to calculate and plot the slowness curves in the sagittal

plane for the various cuts of lithium niobate, lithium tantalate and quartz. Finally, a program was written to compute the effective permittivity functions for the substrates in question.

The slowness and effective permittivity curves determined for the selected pure SAW crystals have been shown to compare favourably with the experimental results cited by other authors. From the permittivity function, it is possible to determine the two most important practical parameters used in SAW filter design. i.e. the electromechanical coupling coefficient (K^2) and the SAW velocity (v) . The zero in the permittivity function denotes the free surface velocity while poles denote the metallized velocity. From these two velocities, the electromechanical coupling coefficients were determined for the selected crystal substrates and these were also comparable to values cited by others. Slight discrepancies in the velocities and coupling coefficients can be attributed to the use of slightly different material constants in the calculations.

The development in this thesis showed how the effective permittivity may be used to relate the surface charge density and potential for a piezoelectric half-space, with the region above the piezoelectric assumed to be a vacuum. This method can be extended to the analysis of surface-wave transducers on a half-space by Green's function methods [25, 37] allowing for the prediction of surface charge and field distribution. The concept may also be generalized to analyze a number of other problems such as the coupling between a piezoelectric half-space and a plane above the surface or the coupling to a semiconductor above the piezoelectric surface [6, p.52].

Finally, a number of different types of surface and bulk waves couple to the electric field produced by an interdigital array. These depend on the crystallographic symmetry of the substrate and the orientation of the surface plane and fingers of the array. This study analyzed the case for the most commonly employed surface wave, the Rayleigh wave, which has elliptical particle motion with components normal and parallel to the surface in the direction of propagation. Future work could involve the extension of the programs to allow for the analysis of other modes of propagation prevalent in many SAW devices, namely Bleustein-Guylaev waves and Pseudo SAW or leaky waves.

APPENDIX A

SYMMETRY CHARACTERISTICS FOR CRYSTAL CLASSES

✠ Labelled by symmetry, then class.

A.1 : Symmetry Characteristics of Stiffness Constants

Triclinic

$$\begin{bmatrix} c_{11} & c_{12} & c_{13} & c_{14} & c_{15} & c_{16} \\ c_{12} & c_{22} & c_{23} & c_{24} & c_{25} & c_{26} \\ c_{13} & c_{23} & c_{33} & c_{34} & c_{35} & c_{36} \\ c_{14} & c_{24} & c_{34} & c_{44} & c_{45} & c_{46} \\ c_{15} & c_{25} & c_{35} & c_{45} & c_{55} & c_{56} \\ c_{16} & c_{26} & c_{36} & c_{46} & c_{56} & c_{66} \end{bmatrix}$$

Monoclinic

$$\begin{bmatrix} c_{11} & c_{12} & c_{13} & 0 & c_{15} & 0 \\ c_{12} & c_{22} & c_{23} & 0 & c_{25} & 0 \\ c_{13} & c_{23} & c_{33} & 0 & c_{35} & 0 \\ 0 & 0 & 0 & c_{44} & 0 & c_{46} \\ c_{15} & c_{25} & c_{35} & 0 & c_{55} & 0 \\ 0 & 0 & 0 & c_{46} & 0 & c_{66} \end{bmatrix}$$

Orthorhombic

$$\begin{bmatrix} c_{11} & c_{12} & c_{13} & 0 & 0 & 0 \\ c_{12} & c_{22} & c_{23} & 0 & 0 & 0 \\ c_{13} & c_{23} & c_{33} & 0 & 0 & 0 \\ 0 & 0 & 0 & c_{44} & 0 & 0 \\ 0 & 0 & 0 & 0 & c_{55} & 0 \\ 0 & 0 & 0 & 0 & 0 & c_{66} \end{bmatrix}$$

Tetragonal *4*, $\bar{4}$, *4/m*

$$\begin{bmatrix} c_{11} & c_{12} & c_{13} & 0 & 0 & c_{16} \\ c_{12} & c_{11} & c_{13} & 0 & 0 & -c_{16} \\ c_{13} & c_{13} & c_{33} & 0 & 0 & 0 \\ 0 & 0 & 0 & c_{44} & 0 & 0 \\ 0 & 0 & 0 & 0 & c_{44} & 0 \\ c_{16} & -c_{16} & 0 & 0 & 0 & c_{66} \end{bmatrix}$$

Tetragonal *4mm, 422,* $\bar{4}$*2m , 4/mmm*

$$\begin{bmatrix} c_{11} & c_{12} & c_{13} & 0 & 0 & 0 \\ c_{12} & c_{11} & c_{13} & 0 & 0 & 0 \\ c_{13} & c_{13} & c_{33} & 0 & 0 & 0 \\ 0 & 0 & 0 & c_{44} & 0 & 0 \\ 0 & 0 & 0 & 0 & c_{44} & 0 \\ 0 & 0 & 0 & 0 & 0 & c_{66} \end{bmatrix}$$

Trigonal *3*, $\bar{3}$

$$\begin{bmatrix} c_{11} & c_{12} & c_{13} & c_{14} & -c_{25} & 0 \\ c_{12} & c_{11} & c_{13} & -c_{14} & c_{25} & 0 \\ c_{13} & c_{13} & c_{33} & 0 & 0 & 0 \\ c_{14} & -c_{14} & 0 & c_{44} & 0 & c_{25} \\ -c_{25} & c_{25} & 0 & 0 & c_{44} & c_{14} \\ 0 & 0 & 0 & c_{25} & c_{14} & \frac{1}{2}(c_{11}-c_{12}) \end{bmatrix}$$

Trigonal *32, 3m,* $\bar{3}m$

$$\begin{bmatrix} c_{11} & c_{12} & c_{13} & c_{14} & 0 & 0 \\ c_{12} & c_{11} & c_{13} & -c_{14} & 0 & 0 \\ c_{13} & c_{13} & c_{33} & 0 & 0 & 0 \\ c_{14} & -c_{14} & 0 & c_{44} & 0 & 0 \\ 0 & 0 & 0 & 0 & c_{44} & c_{14} \\ 0 & 0 & 0 & 0 & c_{14} & \frac{1}{2}(c_{11}-c_{12}) \end{bmatrix}$$

Hexagonal

$$\begin{bmatrix} c_{11} & c_{12} & c_{13} & 0 & 0 & 0 \\ c_{12} & c_{11} & c_{13} & 0 & 0 & 0 \\ c_{13} & c_{13} & c_{33} & 0 & 0 & 0 \\ 0 & 0 & 0 & c_{44} & 0 & 0 \\ 0 & 0 & 0 & 0 & c_{44} & 0 \\ 0 & 0 & 0 & 0 & 0 & \frac{1}{2}(c_{11}-c_{12}) \end{bmatrix}$$

Cubic

$$\begin{bmatrix} c_{11} & c_{12} & c_{12} & 0 & 0 & 0 \\ c_{12} & c_{11} & c_{12} & 0 & 0 & 0 \\ c_{12} & c_{12} & c_{11} & 0 & 0 & 0 \\ 0 & 0 & 0 & c_{44} & 0 & 0 \\ 0 & 0 & 0 & 0 & c_{44} & 0 \\ 0 & 0 & 0 & 0 & 0 & c_{44} \end{bmatrix}$$

A.2 : Symmetry Characteristics of Piezoelectric Constants

Triclinic *1*

$$\begin{bmatrix} e_{11} & e_{12} & e_{13} & e_{14} & e_{15} & e_{16} \\ e_{21} & e_{22} & e_{23} & e_{24} & e_{25} & e_{26} \\ e_{31} & e_{32} & e_{33} & e_{34} & e_{35} & e_{36} \end{bmatrix}$$

Monoclinic *2*

$$\begin{bmatrix} 0 & 0 & 0 & e_{14} & 0 & e_{16} \\ e_{21} & e_{22} & e_{23} & 0 & e_{25} & 0 \\ 0 & 0 & 0 & e_{34} & 0 & e_{36} \end{bmatrix}$$

Monoclinic *m*

$$\begin{bmatrix} e_{11} & e_{12} & e_{13} & 0 & e_{15} & 0 \\ 0 & 0 & 0 & e_{24} & 0 & e_{26} \\ e_{31} & e_{32} & e_{33} & 0 & e_{35} & 0 \end{bmatrix}$$

Orthorhombic *222*

$$\begin{bmatrix} 0 & 0 & 0 & e_{14} & 0 & 0 \\ 0 & 0 & 0 & 0 & e_{25} & 0 \\ 0 & 0 & 0 & 0 & 0 & e_{36} \end{bmatrix}$$

Orthorhombic *2mm*

$$\begin{bmatrix} 0 & 0 & 0 & 0 & e_{15} & 0 \\ 0 & 0 & 0 & e_{24} & 0 & 0 \\ e_{31} & e_{32} & e_{33} & 0 & 0 & 0 \end{bmatrix}$$

Tetragonal $\bar{4}$

$$\begin{bmatrix} 0 & 0 & 0 & e_{14} & e_{15} & 0 \\ 0 & 0 & 0 & -e_{15} & e_{14} & 0 \\ e_{31} & -e_{31} & 0 & 0 & 0 & e_{36} \end{bmatrix}$$

Tetragonal *4*

$$\begin{bmatrix} 0 & 0 & 0 & e_{14} & e_{15} & 0 \\ 0 & 0 & 0 & e_{15} & -e_{14} & 0 \\ e_{31} & e_{31} & e_{33} & 0 & 0 & 0 \end{bmatrix}$$

Tetragonal $\bar{4}2m$

$$\begin{bmatrix} 0 & 0 & 0 & e_{14} & 0 & 0 \\ 0 & 0 & 0 & 0 & e_{14} & 0 \\ 0 & 0 & 0 & 0 & 0 & e_{36} \end{bmatrix}$$

Tetragonal *422*

$$\begin{bmatrix} 0 & 0 & 0 & e_{14} & 0 & 0 \\ 0 & 0 & 0 & 0 & -e_{14} & 0 \\ 0 & 0 & 0 & 0 & 0 & 0 \end{bmatrix}$$

Tetragonal *4mm*

$$\begin{bmatrix} 0 & 0 & 0 & 0 & e_{15} & 0 \\ 0 & 0 & 0 & e_{15} & 0 & 0 \\ e_{31} & e_{31} & e_{33} & 0 & 0 & 0 \end{bmatrix}$$

Trigonal *3*

$$\begin{bmatrix} e_{11} & -e_{11} & 0 & e_{14} & e_{15} & -e_{22} \\ -e_{22} & e_{22} & 0 & e_{15} & -e_{14} & -e_{11} \\ e_{31} & e_{31} & e_{33} & 0 & 0 & 0 \end{bmatrix}$$

Trigonal *32*

$$\begin{bmatrix} e_{11} & -e_{11} & 0 & e_{14} & 0 & 0 \\ 0 & 0 & 0 & 0 & -e_{14} & -e_{11} \\ 0 & 0 & 0 & 0 & 0 & 0 \end{bmatrix}$$

Trigonal *3m*

$$\begin{bmatrix} 0 & 0 & 0 & 0 & e_{15} & -e_{22} \\ -e_{22} & e_{22} & 0 & e_{15} & 0 & 0 \\ e_{31} & e_{31} & e_{33} & 0 & 0 & 0 \end{bmatrix}$$

Hexagonal *6*

$$\begin{bmatrix} 0 & 0 & 0 & e_{14} & e_{15} & 0 \\ 0 & 0 & 0 & e_{15} & -e_{14} & 0 \\ e_{31} & e_{31} & e_{33} & 0 & 0 & 0 \end{bmatrix}$$

Hexagonal *622*

$$\begin{bmatrix} 0 & 0 & 0 & e_{14} & 0 & 0 \\ 0 & 0 & 0 & 0 & -e_{14} & 0 \\ 0 & 0 & 0 & 0 & 0 & 0 \end{bmatrix}$$

Hexagonal *6mm*

$$\begin{bmatrix} 0 & 0 & 0 & 0 & e_{15} & 0 \\ 0 & 0 & 0 & e_{15} & 0 & 0 \\ e_{31} & e_{31} & e_{33} & 0 & 0 & 0 \end{bmatrix}$$

Hexagonal $\bar{6}$

$$\begin{bmatrix} e_{11} & -e_{11} & 0 & 0 & 0 & -e_{22} \\ -e_{22} & e_{22} & 0 & 0 & 0 & -e_{11} \\ 0 & 0 & 0 & 0 & 0 & 0 \end{bmatrix}$$

Hexagonal $\bar{6}m2$

$$\begin{bmatrix} e_{11} & -e_{11} & 0 & 0 & 0 & 0 \\ 0 & 0 & 0 & 0 & 0 & -e_{11} \\ 0 & 0 & 0 & 0 & 0 & 0 \end{bmatrix}$$

Cubic *23* and $\bar{4}3m$

$$\begin{bmatrix} 0 & 0 & 0 & e_{14} & 0 & 0 \\ 0 & 0 & 0 & 0 & e_{14} & 0 \\ 0 & 0 & 0 & 0 & 0 & e_{14} \end{bmatrix}$$

A.3 : Symmetry Characteristics of Dielectric Constants

Triclinic

$$\begin{bmatrix} \varepsilon_{11}^S & \varepsilon_{12}^S & \varepsilon_{13}^S \\ \varepsilon_{12}^S & \varepsilon_{22}^S & \varepsilon_{23}^S \\ \varepsilon_{13}^S & \varepsilon_{23}^S & \varepsilon_{33}^S \end{bmatrix}$$

Monoclinic

$$\begin{bmatrix} \varepsilon_{11}^S & 0 & \varepsilon_{13}^S \\ 0 & \varepsilon_{22}^S & 0 \\ \varepsilon_{13}^S & 0 & \varepsilon_{33}^S \end{bmatrix}$$

Orthorhombic

$$\begin{bmatrix} \varepsilon_{11}^S & 0 & 0 \\ 0 & \varepsilon_{22}^S & 0 \\ 0 & 0 & \varepsilon_{33}^S \end{bmatrix}$$

Hexagonal, Trigonal, Tetragonal

$$\begin{bmatrix} \varepsilon_{11}^S & 0 & 0 \\ 0 & \varepsilon_{11}^S & 0 \\ 0 & 0 & \varepsilon_{33}^S \end{bmatrix}$$

Cubic, Isotropic

$$\begin{bmatrix} \varepsilon_{11}^S & 0 & 0 \\ 0 & \varepsilon_{11}^S & 0 \\ 0 & 0 & \varepsilon_{11}^S \end{bmatrix}$$

APPENDIX B

PHYSICAL CONSTANTS OF SELECTED CRYSTALS

Table B.1 : Summary of the Material Constants for Common SAW Crystals.

	Lithium niobate ($LiNbO_3$)	Lithium tantalate ($LiTaO_3$)	Quartz (SiO_2)
Mass density (kg/m^3)	4628	7454	2651
Elastic Constants (10^{10} N/m^2)	$c_{11}^E = 19.839$ $c_{12}^E = 5.472$ $c_{13}^E = 6.513$ $c_{14}^E = 0.788$ $c_{33}^E = 22.79$ $c_{44}^E = 5.965$	$c_{11}^E = 23.28$ $c_{12}^E = 4.65$ $c_{13}^E = 8.36$ $c_{14}^E = -1.05$ $c_{33}^E = 27.59$ $c_{44}^E = 9.49$	$c_{11}^E = 8.674$ $c_{12}^E = 0.699$ $c_{13}^E = 1.191$ $c_{14}^E = -1.791$ $c_{33}^E = 10.72$ $c_{44}^E = 5.794$
Piezoelectric Constants (C/m^2)	$e_{15} = 3.69$ $e_{22} = 2.42$ $e_{31} = 0.30$ $e_{33} = 1.77$	$e_{15} = 2.64$ $e_{22} = 1.86$ $e_{31} = -0.22$ $e_{33} = 1.71$	$e_{11} = 0.171$ $e_{14} = -0.0436$
Dielectric Constants (in ε_0)	$\varepsilon_{11}^S = 45.6$ $\varepsilon_{33}^S = 26.3$	$\varepsilon_{11}^S = 40.9$ $\varepsilon_{33}^S = 42.5$	$\varepsilon_{11}^S = 4.5$ $\varepsilon_{33}^S = 4.6$

APPENDIX C : SIMULATION SOFTWARE

main.m

```
% This is the main program that controls the entire software.
% It allows the user to choose from a select list of substrates
% and will display the standard material tensors.  The user is then
% prompted to enter the cut of the crystal using the Euler angle convention.
% A subroutine is then called that transforms the standard material tensors
% and displays the results. The user is then prompted to choose from
% three desired tasks (i) to simulate the slowness surface, (ii) to simulate
% the effective permittivity function or (iii) to precisely determine the
% free and metallized velocities. In each case, the appropriate function
% is invoked and the results are displayed.

% declaration of global variables

global subs phi theta ci c pes perm crot pesrot permrot dens c0 perm0

% multiplication factors for material constants

perm0=8.854e-12;  %(F/m)
c0=10^10;         %(N/m^2)

%-------------------------------------------------------------------------
% choosing a substrate
%
subs = menu('Choose a substrate', 'Lithium Niobate','Lithium tantalate','Quartz', 'Gallium
Arsenide');

%-------------------------------------------------------------------------

% intialize the standard material tensors

stastiff(subs); stapes(subs); staperm(subs);
```

```
% display standard material tensors

disp('STANDARD stiffness, piezoelectric stress and permittivity tensors:');

c=c*c0
x=input('prompt');
pes
x=input('prompt');
perm=perm*perm0
x=input('prompt');

%-------------------------------------------------------------------------
%
% enter the desired cut of the crystal using the Euler Angle Method

disp('Please enter the cut of the cut of the crystal using Euler angles;');
disp('********** Enter the Euler angles in degrees**********');

phi = input('enter phi   : ');
theta = input('enter theta : ');
ci = input('enter ci    : ');


%-------------------------------------------------------------------------
% convert Euler angles to radians

phi=phi*pi/180;
theta=theta*pi/180;
ci=ci*pi/180;

%-------------------------------------------------------------------------
% transform standard material tensors to appropriate values for particular
% crystal cut defined by Euler angles using Bond transformation method [ ]

tracon(c,pes,perm);    % calls transformation function


% display rotated material tensors

disp('TRANSFORMED stiffness, piezoelectric stress and permittivity tensors:');

crot
```

```
x=input('prompt');
pesrot
x=input('prompt');
permrot
x=input('prompt');

%-----------------------------------------------------------------------

% allows user to choose from three tasks

choice = menu('Choose a function','Slowness Curve','Effective Permittivity Function',...
'Precise Determination of vo and vm');

if choice == 1

invel(crot,pesrot,permrot); % call function to calculate slowness surface

elseif choice ==2

epcalc(crot,pesrot,permrot); % call function to calculate eff. perm.

else

detvel(crot,pesrot,permrot);    % call function to determine free and
                                % metallized velocities, vo and vm.
end;


%-----------------------------------------------------------------------
```

stastiff.m

```
function c = stastiff(subs)

% this subroutine initiallizes the 'standard' elastic constants for the selected substrates

global subs c dens

for m = 1:6;
        for l = 1:6;
                c(m,l) = 0;
        end;
end;


if subs == 1

        dens = 4628;   % density in (kg/m^3)

        % stiffness constants matrix, for lithium niobate  [38]

        c(1,1) = 19.839;        %(10^10 N/m^2);
        c(1,2) = 5.472;
        c(1,3) = 6.513;
        c(1,4) = 0.788;
        c(3,3) = 22.79;
        c(4,4) = 5.965;
        c(2,2) = c(1,1);
        c(2,3) = c(1,3);
        c(2,4) = -c(1,4);
        c(5,6) = c(1,4);
        c(5,5) = c(4,4);
        c(6,6) = (c(1,1)-c(1,2))/2;
        c(2,1) = c(1,2);
        c(3,1) = c(1,3);
        c(4,1) = c(1,4);
        c(3,2) = c(1,3);
        c(4,2) = -c(1,4);
        c(6,5) = c(1,4);
```

```
%-----------------------------------------------------------------------

elseif subs ==2

        dens = 7454;   % density in (kg/m^3)

        % stiffness constants matrix, for lithium tantalate [38]

        c(1,1) = 23.28;          % (10^10 N/m^2);
        c(1,2) = 4.65;
        c(1,3) = 8.36;
        c(1,4) = -1.05;
        c(3,3) = 27.59;
        c(4,4) = 9.49;
        c(2,2) = c(1,1);
        c(2,3) = c(1,3);
        c(2,4) = -c(1,4);
        c(5,6) = c(1,4);
        c(5,5) = c(4,4);
        c(6,6) = (c(1,1)-c(1,2))/2;
        c(2,1) = c(1,2);
        c(3,1) = c(1,3);
        c(4,1) = c(1,4);
        c(3,2) = c(1,3);
        c(4,2) = -c(1,4);
        c(6,5) = c(1,4);

%-----------------------------------------------------------------------

elseif subs == 3;
        dens = 2651;   % density in (kg/m^3)

        % stiffness constants matrix, for quartz [17]


        c(1,1) = 8.674;          % (10^10 N/m^2);
        c(1,2) = 0.699;
        c(1,3) = 1.191;
        c(1,4) = -1.791;
        c(3,3) = 10.72;
        c(4,4) = 5.794;
```

```
c(2,2) = c(1,1);
c(2,3) = c(1,3);
c(2,4) = -c(1,4);
c(5,6) = c(1,4);
c(5,5) = c(4,4);
c(6,6) = (c(1,1)-c(1,2))/2;
c(2,1) = c(1,2);
c(3,1) = c(1,3);
c(4,1) = c(1,4);
c(3,2) = c(1,3);
c(4,2) = -c(1,4);
c(6,5) = c(1,4);

% ------------------------------------------------------------------------

else

    dens = 5307;   % density in (kg/m^3);

    % stiffness constants matrix, for GaAs [17]

    c(1,1) = 11.88;          %(10^10 N/m^2);
    c(1,2) = 5.38;
    c(1,3) = c(1,2);
    c(2,2) = c(1,1);
    c(3,3) = c(1,1);
    c(4,4) = 5.94;
    c(2,3) = c(1,2);
    c(5,5) = c(4,4);
    c(6,6) = c(4,4);
    c(2,1) = c(1,2);
    c(3,1) = c(1,3);
    c(3,2) = c(2,3);


end
```

stapes.m

```
function pes = stapes(subs)

% this subroutine initiallizes the 'standard' piezoelectric constants for the substrates

global subs pes

for m = 1 : 3;
        for l = 1 : 6;
                pes(m,l)=0;
        end;
end;


if subs == 1

        % piezoelectric constants matrix, for lithium niobate [38]

        pes(1,5) = 3.69;        %(C/m^2);
        pes(2,2) = 2.42;
        pes(3,1) = 0.30;
        pes(3,3) = 1.77;
        pes(1,6) = -pes(2,2);
        pes(2,1) = -pes(2,2);
        pes(2,4) = pes(1,5);
        pes(3,2) = pes(3,1);


%-------------------------------------------------------------------

elseif subs ==2

        % piezoelectric constants matrix, for lithium tantalate [38]

        pes(1,5) = 2.64;        %(C/m^2);
        pes(2,2) = 1.86;
        pes(3,1) = -0.22;
        pes(3,3) = 1.71;
        pes(1,6) = -pes(2,2);
```

```
        pes(2,1) = -pes(2,2);
        pes(2,4) = pes(1,5);
        pes(3,2) = pes(3,1);

%-------------------------------------------------------------------------

elseif subs == 3;

        % piezoelectric constants matrix, for quartz [17]

        pes(1,1) = 0.171;       % (C/m^2);
        pes(1,4) = -0.0436;
        pes(1,2) = -pes(1,1);
        pes(2,5) = -pes(1,4);
        pes(2,6) = -pes(1,1);

% -------------------------------------------------------------------------

else

        % piezoelectric constants matrix, for gallium arsenide [17]

        pes(1,4) = 0.154;       % (C/m^2);
        pes(2,5) = 0.154;
        pes(3,6) = 0.154;


end
```

staperm.m

```
function perm = staperm(subs)

% this subroutine initiallizes the 'standard' permittivity constants for the substrates

global subs perm

for m = 1 : 3;
        for l = 1 : 3;
                perm(m,l) = 0;
        end;
end;


if subs == 1

        % permittivity constants matrix for lithium niobate [38]

        perm(1,1) = 45.6;               % ( in perm0);
        perm(3,3) = 26.3;
        perm(2,2) = perm(1,1);

%-------------------------------------------------------------------------

elseif subs ==2

        % permittivity constants matrix, for lithium tantalate [38]

        perm(1,1) = 40.9;               % (in perm0);
        perm(3,3) = 42.5;
        perm(2,2) = perm(1,1);

%-------------------------------------------------------------------------

elseif subs == 3;

        % permittivity constants matrix, for quartz [17]

        perm(1,1) = 4.5;                % ( in perm0);
```

```
        perm(3,3) = 4.6;
        perm(2,2) = perm(1,1);

% ------------------------------------------------------------------------

else

        % permittivity constants matrix, for GaAs [17]

        perm(1,1) = 12.5;
        perm(2,2) = perm(1,1);                  % ( in perm0);
        perm(3,3) = perm(1,1);


end
```

tracon.m

```
function [crot,pesrot,permrot] = tracon(cl,pesl,perml)

% this subroutine transforms the standard material tensors to
% to the appropriate frame of reference defined by the cut of the
% crystal (note that cut is defined by the Euler Angles)

global phi theta ci crot pesrot permrot c0 perm0

% calculate the standard 'coordinate rotation matrix', a, for each Euler angle

for n=1:3;              % must repeat for each Euler angle

    if n==1;

        a(1,1) = cos(phi);
        a(1,2) = sin(phi);
        a(1,3) = 0;
        a(2,1) = -sin(phi);
        a(2,2) = cos(phi);
        a(2,3) = 0;
        a(3,1) = 0;
        a(3,2) = 0;
        a(3,3) = 1.0;

    elseif n==2;

        a(1,1) = 1;
        a(1,2) = 0;
        a(1,3) = 0;
        a(2,1) = 0;
        a(2,2) = cos(theta);
        a(2,3) = sin(theta);
        a(3,1) = 0;
        a(3,2) = -sin(theta);
        a(3,3) = cos(theta);

    else;
```

```
        a(1,1) = cos(ci);
        a(1,2) = sin(ci);
        a(1,3) = 0;
        a(2,1) = -sin(ci);
        a(2,2) = cos(ci);
        a(2,3) = 0;
        a(3,1) = 0;
        a(3,2) = 0;
        a(3,3) = 1.0;

    end;

%-----------------------------------------------------------------

%   Calculate the Bond stress transformation matrix, M  [17]

    for m = 1 : 3;
        for l = 1 : 3;
            M(m,l) = a(m,l)^2;
        end;
    end;

    M(1,4) = 2*a(1,2)*a(1,3);
    M(1,5) = 2*a(1,3)*a(1,1);
    M(1,6) = 2*a(1,1)*a(1,2);

    M(2,4) = 2*a(2,2)*a(2,3);
    M(2,5) = 2*a(2,3)*a(2,1);
    M(2,6) = 2*a(2,1)*a(2,2);

    M(3,4) = 2*a(3,2)*a(3,3);
    M(3,5) = 2*a(3,3)*a(3,1);
    M(3,6) = 2*a(3,1)*a(3,2);

    M(4,1) = a(2,1)*a(3,1);
    M(4,2) = a(2,2)*a(3,2);
    M(4,3) = a(2,3)*a(3,3);
    M(4,4) = a(2,2)*a(3,3) + a(2,3)*a(3,2);
    M(4,5) = a(2,1)*a(3,3) + a(2,3)*a(3,1);
    M(4,6) = a(2,2)*a(3,1)+a(2,1)*a(3,2);
```

```
        M(5,1) = a(3,1)*a(1,1);
        M(5,2) = a(3,2)*a(1,2);
        M(5,3) = a(3,3)*a(1,3);
        M(5,4) = a(1,2)*a(3,3)+a(1,3)*a(3,2);
        M(5,5) = a(1,3)*a(3,1)+a(1,1)*a(3,3);
        M(5,6) = a(1,1)*a(3,2)+a(1,2)*a(3,1);

        M(6,1) = a(1,1)*a(2,1);
        M(6,2) = a(1,2)*a(2,2);
        M(6,3) = a(1,3)*a(2,3);
        M(6,4) = a(1,2)*a(2,3)+a(1,3)*a(2,2);
        M(6,5) = a(1,3)*a(2,1)+a(1,1)*a(2,3);
        M(6,6) = a(1,1)*a(2,2)+a(1,2)*a(2,1);

%-------------------------------------------------------------------

%       Calculate the rotated stiffness matrix

        cl = M*cl*(M');

%       Calculate the rotated piezoelectric stress matrix

        pesl = a*pesl*(M');

%       Calculate the rotated permittivity matrix

        perml = a*perml*(a');

end;

crot=cl;
permrot=perml;
pesrot=pesl;

M = [];
a = [];

end
```

invel.m

```
function [x1comp,x3comp] = invel(crot,pesrot,permrot)

% This subroutine calculates the slowness curves in the sagittal plane
% for the selected crystal substrate using the Christoffel Equation
% outlined in Chapter 5.

global dens

% density used in Christoffel Matrix

P0=dens*[1 0 0 0
      0 1 0 0
      0 0 1 0
      0 0 0 0];

I0=1e-8*[1 0 0 0
       0 1 0 0
       0 0 1 0
       0 0 0 1];

% range for plot including interval
ang = 0:0.01:2*pi;

% determines number of points for plot
ns = fix(2*pi/0.01);

for n=1:ns;

  % form Christoffel matrix to get the solution of 'slowness' in dispersion
  % relation - see equation (5.10) in Chapter 5.

  CM(1,1)=-(sin(ang(n)))^2*crot(5,5)-2*sin(ang(n))*cos(ang(n))*crot(1,5)...
              -crot(1,1)*(cos(ang(n)))^2;

  CM(1,2)=-(sin(ang(n)))^2*crot(4,5)-sin(ang(n))*cos(ang(n))*(crot(1,4)+crot(5,6))...
              -crot(1,6)*(cos(ang(n)))^2;
```

```
CM(1,3)=-(sin(ang(n)))^2*crot(3,5)-sin(ang(n))*cos(ang(n))*(crot(1,3)+crot(5,5))...
        -crot(1,5)*(cos(ang(n)))^2;

CM(1,4)=-(sin(ang(n)))^2*pesrot(3,5)-pesrot(1,1)*(cos(ang(n)))^2...
        -sin(ang(n))*cos(ang(n))*(pesrot(1,5)+pesrot(3,1));


CM(2,1)=-(sin(ang(n)))^2*crot(4,5)-sin(ang(n))*cos(ang(n))*(crot(1,4)+crot(5,6))...
        -crot(1,6)*(cos(ang(n)))^2;

CM(2,2)=-(sin(ang(n)))^2*crot(4,4)-2*sin(ang(n))*cos(ang(n))*crot(4,6)...
        -crot(6,6)*(cos(ang(n)))^2;

CM(2,3)=-(sin(ang(n)))^2*crot(3,4)-sin(ang(n))*cos(ang(n))*(crot(3,6)+crot(4,5))...
        -crot(5,6)*(cos(ang(n)))^2;

CM(2,4)=-(sin(ang(n)))^2*pesrot(3,4)-pesrot(1,6)*(cos(ang(n)))^2...
        -sin(ang(n))*cos(ang(n))*(pesrot(1,4)+pesrot(3,6));


CM(3,1)=-(sin(ang(n)))^2*crot(3,5)-sin(ang(n))*cos(ang(n))*(crot(1,3)+crot(5,5))...
        -crot(1,5)*(cos(ang(n)))^2;

CM(3,2)=-(sin(ang(n)))^2*crot(3,4)-sin(ang(n))*cos(ang(n))*(crot(3,6)+crot(4,5))...
        -crot(5,6)*(cos(ang(n)))^2;

CM(3,3)=-(sin(ang(n)))^2*crot(3,3)-2*sin(ang(n))*cos(ang(n))*crot(3,5)...
        -crot(5,5)*(cos(ang(n)))^2;

CM(3,4)=-(sin(ang(n)))^2*pesrot(3,3)-pesrot(1,5)*(cos(ang(n)))^2...
        -sin(ang(n))*cos(ang(n))*(pesrot(1,3)+pesrot(3,5));


CM(4,1)=-(sin(ang(n)))^2*pesrot(3,5)-pesrot(1,1)*(cos(ang(n)))^2...
        -sin(ang(n))*cos(ang(n))*(pesrot(1,5)+pesrot(3,1));

CM(4,2)=-(sin(ang(n)))^2*pesrot(3,4)-pesrot(1,6)*(cos(ang(n)))^2...
        -sin(ang(n))*cos(ang(n))*(pesrot(1,4)+pesrot(3,6));

CM(4,3)=-(sin(ang(n)))^2*pesrot(3,3)-pesrot(1,5)*(cos(ang(n)))^2...
        -sin(ang(n))*cos(ang(n))*(pesrot(1,3)+pesrot(3,5));
```

```
CM(4,4)=(sin(ang(n)))^2*permrot(3,3)+2*sin(ang(n))*cos(ang(n))*permrot(1,3)...
              -permrot(1,1)*(cos(ang(n)))^2;


% intiallize matrices that will store roots of Christoffel Equation

 slrt00 = []; slrt = [];

% get the eigenvalues of matrix equation; these will correspond to (k/w)^2

 slrt00(n,:) = eig(-P0/(CM+I0))';


% take square root to obtain (k/w)

 for m=1:3;
       slrt(m)=sqrt(slrt00(n,m));
 end;

 for m=1:3;
       [smax,pos]=max(slrt);                  % arranges slownesses in descending
       x3comp(n,m)=-cos(ang(n))*smax;         % order for plotting purposes.
       x1comp(n,m)=sin(ang(n))*smax;
       slrt(pos)=slrt(pos)/100;
 end;


end;

% plot the slowness surface

figure('position',[640 550 650 650]) ;

plot(x1comp(1:ns,1),x3comp(1:ns,1),'w-',x1comp(1:ns,2),x3comp(1:ns,2),...
       'w-',x1comp(1:ns,3),x3comp(1:ns,3),'w--')

xlabel('Sx3 - slowness (s/m)');
ylabel('Sx1 - slowness (s/m)');

end
```

epcalc.m

```
function [rep,iep] = epcalc(crot,pesrot,permrot)

% This subroutine calculates and plots the effective permittivity function
% for the selected crystal substrates using the method outlined
% in chapter 6 of the Thesis.

global dens rep iep

% choose suitable range for surface wave velocities

s1=1e-6;                    % v1=1e+006 m/s;
s2=500e-6;                  % v2=2000 m/s;

ns=input('Input the number of points desired for the analysis:');

ep(s1,s2,ns);   % call 'general' function to calculate effective permittivity

% this section specifies the range of interest on the y-axis
% for the effective permittivity.

for n=1:ns+1;

        if rep(n) > 100;
                rep(n) = 100;
        end;

        if rep(n) < -100;
                rep(n) = -100;
        end;

        if iep(n) > 400;
                 iep(n) = 400;
        end;

        if iep(n) < -400;
                iep(n) = -400;
        end;
end;
```

```
% plot the real and imaginary parts of the effective permittivity

ds=(s2-s1)/ns;          % determine distance between each step
s=s1:ds:s2;             % range of plot

figure;

plot(s(10:ns),rep(10:ns),'w',s(10:ns),iep(10:ns),'y--')

% label the axis

xlabel('Slowness (s/m)');
ylabel('Effective permittivity / free space permittivity');

% ------------------------------------------------------------------
```

detvel.m

```
function [v0,vm,ECC] = detvel(crot,pesrot,permrot)

% The following subroutine calculates the free and metallized velocities
% by determining the accurate locations of zeros and poles in the
% effective permittivity function. The program chooses a predetermined
% range of the effective permittivity function containing the poles and
% zeros and then recalculates the function in this range using a great
% many number points to obtain a high level of accuracy. The location of
% the poles and zeros are then used to calculate the respective
% velocities. The electromechanical coupling coeefficient (K^2) is then
% computed using these velocities.

global phi theta ci dens effperm ieffperm rep iep

% determine range for analysis by examining Euler angles

if ci == 0;                     % Regular SAW;
        s1 = 1/4050;            % establish range of analysis as
        s2 = 1/3100;            % determined by inspection from plots.
        ns = 4000;              % number of points in range (accuracy).

elseif abs(theta) == abs(ci);   %  Pure Rayleigh Wave type(YZ cut of LiNbO3
                                 % and LiTaO3);

        s1 = 1/3500;
        s2 = 1/3100;
        ns = 2000;

else

        s1 = 1/3450;
        s2 = 1/3100;
        ns = 2000;

end;
```

```
ep(s1,s2,ns);                % determine eff. perm. in prescribed range
                             % using many more steps (ns) for greater accuracy


ds=(s2-s1)/ns;
s=s1:ds:s2;

[pv0,mv0]=max(abs(ieffperm));    % find location of zero (s0)
v0=1/s(mv0);                     % free surface velocity (=1/s0)

[pvm,mvm]=max(rep+i*iep);        % find location of pole (sm)
vm=1/s(mvm);                             % metallized velocity   (=1/sm)

% calculate K^2 (coupling coefficient)

ECC=2*(v0-vm)/v0;

% display the results

disp('free surface velocity : '); v0
disp('metallized velocity   : '); vm
disp('electromechanical coupling coefficient : ');  ECC

% ---------------------------------------------------------------
```

ep.m

```
function [effperm,ieffperm,rep,iep] = ep(ss1,ss2,nss)

% This is a general subroutine that calculates the effective permittivity
% function for the selected crystal substrates using the method outlined
% in chapter 6 of the Thesis. It is invoked to calculate and plot the
% permittivity as well as to determine the free and metallized velocities.

global dens crot pesrot permrot perm0 rep iep ieffperm

TD0=[0 0 0 1];          % vector specifying stress-free boundary condition and
                        % condition that total electric displacement must equal
                        % charge density (assumed to be 1 in this case).

Ds = (s2-s1)/nss;       % determine the increment between points
s = s11: ds : ss2;      % range for analysis with increment(determined by calling
                        % program)

for n=1:ns+1;

        % form the matrix of polynomial coefficients as in equation (4.14)

        pn11 = [crot(5,5) -2*i*crot(1,5) -crot(1,1)+dens/s(n)^2];
        pn12 = [crot(4,5) -i*(crot(1,4)+crot(5,6)) -crot(1,6)];
        pn13 = [crot(3,5) -i*(crot(1,3)+crot(5,5)) -crot(1,5)];
        pn14 = [pesrot(3,5) -i*(pesrot(1,5)+pesrot(3,1)) -pesrot(1,1)];

        pn21 = [crot(4,5) -i*(crot(1,4)+crot(5,6)) -crot(1,6)];
        pn22 = [crot(4,4) -2*i*crot(4,6) -crot(6,6)+dens/s(n)^2];
        pn23 = [crot(3,4) -i*(crot(3,6)+crot(4,5)) -crot(5,6)];
        pn24 = [pesrot(3,4) -i*(pesrot(1,4)+pesrot(3,6)) -pesrot(1,6)];

        pn31 = [crot(3,5) -i*(crot(1,3)+crot(5,5)) -crot(1,5)];
        pn32 = [crot(3,4) -i*(crot(3,6)+crot(4,5)) -crot(5,6)];
        pn33 = [crot(3,3) -2*i*crot(3,5) -crot(5,5)+dens/s(n)^2];
        pn34 = [pesrot(3,3) -i*(pesrot(1,3)+pesrot(3,5)) -pesrot(1,5)];

        pn41 = [pesrot(3,5) -i*(pesrot(1,5)+pesrot(3,1)) -pesrot(1,1)];
        pn42 = [pesrot(3,4) -i*(pesrot(1,4)+pesrot(3,6)) -pesrot(1,6)];
        pn43 = [pesrot(3,3) -i*(pesrot(1,3)+pesrot(3,5)) -pesrot(1,5)];
```

```
pn44 = [-permrot(3,3) 2*i*permrot(1,3) permrot(1,1)];

%-----------------------------------------------------------------

% takes the determinant of the 4x4 matrix of polynomials using
% standard algebraic techniques (cofactor expansion)

% eliminate first row and first column
% in matrix to form 3x3 matrix

pn011 = pn22; pn012 = pn23; pn013 = pn24;
pn021 = pn32; pn022 = pn33; pn023 = pn34;
pn031 = pn42; pn032 = pn43; pn033 = pn44;

% take determinant of 3x3 matrix using 'conv' function to multiply
% polynomials.

aa = conv(pn011, pn022);
pn01 = conv(aa, pn033);
aa = conv(pn021, pn032);
pn02 = conv(aa, pn013);
aa = conv(pn031, pn023);
pn03 = conv(aa, pn012);
aa = conv(pn013, pn022);
pn04 = conv(aa, pn031);
aa = conv(pn032, pn023);
pn05 = conv(aa, pn011);
aa = conv(pn033, pn012);
pn06 = conv(aa, pn021);
pnsum1 = pn01+pn02+pn03-pn04-pn05-pn06;

% eliminate second row and second column
% in matrix to form 3x3 matrix

pn011 = pn21; pn012 = pn23; pn013 = pn24;
pn021 = pn31; pn022 = pn33; pn023 = pn34;
pn031 = pn41; pn032 = pn43; pn033 = pn44;


% take determinant of 3x3 matrix using 'conv' function to multiply
% polynomials.
```

```
aa = conv(pn011, pn022);
pn01 = conv(aa, pn033);
aa = conv(pn021, pn032);
pn02 = conv(aa, pn013);
aa = conv(pn031, pn023);
pn03 = conv(aa, pn012);
aa = conv(pn013, pn022);
pn04 = conv(aa, pn031);
aa = conv(pn032, pn023);
pn05 = conv(aa, pn011);
aa = conv(pn033, pn012);
pn06 = conv(aa, pn021);
pnsum2 = pn01+pn02+pn03-pn04-pn05-pn06;

% eliminate first row and third column
% in matrix to form 3x3 matrix

pn011 = pn21; pn012 = pn22; pn013 = pn24;
pn021 = pn31; pn022 = pn32; pn023 = pn34;
pn031 = pn41; pn032 = pn42; pn033 = pn44;

% take determinant of 3x3 matrix using 'conv' function to multiply
% polynomials.

aa = conv(pn011, pn022);
pn01 = conv(aa, pn033);
aa = conv(pn021, pn032);
pn02 = conv(aa, pn013);
aa = conv(pn031, pn023);
pn03 = conv(aa, pn012);
aa = conv(pn013, pn022);
pn04 = conv(aa, pn031);
aa = conv(pn032, pn023);
pn05 = conv(aa, pn011);
aa = conv(pn033, pn012);
pn06 = conv(aa, pn021);
pnsum3 = pn01+pn02+pn03-pn04-pn05-pn06;

% eliminate first row and fourth column
% in matrix to form 3x3 matrix

pn011 = pn21; pn012 = pn22; pn013 = pn23;
```

```
pn021= pn31; pn022 = pn32; pn023 = pn33;
pn031=pn41;pn032=pn42;pn033=pn43;

% take determinant of 3x3 matrix using 'conv' function to multiply
% polynomials.

aa = conv(pn011, pn022);
pn01 = conv(aa, pn033);
aa = conv(pn021, pn032);
pn02 = conv(aa, pn013);
aa = conv(pn031, pn023);
pn03 = conv(aa, pn012);
aa = conv(pn013, pn022);
pn04 = conv(aa, pn031);
aa = conv(pn032, pn023);
pn05 = conv(aa, pn011);
aa = conv(pn033, pn012);
pn06 = conv(aa, pn021);
pnsum4 = pn01+pn02+pn03-pn04-pn05-pn06;

% multiply individual 3x3 determinants by cofactors of first row

pn1 = conv(pn11,pnsum1);
pn2 = -conv(pn12,pnsum2);
pn3 = conv(pn13,pnsum3);
pn4 = -conv(pn14,pnsum4);

% ********** calculate total determinant of 4x4 matrix ***********

pnsum = pn1+pn2+pn3+pn4;

% initiallize matrices used in selecting and storing acceptable roots

rt = []; rt0 = []; rt00 = []; rt000 = []; mrt = [];

rt000 = roots(pnsum);          % finds the roots of the characteristic equation

rt00 = rt000;
```

```
% ----------the following section chooses the acceptable roots----------


% this sections cuts the pure image conjugate roots

for m = 2:8;
        if abs(imag(rt00(m))-imag(rt00(m-1)')) < 1e-10;
                if abs(real(rt00(m))) < 1e-15;
                        rt00(m) = rt00(m)-1e10;
                        rt00(m-1) = real(rt00(m-1))+abs(imag(rt00(m-1)))*i;
                end;
        end;
end;

l = 1;

for m = 1 : 8;
        if real(rt00(m)) > -1e-10;
                if imag(rt00(m)) > -6.8;
                        rt0(l) = rt00(m);
                        l = l+1;
                end;
        end;
end;

if l == 5;
        rt = rt0;
elseif l > 5 ;      % this section eliminates surplus pure imaginary roots
        k = 1;
        for m = 1 : l-1;
                if real(rt0(m)) > 1e-10;
                        rt(k) = rt0(m);
                        rt0(m) = rt0(m)-1e10*(1+i);
                        k = k+1;
                end;
        end;
        k0 = 5-k;
        for m = 1:k0;
                [kmax,m0] = max(imag(rt0));
                rt(k) = rt0(m0);
                rt0(m0) = rt0(m0)-1e10*(1+i);
                k = k+1;
```

```
        end;
end;

% ------------------------------------------------------------------------

% this section evaluates the coefficient matrix for 'each' of
% the four acceptable roots, alpha, of the characteristic equation

for  m=1:4;

        yy(1,1) = polyval(pn11,rt(m));
        yy(1,2) = polyval(pn12,rt(m));
        yy(1,3) = polyval(pn13,rt(m));
        yy(1,4) = polyval(pn14,rt(m));

        yy(2,1) = polyval(pn21,rt(m));
        yy(2,2) = polyval(pn22,rt(m));
        yy(2,3) = polyval(pn23,rt(m));
        yy(2,4) = polyval(pn24,rt(m));

        yy(3,1) = polyval(pn31,rt(m));
        yy(3,2) = polyval(pn32,rt(m));
        yy(3,3) = polyval(pn33,rt(m));
        yy(3,4) = polyval(pn34,rt(m));

        yy(4,1) = polyval(pn41,rt(m));
        yy(4,2) = polyval(pn42,rt(m));
        yy(4,3) = polyval(pn43,rt(m));
        yy(4,4) = polyval(pn44,rt(m));

        % find u1, u2, u3 for each root that satisfies matrix equation
        % Normallize with respect to potential which is assumed to be 1
        % for convenience

        vector1 = yy(1:3,1:3)\(-yy(1:3,4));

        % The matrix U stores the displacement components for each root
        % in respective columns.

        U(1:3,m) = vector1; U(4,m) = 1;
 end;
```

```
% This section calculates the normal components of stress
% T13, T23, T33 and displacement D3 in the substrate and stores
% the information in a coefficient matrix, B. Each element of B is
% a coefficient of one of three displacement components or potential

for  m = 1 : 4;

        B(1,1) = crot(5,5)*rt(m)-crot(1,5)*i;
        B(1,2) = crot(4,5)*rt(m)-crot(5,6)*i;
        B(1,3) = crot(3,5)*rt(m)-crot(5,5)*i;
        B(1,4) = pesrot(3,5)*rt(m)-pesrot(1,5)*i;

        B(2,1) = crot(4,5)*rt(m)-crot(1,4)*i;
        B(2,2) = crot(4,4)*rt(m)-crot(4,6)*i;
        B(2,3) = crot(3,4)*rt(m)-crot(4,5)*i;
        B(2,4) = pesrot(3,4)*rt(m)-pesrot(1,4)*i;

        B(3,1) = crot(3,5)*rt(m)-crot(1,3)*i;
        B(3,2) = crot(3,4)*rt(m)-crot(3,6)*i;
        B(3,3) = crot(3,3)*rt(m)-crot(3,5)*i;
        B(3,4) = pesrot(3,3)*rt(m)-pesrot(1,3)*i;

        B(4,1) = pesrot(3,5)*rt(m)-pesrot(3,1)*i;
        B(4,2)= pesrot(3,4)*rt(m)-pesrot(3,6)*i;
        B(4,3) = pesrot(3,3)*rt(m)-pesrot(3,5)*i;
        B(4,4) = -permrot(3,3)*rt(m)+permrot(1,3)*i;

        % t is a 4x1 column vector storing the normal stresses and
        % displacement (T13,T23,T33,D3) for each root. It is calculated
        % by taking the product of the coefficient matrix B and columns
        % in U representing displacement components for each respective
        % root.

        t = B*U(:,m);

        % T4 is a 4x4 matrix that stores the normal stress and displacement
        % components for each respective root in columns vectors

        T4(:,m) = t;

end;
```

```
TT4(4,1:4) = perm0*[1 1 1 1];

% the matrix TD4 stores the normal components of stress and total normal
% component of electric displacement for each root in respective columns

TD4(1:3,1:4) = -T4(1:3,1:4);

% calculate the 'total' normal electric displacement component
% at surface by summing contributions from both sides.

TD4(4,1:4) = (TT4(4,1:4)-T4(4,1:4));
TD4 = TD4;

% find the coefficients A required to satisfy the boundary conditions
% defined by TD0 where the normal components of stress dissappear
% (stress-free bounadary condition) and the total electric
% displacement D3 is equal to the charge density which is assumed
% to be 1 for simplicity.

coeff = TD4(1:4,1:4)\TD0';

A(1:4) = coeff;          % store the coefficients in row vector A

% determine effective permittivity by forming ratio of charge density
% to potential where the general potential is a linear combination
% of the potentials determined for each respective root. Note that
% it is only necessary to add the coefficients A since the solutions
% were normaliized with respect to potential (assumed to be 1).

effperm(n) = 1/(U(4,1)*A(1)+U(4,2)*A(2)+U(4,3)*A(3)+U(4,4)*A(4));

ieffperm(n) = 1/effperm(n);

rep(n) = real(effperm(n))/perm0;     % find the real part of the eff. perm.
iep(n) = imag(effperm(n))/perm0;     % find the imaginary part of the eff. perm.


end
```

REFERENCES

1. Lord Rayleigh, "On Waves Propagated along the Plane Surface of an Elastic Solid", Proceedings London Mathematical Society, Vol. 17, 1885, pp. 4-11.

2. H. Matthews (Ed.), Surface Wave Filters: Design, Construction and Use, New York : John Wiley, 1977.

3. K. Dransfeld and E. Salzmann, "Excitation, Detection and Attenuation of High-Frequency Elastic Surface Waves", Physical Acoustics, Vol. VII, 1970, pp.219-272.

4. N. Braithwaite and G. Weaver, Electronic Materials, London : The Open University, 1990.

5. L.A. Coldren and H. J. Shaw, "Surface-Wave Long Delay Lines", Proceedings IEEE, Vol. 64, 1976, pp. 598-609.

6. D. P. Morgan, Surface-Wave Devices for Signal Processing, New York: ELSEVIER Science Publishing Company Inc., 1985.

7. C. K. Campbell, Notes on Surface Acoustic Wave Devices, Hamilton : McMaster University, 1982.

8. B. J. Darby, D. J. Gunton and M. F. Lewis, "Efficient Miniature SAW Convolver", Proceedings 1980 IEEE Ultrasonics Symposium, pp. 53-58.

9. R. Bracewell, The Fourier Transform and Its Applications, New York : McGraw-Hill Inc., 1986.

10. D.T. Bell and R. C. M. Li, "Surface Acoustic Wave Resonators", Proceedings IEEE, Vol. 64, 1976, pp. 711-721.

25. R. F. Milsom, N. H. C. Reilly and M. Redwood, "Analysis of Generation and Detection of Surface and Bulk Acoustic Waves by Interdigital Transducers", IEEE Transactions on Sonics and Ultrasonics, Vol. SU-24, No. 3, May 1977, pp. 147-166.

26. R. F. Milsom, M. Redwood and N. H. C. Reilly, "The Interdigital Transducer", in Matthews [2], pp. 55-108

27. K. M. Lakin, "Perturbation Theory for Electromagnetic Coupling to Elastic Surface Waves on Piezoelectric Substrates", Journal of Applied Physics, Vol. 42, 1971, pp. 899-906.

28. B. A. Auld and G. S. Kino, "Normal Mode Theory for Acoustic Waves and its Application to the Interdigital Transducer", IEEE Transactions, Vol. ED-18, 1971, pp. 898-908.

29. H. Jeffreys, Cartesian Tensors, New York : Cambridge University Press, 1952

30. H. Anton, Elementary Linear Algebra 5e, New York : John Wiley, 1987.

31. M. Feldmann and J. Henaff, Surface Acoustic Waves for Signal Processing, Boston, MA : Artech House, 1989 (English edition).

32. A. A. Oliner, Acoustic Surface Waves, Germany : Springer-Verlag Berlin Heidelberg, 1978

33. J. Henaff and M. Feldmann, "Monolithic acoustoelectric amplifier using pseudo-surfave waves", Appl. Phys. Lett., **24**, 1974, pp. 447-449.

34. C. S. Hartmann and Jen, "Improved Accuracy for Determining SAW Transducer Capicitance and K^2", Proceedings 1987 IEEE Ultrasonics Symposium, pp.161-167.

35. J. J. Campbell and W. R. Jones, "A Method for Estimating Optimal Crystal Cuts and Propagation Directions for Excitation of Piezoelectric Surface Waves", IEEE Transactions on Sonics and Ultrasonics, Vol. SU-15, No. 4, October 1968, pp. 209-217.

36. L. Boyer, J. Debois, Y. Zhang and J. M. Hode', "Theoretical Determination of the Pseudo Surface Acoustic Wave Characteristic Parameters", Proceedings 1991 IEEE Ultrasonics Symposium, pp. 353-357.

37. V. P. Plessky and T. Thorvaldson, "Periodic Green's Function Analysis of SAW and Leaky SAW Propagation in a Periodic System of Electrodes on a Piezoelectric Crystal", IEEE Transactions on Ultrasonics, Ferroelectrics and Frequency Control, Vol. 42, No. 2, March 1995, pp. 280-293.

38. G. Kovacs, M. Anhorn, H. E. Engan, G. Visintini and C. C. W. Ruppel, "Improved Material Constants for $LiNbO_3$ and $LiTaO_3$", Proceedings 1990 IEEE Ultrasonics Symposium, pp. 435-438.